Study on Phosphorus Accumulation and Inorganic Carbon/Nitrogen Fixation in Algal-bacterial Aerobic Granular Sludge

January 2024

Li Zejiao

Study on Phosphorus Accumulation and Inorganic Carbon/Nitrogen Fixation in Algal-bacterial Aerobic Granular Sludge

A Dissertation Submitted to
the Graduate School of Science and Technology,
University of Tsukuba
in Partial Fulfillment of the Requirements
for the Degree of Doctor of Philosophy in Environmental Studies

Doctoral Program in Environmental Studies,
Degree Programs in Life and Earth Sciences

Li Zejiao

Abstract

Under the increasing demand of carbon (C) neutrality and Sustainable Development Goal (SDG) 6, the conventional activated sludge (CAS) technology treating domestic/industrial wastewater is facing new challenges including high energy consumption and C emissions. The newly developed algal-bacterial aerobic granular sludge (AGS), on the other hand, shows great potentials to overcome these challenges and is thus regarded as the next generation of biological wastewater treatment technology. In this algal-bacterial AGS system, besides the advantage of energy saving resulting from the granular structure, the coexisting microalgae can fix carbon dioxide (CO_2) and photosynthetically produce oxygen (O_2) for aerobic removal of organics, nitrogen (N), and phosphorus (P), which largely reduces direct CO_2 emissions and aeration cost compared with CAS-based wastewater treatment plants (WWTPs). Although microalgae can remove N/P from wastewater through assimilation, its efficiency is relatively low compared with the functional bacteria including nitrifying/denitrifying bacteria and polyphosphate-accumulating organisms (PAOs), which are important to maintain stable granular structure. However, the interaction mechanisms between microalgae and functional bacteria are still unclear, especially in the substance exchange of C and O_2, C removal/fixation, and their contributions to nutrients removal. Specifically, it was found that the functionality of PAOs would gradually lose with the growth of microalgae in the algal-bacterial AGS system.

Therefore, more fundamental works are necessary for its practical application. This study aimed to coordinate microalgae and functional bacteria to establish a photosynthetic O_2-supported algal-bacterial AGS-based wastewater treatment system and clarify the interactions between microalgae and bacteria. The main results can be summarized as follows.

(1) Batch tests show that a strong illumination may induce a high pH due to the uptake of inorganic C by microalgae in the external O_2-supported algal-bacterial AGS (i.e., mechanical aeration was used as the major O_2 supplier), in which chemical P precipitates were formed at a molar Ca/P ratio of 0.99. The chemical P precipitation may account for up to 48% of the total P removal from the bulk liquid under a light illuminance of 560 $\mu mol \cdot m^{-2} \cdot s^{-1}$. On the other hand, the contribution of microalgae growth to P removal from the bulk liquid was negligible. During the aerobic P uptake process, the profile of P uptake was similar ($p > 0.05$) under different light illuminance (0, 90, 280, and 560 $\mu mol \cdot m^{-2} \cdot s^{-1}$), implying that P removal may not be promoted with the enhancement of microalgae growth. Results indicated that the coexisting microalgae significantly inhibited the P removal by PAOs due to the increased liquid pH. In addition, the kinetic process of aerobic P uptake was found to be controlled by macropore (contributing to

64 - 75% P removal) and micropore diffusion.

(2) Photosynthetic O_2 as the sole O_2 supplier can implement aerobic P uptake by PAOs and ammonia oxidation by nitrifying bacteria under the test illumination range even at low dissolved oxygen (DO) concentration < 0.5 mg/L in the algal-bacterial AGS system under stirring operation. An obvious O_2 accumulation occurred after 60 - 90% of N and P were removed under 330 - 1400 $\mu mol \cdot m^{-2} \cdot s^{-1}$. Besides, a net removal of dissolved inorganic C was detected, indicating efficient C fixation. High ammonia removal and P uptake were achieved primarily through functional bacteria under light intensities of 670 - 1400 $\mu mol \cdot m^{-2} \cdot s^{-1}$. On the other hand, photosynthesis as an O_2 supplier showed little effect on the changes of major ions except K^+.

(3) A photosynthetic O_2-supported algal-bacterial AGS system with a low CO_2 emission of 0.25 kg-CO_2/kg-COD was established for highly efficient C assimilation and N/P removal. The photosynthetic O_2 by microalgae could maintain the DO level at 3 - 4 mg/L in the bulk liquid, in which an LED light control system reduced 10 - 30% of light energy consumption. Results showed that the biomass assimilated 52% of input dissolved total C, and the produced O_2 simultaneously facilitated aerobic nitrification and P uptake with the coexisting microalgae serving as the C fixer and O_2 supplier. This resulted in a stably high total N removal of 81 ± 7% and an N assimilation rate of 7.55 mg/(g-mixed liquor volatile suspended solids (MLVSS)·d) with enhanced microbial assimilation and simultaneous nitrification/denitrification. Good P removal of 92 - 98% was maintained during the test period with high P release and uptake rates of 10.84 ± 0.41 and 7.18 ± 0.24 mg/(g-MLVSS·h), respectively. This study found that photosynthetic O_2 was more advantageous for N and P removal than mechanical aeration, and the latter was not economical when compared to the only mixing operation for the proposed algal-bacterial AGS system.

Results from this study can provide a more in-depth and scientific understanding of interactions between microalgae and bacteria in the algal-bacterial AGS system. The proposed system in this study can contribute to a better design and sustainable operation of WWTPs.

Keywords: Algal-bacterial aerobic granular sludge; Carbon fixation; Nitrogen assimilation; Photosynthetic oxygen; Simultaneous nitrogen and phosphorus removal

Contents

List of tables

List of figures

Abbreviations

AGS	Aerobic granular sludge
ANOVA	Analysis of variance
A/O	Anoxic/oxic or anaerobic/oxic
A^2/O	Anaerobic/anoxic/oxic
AOB	Ammonia-oxidizing bacteria
AP	Apatite phosphorus
AS	Activated sludge
BOD	Biochemical oxygen demand
CAS	Conventional activated sludge
CH_4	Methane
Chl-*a/b/c*	Chlorophyll *a/b/c*
CO_2	Carbon dioxide
COD	Chemical oxygen demand
DIC	Dissolved inorganic carbon
DOC	Dissolved organic carbon
DO	Dissolved oxygen
DTC	Dissolved total carbon
EPA	Environmental Protection Agency
EPS	Extracellular polymeric substances
GAOs	Glycogen-accumulating organisms
GHGs	Greenhouse gases
HRT	Hydraulic retention time
IP	Inorganic phosphorus
IPCC	Intergovernmental panel on climate change
IPD	Intra-particle diffusion
LB-EPS	Loosely bound extracellular polymeric substances
MLSS	Mixed liquor suspended solids
MLVSS	Mixed liquor volatile suspended solids
N	Nitrogen
N_2	Nitrogen gas
NAIP	Non-apatite inorganic phosphorus

NH_4^+-N	Ammonia nitrogen
N_2O	Nitrous oxide
NO_2^--N	Nitrite nitrogen
NO_3^--N	Nitrate nitrogen
NOB	Nitrite-oxidizing bacteria
O_2	Oxygen gas
O&M	Operation and maintenance
OP	Organic phosphorus
P	Phosphorus
PAOs	Polyphosphate-accumulating organisms
PFO	Pseudo-first order
PHAs	Poly-β-hydroxyalkanoates
PN	Proteins
PolyP	Polyphosphate
PS	Polysaccharides
PSBR	Photo-sequencing batch reactor
PSO	Pseudo-second order
SBR	Sequencing batch reactor
SMP	Soluble microbial products
SMT	Standards, Measurements, and Testing
SOUR	Specific oxygen uptake rate
SRT	Sludge retention time
SVI	Sludge volume index
TB-EPS	Tightly bound extracellular polymeric substances
TC	Total carbon
TN	Total nitrogen
TP	Total phosphorus
VER	Volumetric exchange ratio
VFAs	Volatile fatty acids
WWTPs	Wastewater treatment plants

Chapter 1 Introduction

1.1 Water pollution and typical treatment units in wastewater treatment plants

1.1.1 Water pollution

Since the first industrial revolution, environmental pollution including water, air and soil problems, has become increasingly serious, which began to draw the attention of society and authorities from the end of the 20th century on (Garcés-Pastor et al., 2023; Whelan et al., 2022). Especially, with the rapid urbanization and associated population growth, the water environment, on which human beings depend, is suffering from pollutions caused by industrial and municipal wastewaters. The global wastewater generation is estimated at 359.4 billion cubic meters annually, with only 53% being adequately treated (Jones et al., 2021). There are a large variety of pollutants in wastewater produced, such as organic matter, nitrogen (N), phosphorus (P), heavy metals, pharmaceutical compounds, and so on (Whelan et al., 2022). The biological degradation of organics easily depletes the dissolved oxygen (DO) in water body, which may cause large amounts of aquatic organisms' death. N and P are the main factors for eutrophication, a water pollution phenomenon worldwide. Heavy metals and other pollutants, on the other hand, are generally toxic to most of organisms. The water bodies polluted by different wastewater sources present different characteristics, which generally requires different treatment methods. Among the various water pollutions, domestic and/or municipal wastewaters mainly containing excessive organics, N, and P have been one major research focus for environmental researchers due to its substantial volume and directly being related to human life. Increasing pressure in the treatment of domestic and/or municipal wastewater production has been driving the development of wastewater treatment techniques.

1.1.2 Typical treatment units in wastewater treatment plants

A typical wastewater treatment plant (WWTP), targeting domestic and/or municipal wastewater treatment, is generally composed of primary, secondary, and tertiary treatment units (Crini and Lichtfouse, 2019; Pei et al., 2019). Primary treatment is mainly to remove floatable and easily settleable matters through sedimentation, coagulation/flocculation, filtration, etc. by using physical methods. Secondary treatment is to remove dissolved and colloidal organic pollutants, N, and P by biological means. Tertiary treatment involves refining the effluents from the secondary treatment, aiming to eliminate some specific contaminants in addition to the residual N and P through membrane filtration, advanced oxidation, ion exchange, adsorption, and so on. The above-mentioned methods are not fixed in the whole WWTP, and they can be

adjusted according to the practical operation requirements. As such, most of organic pollutants, N, and P are removed during the secondary treatment. Among all the treatment methods, the biological treatment is well accepted in WWTPs due to its simplicity, cost-effectiveness, and no production of secondary byproducts (Crini and Lichtfouse, 2019). Thus, the development of various biological treatment technologies has been a research hot spot.

1.2 Conventional activated sludge and its challenges

1.2.1 Conventional activated sludge

Conventional activated sludge (CAS), a well-known biotechnology for wastewater treatment, has being widely applied in the WWTPs in the world since its discovery 100 years ago (Stensel and Makinia, 2014). Activated sludge is usually brown and flocculent with microbial aggregates containing various microorganisms that can utilize organic pollutants, N, and P from wastewater for their own growth. The efficient pollutant removal can be realized through separating the grown biomass from the treated wastewater, and in general the separation process can be easily implemented via gravity sedimentation.

With the development of molecular biotechnology, functional bacteria are gradually identified in activated sludge, and most of the pollutants removal mechanisms have been well illustrated (Aitken et al., 2014). During the CAS process, organic pollutants indicated by biochemical oxygen demand (BOD) or chemical oxygen demand (COD) are biologically degraded into carbon dioxide (CO_2), and partial organic carbon (C) are assimilated by heterotrophic microorganisms under aerobic and/or anaerobic conditions. As for P removal, besides microbial assimilation, polyphosphate accumulating microorganisms (PAOs) have been well recognized as the major bacteria for P accumulation and removal from wastewater, which require specific organic C sources (i.e., volatile fatty acids (VFAs)) and an alternative anaerobic/aerobic operation mode: under anaerobic condition, PAOs hydrolyze polyphosphates inside the cells by utilizing VFAs; while under aerobic condition, PAOs can excessively uptake P for a net P removal from wastewater. Due to its multiple forms, N removal is relatively complex: the removal of ammonia nitrogen (NH_4^+-N) is generally achieved through nitrification process, during which NH_4^+-N is first oxidized into nitrite nitrogen (NO_2^--N) and then further oxidized into nitrate nitrogen (NO_3^--N) under aerobic condition. The produced NO_3^--N can be reduced into nitrogen gas (N_2) under the anoxic or anaerobic condition (namely denitrification), which also requires organic C source. In addition, bacterial assimilation may contribute to N removal.

The CAS process can be properly designed to achieve highly efficient COD, N, and P removals for meeting different effluent emission standards, such as anaerobic/anoxic/oxic (A^2/O), anoxic/oxic (A/O), sequencing batch reactor (SBR), oxidation ditch, etc.

1.2.2 New challenges

However, under the pressures of global climate change and C neutralization goals, the intrinsic characteristics of high energy consumption and CO_2 emission are challenging the sustainable development of wastewater industries.

(1) High energy consumption

First of all, CAS is an energy-intensive process, especially the mechanical aeration unit. The energy consumption by the WWTP varies largely from 0.3 to 2.1 kWh/m^3 of treated wastewater, depending on the regions, techniques, WWTP scale, and so on, which accounts for about 25 - 40% of the total operation costs of a conventional WWTP in the European Union (Capodaglio and Olsson, 2020; Gandiglio et al., 2017; Hao et al., 2015; Panepinto et al., 2016). In Germany the WWTPs have a high energy consumption of about 0.7 kWh/m^3 while the WWTPs in China have a low energy consumption of about 0.3 kWh/m^3 (Gandiglio et al., 2017; Hao et al., 2015). In addition, the energy consumption is negatively correlated to the scale of WWTP within a certain scale range (He et al., 2019). Generally, it is well recognized that aeration operation accounts for more than half of energy consumption in the WWTP. The energy consumption of the wastewater treatment facilities were estimated to be up to 1 - 3% of the total electrical energy consumption of a country (Capodaglio and Olsson, 2019; Hao et al., 2015). Such a high electricity consumption also indirectly contributes to CO_2 emissions considering the process by which electricity is generated (Campos et al., 2016).

(2) Greenhouse gases emission

Secondly, WWTPs are also a big contributor of greenhouse gases (GHGs) emission (Campos et al., 2016; Larsen, 2015). Their main GHGs include CO_2, nitrous oxide (N_2O), and methane (CH_4). As addressed in Chapter 1.2.1, the oxidation of organics and the removal of N and P are companied by the direct emission of CO_2. Bao et al. (2015) investigated four full-scale WWTPs and found that the CO_2 emission factor was about 0.58 kg-CO_2/kg-COD, 0.68 kg-CO_2/kg-COD, 0.76 kg-CO_2/kg-COD, and 0.97 kg-CO_2/kg-COD in A^2/O, A/O, oxidation ditch, and SBR-based WWTPs, respectively. Low CO_2 emissions were also reported in full-scaled WWTPs with the Orbal oxidation ditch (0.26 kg-CO_2/kg-COD), reversed A^2/O (0.23 kg-CO_2/kg-COD), and A^2/O (0.32 kg-CO_2/kg-COD) processes (Yan et al., 2014). The GHGs emission from WWTPs may account for 1 - 3% of total anthropogenic emissions (Belloir et al.,

2015; Knappe et al., 2022; Tian et al., 2022; Xi et al., 2021). N_2O is mainly released in aerobic and anoxic processes, which is largely dependent on process operation and conditions, during which N_2O as a by-product is generated and stripped out by aeration, ranging from 0.05 to 25% (kg-N_2O-N/kg-loaded N) (Kampschreur et al., 2009). The emission of CH_4 is generally from the anaerobic fermentation of sludge, and thus has a relatively low emission factor. Recently, however, Moore et al. (2023) found a serious underestimation of CH_4 emission from WWTPs with a median emission factor of 3.4% kg-CH_4/kg-BOD, 1.9 times higher than the estimates by the Intergovernmental Panel on Climate Change (IPCC) and the Unites States Environmental Protection Agency (USEPA).

To sum up, the new challenges for sustaining the sustainable development of WWTPs push the researchers worldwide to focus more on the development of new wastewater treatment technologies with low energy consumption and CO_2 emissions.

1.3 Bacterial aerobic granular sludge for energy saving

Aerobic granular sludge (AGS) can be regarded as self-immobilized microbial aggregates, which are characteristic of compact structure with a diameter of 0.2 - 5 mm, excellent settleability with settling velocity of 10 - 90 m/h, and the ratio of 5 min sludge volume index (SVI_5) to 30 min SVI (SVI_{30}) being nearly "1" (de Kreuk et al., 2007; de Sousa Rollemberg et al., 2018; Nancharaiah and Reddy, 2018). Bacterial AGS was first reported in the 1990s (Morgenroth et al., 1997), which has been applied in over 100 WWTPs in more than 20 countries up to now (Nereda, 2023).

Bacterial AGS is generally cultivated from CAS in SBRs through controlling selective pressures. The key selective pressures have been identified as the volumetric exchange ratio (VER) and settling time (Liu et al., 2005). Thus, the removal mechanisms of COD, N, and P by bacterial AGS are similar as CAS (Chapter 1.2.1). Due to its compact granular structure, bacterial AGS holds a longer biomass retention, higher tolerance to toxicity, and stronger ability to cope with high organic loading rate, etc. compared to CAS (Adav et al., 2008; de Sousa Rollemberg et al., 2018). Furthermore, its big size allows aerobic/anoxic/anerobic zones in one granule, in which nitrifying bacteria, denitrifying bacteria, and PAOs coexist (He et al., 2016). Therefore, it does not need separated anaerobic and aerobic tanks, and even secondary sedimentation tank. As such, simultaneous removal of C, N, and P can be achieved in one reactor. These properties can significantly reduce operation cost of a bacterial AGS-based WWTP. It was estimated that an AGS system presents about 23 - 40% less electricity, 50 - 75%

reduction in space requirements, and 20 - 25% reduction in operation costs in comparison to a CAS system (Adav et al., 2008; de Sousa Rollemberg et al., 2018). Therefore, bacterial AGS technology can reduce CO_2 emission from the perspective of electricity consumption.

However, the bacterial AGS process seems not to largely reduce CO_2 emissions but even sometimes may increase CO_2 emissions. Daudt et al. (2022) reported that the bacterial AGS process emitted up to 0.85 kg-CO_2/kg-$COD_{removed}$ in a pilot-scale SBR treating the real wastewater. A high CO_2 emission factor of 0.93 kg-CO_2/kg-COD was also reported in a lab-scale bacterial AGS system (Wang et al., 2023b). Such CO_2 emission factors are significantly higher than those in the A^2/O and A/O-based WWTPs described in Chapter 1.2.3. Thereby, it is necessary to further reduce the CO_2 emission from the biological process for a carbon-neutral WWTP.

1.4 Microalgae for C fixation

Microalgae cultivation is a promising way to achieve zero CO_2 emission in a WWTP (Jiang et al., 2021; Xu et al., 2023). Under light condition, microalgae can fix CO_2 from bacterial respiration and simultaneously absorb N and P for growth. Unlike CAS and bacterial AGS, the major removal mechanisms of N and P by microalgae are assimilation. In fact, photoheterotrophic microalgae can also absorb specific organics, while it is seldomly designed to remove organic pollutants. When microalgae cultivation is used for nutrients removal, in addition to no CO_2 generation, the harvested algal biomass are more valuable for biofuel production compared to CAS (Vasconcelos Fernandes et al., 2015). It was reported that 1.88 kg CO_2 can be fixed when 1 kg microalgal biomass is generated (Ho et al., 2011). Campos et al. (2016) pointed out that the WWTP coupled with high-rate microalgae pond has potential to achieve a negative CO_2 emission since microalgae can fix CO_2 and then produce O_2 for bacteria with low aeration demand.

It is worth mentioning that phototrophic bacteria can play the same roles as microalgae do. Therefore, the “microalgae” mentioned in this dissertation generally include phototrophic bacteria unless otherwise stated.

The practical application of microalgae cultivation in WWTPs is however greatly limited since the tiny microalgae cells are easily contaminated and difficult to be separated. More attention is thus paid to algal-bacterial consortia, which has been applied in wastewater treatment since 1950s (Jiang et al., 2021). In this kind of system as shown in Fig. 1-1, the coexisting bacteria can improve microalgal settleability to some extent and provide some

growth substances (such as CO_2 and vitamin) for microalgae, while microalgae can elevate biomass value and also provide growth substances (such oxygen (O_2) and amino acids) for bacteria besides absorbing some N and P (Cai et al., 2013; Jiang et al., 2021). Of course, antagonistic effects are sometimes observed between microalgae and bacteria. For example, some red microalgae show strong antibacterial activities (Vairappan, 2003).

Therefore, this kind of consortia still face some challenges before its wide applications. The commonly applied suspended cultivation is challenging the sustainable wastewater industry, including low settleability thus high cost for harvesting, high liquid pH, and possible microalgae pollution during the downstream processing, etc. (Gonçalves et al., 2017; Q. Wang et al., 2020; Yong et al., 2021). In addition, the cultivation of microalgae for nutrients removal requires a long hydraulic retention time (HRT) of 2 - 6 days (Muñoz and Guieysse, 2006), resulting in lower efficiencies when compared to N removal by nitrifiers/denitrifiers and P removal by PAOs in the conventional biological WWTPs.

1.5 Algal-bacterial aerobic granular sludge

In recent years, to simultaneously enhance the reduction of energy consumption and CO_2 emission from wastewater treatment processes, the granular symbiosis of microalgae and bacteria, namely algal-bacterial AGS, firstly reported in 2015 (Huang et al., 2015; Kumar and Venugopalan, 2015), has been attracting more and more attention. Under appropriate artificial or natural light conditions, algal-bacterial AGS system can be established from various inoculums including CAS, bacterial AGS, microalgae, or their mixed cultures in photo-SBRs (Abouhend et al., 2018; He et al., 2018a; Huang et al., 2015; Kumar and Venugopalan, 2015; Liu et al., 2017; Tiron et al., 2015; J. Wang et al., 2020; Wang et al., 2022b; Q. Wang et al., 2020). As summarized in Table 1-1, this technology holds great potentials to inherit the excellent properties of microalgae and bacterial AGS, such as excellent settleability, high heat value of biomass, low energy consumption, low CO_2 emissions, and so on.

From the viewpoint of O_2 supply strategy, algal-bacterial AGS can be classified into two types. The first type is the external O_2-supported algal-bacterial AGS, in which mechanical aeration is still the major O_2 supplier like in the bacterial AGS system. The second type is the photosynthetic O_2-supported algal-bacterial AGS (or photogranule), in which photosynthesis instead of mechanical aeration is the sole O_2 supplier. Obviously, the photosynthetic O_2-supported system has a higher potential for energy saving compared with the external O_2-supported system due to its removal of the most energy-intensive aeration operation. In other

words, the potentials including C fixation and photosynthetic O_2 of microalgae can be fully realized in this kind of system.

1.5.1 Cultivation of algal-bacterial aerobic granular sludge

Firstly, in the external O_2-supported photo-SBRs, similar with the cultivation of bacterial AGS, algal-bacterial AGS can be developed from the sole activated sludge sources under light conditions through gradually shortening settling time (Huang et al., 2015; Zhang et al., 2018). In addition, exogenous microalgae are not a necessary condition for the formation of algal-bacterial AGS (Liu et al., 2022). It is believed that there are some microalgae or phototrophic bacteria seeds in raw activated sludge. When light is applied, these microalgae seeds start to grow together with bacteria, and finally a balance between microalgae and bacteria may be automatically established for a stable algal-bacterial AGS system. When bacterial AGS is as inoculum, algal-bacterial AGS can be faster developed, in which microalgae gradually grow on granules (He et al., 2018a; Wang et al., 2022b). Of course, some exogenous microalgae can be introduced into this granular system. Liu et al. (2017) obtained the algal-bacterial AGS from mixed cultures of *Chlorella*, *Scenedesmus*, and bacterial AGS in external O_2-supported SBRs through controlling the VER, in which *Chlorella* and *Scenedesmus* became dominant algal species. In addition, pure microalgae can be as sole inoculum for algal-bacterial AGS although long cultivation (about 90 days) is required (Q. Wang et al., 2020). During the granulation of pure microalgae, bacteria from air and wastewater would gradually enrich the biomass. It is believed that the accumulation of bacteria is a vital step for granulation.

Secondly, the algal-bacterial AGS can be also established in photosynthetic O_2 supported photo-SBRs. Tiron et al. (2015) successfully performed granulation of microalgae and bacteria through managing the HRT under a stirring operation at a strong light intensity of 235 $\mu mol \cdot m^{-2} \cdot s^{-1}$. Moreover, algal-bacterial AGS can be formed from the sole activated sludge inoculum under a static condition (namely, no mixing of the culture) under 160 - 200 $\mu mol \cdot m^{-2} \cdot s^{-1}$ (Abouhend et al., 2018; Milferstedt et al., 2017), in which microorganisms (especially Cyanobacteria) can grow as dense aggregates resulting from their response to the environment under light condition.

Despite of different cultivation systems, biopolymers are believed to play an vital role in the aggregation of microalgae and bacteria (He et al., 2018a; Liu et al., 2022; Tiron et al., 2017; Zhang et al., 2018). The extracellular polymeric substances (EPS) largely secreted by microorganisms possibly serve as a biological glue to bind microalgae and bacteria for their granulation under the selective pressure. In addition, filamentous phototrophs (cyanobacteria)

can also serve as the skeletal structure for stronger granules (Milferstedt et al., 2017).

Light intensity, as the most critical driving force of microalgae growth, has been extensively investigated in the external O_2-supported system. Light intensity not only dominates the microalgae content in biomass, but also shapes the microbial community (Meng et al., 2019; Zhang et al., 2019). These previous works also pointed out that a stronger light intensity would shift microbial communities and finally cause loose surface and low density of granules, and even led to nitrite nitrogen (NO_2^--N) accumulation. In addition, photoperiodicity is important to develop algal-bacterial AGS. Wang et al. (2022b) claimed that the illumination during the anaerobic phase would decrease PAOs activity in the external O_2-supported SBRs. Therefore, to select appropriate light intensity and operation strategy is the primary step for maintaining good synergic relationships between microalgae and bacteria. However, such studies on photosynthetic O_2-systems are still limited up to date.

1.5.2 Organics and nutrients removal

(1) COD removal

According to the reports on the algal-bacterial AGS, high COD removal efficiency can be achieved in most of test conditions, especially in the photo-SBRs with mechanical aeration. Zhang et al. (2018) claimed that the algal-bacteria AGS can improve COD removal efficiency possibly due to the improved O_2 utilization rate. In most of the previous works, easily biodegradable acetate and glucose were used as the sole organic C. Irrespective of CAS or bacterial AGS, there are large amounts of heterotrophic microorganisms including PAOs and denitrifiers. It can thus be predicted that these heterotrophic microorganisms efficiently utilize this kind of C sources. What's more, several studies used algal-bacterial AGS to treat real wastewaters in the photosynthetic O_2-supported systems and a good COD removal efficiency was also achieved, indicating that photosynthetic O_2 is enough for organic degradation in the test wastewaters (Abouhend et al., 2018; Tiron et al., 2015). Recently, Ji et al. (2020a) pointed out that bacterial assimilation possibly contributed to 49% of total organic carbon (TOC) removal. Of course, photoheterotrophic microorganisms also possibly contribute to COD removal. However, the individual contributions of bacteria or microalgae to C removal are still unclear.

(2) N removal

The removal of N is relatively complex due to the rich microbial diversity of algal-bacterial AGS. The possible removal mechanisms include nitrification, denitrification, microalgae assimilation, bacterial assimilation, etc. In the early stage of algal-bacterial AGS, it was found

that the growth of microalgae inhibited nitrification and caused accumulation of NO_2^--N resulting from the decreased nitrifying bacteria in biomass in the external O_2-supported SBR under natural solar light condition (Huang et al., 2015), which might be due to a strong light intensity (Meng et al., 2019). With the development and progress of this system, such inhibition has been largely ameliorated, in which both nitrifiers and denitrifies can function well (Zhang et al., 2018; Zhao et al., 2018). Namely, nitrification and denitrification are still the major N removal pathways as the same as in bacterial AGS systems. The external O_2-supported system is commonly operated under open conditions, both air and photosynthetic O_2 are possible sources to support aerobic nitrification, especially for the former that can provide enough O_2. Some researchers argued that the photosynthetic O_2 may facilitate O_2 utilization rates and decrease anaerobic zone in the granules (Meng et al., 2019; Zhang et al., 2018). In contrast, the mechanical aeration can strip out dissolved gases (Zhang et al., 2020), and O_2 is not an exception. Therefore, the roles of photosynthetic O_2 in nitrification and denitrification still need further investigation in this system. Although some studies claimed that the total N removal can be enhanced in the algal-bacterial AGS systems (Meng et al., 2019; Zhang et al., 2018), the contributions of microalgal assimilation to N removal remain unclear.

In the photosynthetic O_2-supported system, it is clear that photosynthetic O_2 generated by microalgae can support aerobic bacteria including nitrifying bacteria. Tiron et al. (2015) found that both nitrification and denitrification can coexist in the algal-bacterial granules developed from the mixture of activated sludge and microalgae. Abouhend et al. (2018) claimed that nitrification and denitrification are the main N removal pathways in the photosynthetic O_2 supported system. Overall, microalgae are able to synergize nitrifiers/denitrifiers to achieve an excellent N removal. In recent years, some researchers pointed out that most of ammonia can be assimilated by microorganisms in this photosynthetic O_2 supported system (Ji et al., 2020a). It is believed that both microbial assimilation and nitrification/denitrification pathways are the major NH_4^+-N and total N removal mechanisms.

(3) P removal

Three major removal pathways, including chemical precipitation, microbial assimilation, and bioaccumulation by PAOs, are possibly involved in P removal from wastewater in the algal-bacterial AGS system. Chemical precipitation generally requires a high liquid pH and a high P concentration. Thus, in the algal-bacterial AGS systems, many researchers claimed that it is not the main contributor to P removal due to the low bulk liquid pH condition (Abouhend et al., 2018; Ji et al., 2020b; Meng et al., 2019; Zhang et al., 2018). As for PAOs, there are disputes

on their roles in P removal in the algal-bacterial AGS system. For example, some studies revealed that the release of PO_4^{3-} from anaerobic hydrolysis of polyP become worse or is not significant in the external O_2-supported system (Huang et al., 2015; Meng et al., 2019). In contrast, several reports noticed a significant release of PO_4^{3-} in this kind of photo-SBRs system but inhibitions of microalgae on PAOs activity may also occur (Wang et al., 2021, 2022b). Especially in the photosynthetic O_2-supported system, the contributions of PAOs to P removal are more negligible (Abouhend et al., 2018; Ji et al., 2020b). Ji et al. (2020b) attributed 70% of soluble P removal to algal accumulation.

To sum up, the coexisting microalgae can well coordinate nitrifying/denitrifying bacteria while the microalgae always exert some negative effects on PAOs in the granules. Although a high P removal can be achieved even under no contribution of PAOs in this promising system, PAOs may actually play important roles in granular stability and highly efficient P removal (de Sousa Rollemberg et al., 2018). In addition, PAOs enriched granules hold great potential for P recovery (Wang et al., 2022a). Therefore, taking the Sustainable Development Goal (SDG) 6 into consideration, it is very necessary to coordinate microalgae and functional bacteria (especially PAOs) in this photosynthetic O_2-supported system for the sustainable management of wastewater industry. However, algal-bacterial AGS is a newly developed biotechnology, and limited information relating to the interaction between PAOs and microalgae is available. More detailed research works are needed for its future application in practice.

1.5.3 Contributions to reduced CO_2 emission and energy consumption

Theoretically, the C fixation can be achieved upon microalgae growth in this algal-bacterial AGS. It is thus speculated that the reduction of CO_2 emissions can be realized in this consortia system. Recently, Guo et al. (2021) estimated a low CO_2 emission of 0.08 kg-CO_2/kg-COD in a SBR using the assumed stochiometric formulas of bacteria and microalgae, which was significantly lower than those in CAS or bacterial AGS systems as shown in Chapters 1.2.3 and 1.3. Ji et al. (2020a) combined the measured formula of algal-bacterial AGS and the assumed ones, achieving a low CO_2 emission of 0.14 kg-CO_2/kg-COD (10% of input C) in several small closed systems supported by photosynthetic O_2. Although only a few studies reported CO_2 emissions, it is clear that this consortium system indeed reduces CO_2 emissions. However, the real CO_2 emissions still need to be verified based on C mass balance since the assumed formulas do not indeed represent the real compositions of microalgae and bacteria.

As mentioned in Chapter 1.2.3, aeration is the most energy-intensive operation unit in WWTPs. Besides the advantage of energy saving resulting from granular structure as illustrated

in Chapter 1.3, it is expected that the photosynthetic O_2-supported system can further reduce energy consumption during wastewater treatment compared to the external O_2-supported system. In previous studies, the stirring or shaking operation instead of mechanical aeration are used to mix granules and provide necessary shear force for stably granular structure (Abouhend et al., 2018; Ji et al., 2020a). It can be understood that the system with shaking operation is hardly adopted in practical application. The photosynthetic O_2-supported SBR with stirring operation will be the best choice at present. However, up to now, little information is available on the comparative energy consumption between mechanical aeration and stirring operations in this kind of system. Furthermore, the input light energy is not generally discussed in the previous studies since it is believed that artificial light can be replaced by natural sunlight. In practice, the natural light may not meet the requirements for the photo-SBR system. Therefore, more research works on energy consumption should be conducted to better the development of algal-bacterial AGS system.

1.6 Statement of scientific problems

As discussed above, algal-bacterial AGS is a promising biological technology in wastewater industry when taking the SDG 6 and C neutrality into consideration. The good coordination between microalgae and functional bacteria can facilitate the sustainable operation and maintenance (O&M) of algal-bacterial AGS systems, especially in the photosynthetic O_2-supported system. According to the above review on previous works, the major problems are summarized as follows.

(1) Although the coexisting microalgae can well coordinate with nitrifying/denitrifying bacteria in the algal-bacterial AGS system, the growth of microalgae always exerts negative effects on the PAOs activity. The coexistence of functional bacteria can facilitate granular stability with highly efficient N/P removal. Therefore, it is necessary to coordinate microalgae and functional bacterial in the algal-bacterial system. However, how to coordinate microalgae and PAOs still remains unknown.

(2) Light is the most important factor to drive the algal-bacterial AGS system, but limited information is available on its effects on photosynthetic O_2-supported system. Meanwhile, it is also unclear whether photosynthetic O_2 can simultaneously support P removal by PAOs and N removal by nitrifying/denitrifying bacteria.

(3) Whether a stable photosynthetic O_2-supported system with a well coordination between microalgae and functional bacteria can be established or not remains unknown during the long-

term operation for real practice. In such a system, many questions are pending, for example, what factors can better control or tune this system, how much C emissions can be reduced, how microalgae and bacteria contribute to nutrients removal, whether the energy consumption resulting from the light and stirring operation is lower than that from the mechanical aeration, etc. These questions need to be clarified.

1.7 Research objectives and originality

1.7.1 Research objectives

To solve the above problems, this study aimed to achieve the following objectives.

(1) The first objective was to illuminate the roles of microalgae, especially its effects on PAOs in the algal-bacterial AGS system.

This research would be conducted in the external O_2-supported systems since the growth and accumulation of PAOs in the photosynthetic O_2-supported systems was low according to a previous work (Meng et al., 2019). The possible environmental variations brought by microalgae growth would be fully considered. Meanwhile, the individual contributions of microalgae and PAOs, and chemical precipitation to aerobic P uptake would be systematically investigated in a series of batch tests.

(2) The second objective was to investigate the feasibility of simultaneous removals of P and N by functional bacteria supported by photosynthetic O_2 and reveal roles of light intensity in the algal-bacterial AGS system.

According to the key parameters obtained from the first research work, the feasibility of simultaneous N removal by nitrifying/denitrifying bacteria and P removal by PAOs would be investigated in the photosynthetic O_2-supported algal-bacterial AGS system through batch tests. Exchange of CO_2 and O_2 between microalgae and bacteria, C removal/fixation, nutrient removal mechanisms, etc. would be preliminarily explored.

(3) The third objective was to establish a stable photosynthetic O_2-supported system with highly efficient nutrient removal and low CO_2 emission through coordinating microalgae and functional bacteria.

Finally, to achieve highly efficient nutrient removal and low CO_2 emission, a new photosynthetic O_2-supported system would be established, in which the interaction mechanisms between microalgae and functional bacteria would be clarified regarding substance exchange, C removal/fixation, N/P removal, etc. In addition, preliminary estimations were conducted on energy consumptions by illumination, stirring operation, and aeration.

1.7.2 Research originality

Algal-bacterial AGS is a newly developed wastewater treatment biotechnology, which has demonstrated great potentials to overcome the two new challenges that CAS-based WWTPs are facing. However, up to now,

(1) Little information is available on microalgae and its negative effects on PAOs in the algal-bacterial AGS system with mechanical aeration.

(2) No report can be found on the roles of light intensity that drives the photosynthetic O_2-supported algal-bacterial AGS.

(3) The establishment of a sustainable and scalable algal-bacterial AGS-based SBR system with highly efficient nutrients removal and low CO_2 emissions is rarely reported. In addition, how to easily control and manage its operation remains unclear for practical application.

To sum up, this study firstly tried to coordinate microalgae and functional bacteria to establish a sustainable algal-bacterial AGS-based SBR system with highly efficient nutrients removal and C fixation. Results from this study are expected to contribute the development of C-neutral WWTP and the transformation of WWTP from an energy consumer to energy saver.

1.8 Structure of the dissertation

As shown in Fig. 1-2, this dissertation is divided into five chapters.

In Chapter 1, an overview on the development of wastewater treatment technology on nutrients removal, GHGs emissions, and energy consumption was conducted. Based on the previous studies and the new challenges for WWTPs, the research problems, objectives, and originality were summarized.

In Chapter 2, the effects of the coexisting microalgae on P removal mechanisms during aerobic phases were investigated. Moreover, the limiting factors of microalgae on PAOs were clarified in the algal-bacterial AGS.

In Chapter 3, the feasibility of simultaneous N/P removal by nitrifying/denitrifying bacteria and PAOs supported by photosynthetic O_2 was investigated. The effects of different light intensities on photosynthetic O_2 production, liquid pH, C and O_2 exchange, N/P removal in the photosynthetic O_2-supported algal-bacterial AGS system were explored. In addition, the responses of major ions involving in this system were disclosed.

In Chapter 4, microalgae were attempted to coordinate with functional bacteria for simultaneous high N/P removal efficiency and C fixation in the algal-bacterial AGS. Besides, batch cycle tests, mass balance analysis, and microbial community analysis were performed to

shed light on the mechanisms involved in C/N/P removal and the C and O_2 mass exchanges between microalgae and bacteria. Preliminary estimations of energy consumptions by illumination, stirring, and aeration were also made and compared.

In Chapter 5, main conclusions were summarized with future research directions being proposed.

Table 1-1 Comparison among CAS, microalgae, AGS, and algal-bacteria AGS.

	CAS	Microalgae [a]	AGS	Algal-bacterial AGS	References
Time	Since 1910s	Since 1950s	Since 1990s	Since 2010s	Abouhend et al. (2018) Huang et al. (2015) Barnard and Comeau (2014) Wendell and Pitt (2014) Jiang et al. (2021) Kumar and Venugopalan (2015) Morgenroth et al. (1997)
Nutrient removal mechanisms	COD: Biodegradation, N and P: Bacteria Assimilation, nitrification/denitrification, accumulation by PAOs.	COD: Assimilation by photoheterotrophic microalgae. N and P: Microalgae assimilation.	COD: Similar with CAS N and P: Similar with CAS	Combined mechanisms of microalgae and AGS	
Major processes/ O_2 supply way	A^2/O, A/O, SBR, oxidation ditch, etc. Mechanical aeration	High-rate microalgal pond -	SBR Mechanical aeration	SBR Mechanical aeration or photosynthesis	
Biomass yield	0.6 g-MLVSS/g-BOD	15 kg-dry biomass/kg-N assimilated [b]	0.6 g-MLVSS/g-COD	0.43 - 0.50 g-MLVSS/g-COD	de Sousa Rollemberg et al. (2018) Ho et al. (2011) Mayhew and Stephenson (1997) Muylaert et al. (2017) Świątczak and Cydzik-Kwiatkowska (2018) Wang et al. (2022b) Wang et al. (2020)
Morphology	Filamentous	Tiny and single cell	Compact and near round	Compact and near round	
Settling velocity	2 - 10 m/h	Pure microalgae: 1 cm/h or more.	10 - 90 m/h	Similar with AGS	

Table 1-1 Continued

Heat value	4.57 - 12.51 MJ/kg	18 - 21 MJ/kg	-	-	Scragg et al. (2002) Zakaria et al. (2015)
Energy consumption	0.3 - 2.1 kWh/m^3	-	23 - 40% less compared to AS	Similar to AGS	Bao et al. (2015) de Sousa Rollemberg et al. (2018) Gandiglio et al. (2017) Guo et al. (2021) Ho et al. (2011) Ji et al. (2020a) Wang et al. (2023b) Yan et al. (2014)
CO_2 emission (+) or fixation (-) [b]	+ 0.23 - 0.97 kg-CO_2/kg-COD	- 1.88 kg-CO_2/kg [c]	+ 0.61 kg-CO_2/kg-COD + 0.93 kg-CO_2/kg-COD	+ 0.08 CO_2/kg-COD + 0.14 CO_2/kg-COD	
N_2O emission	0.05 - 25% kg-N_2O/kg-loading N	Low	1 - 21.9% kg-N_2O/kg-TN or removed NH_4^+-N	-	Jahn et al. (2019) Kampschreur et al. (2009)

Note: [a] Only information related to pure microalgal cultivation are provided.

[b] The "+" means emission and "–" means fixation

[c] It was estimated from a general formula ($CO_{0.48}H_{1.83}N_{0.11}P_{0.01}$) of microalgae.

AGS, Aerobic granular sludge; A/O, Anoxic/oxic or anaerobic/oxic; A^2/O, Anaerobic/anoxic/oxic; BOD, biochemical oxygen demand; CAS, Conventional activated sludge; CO_2, carbon dioxide; COD, Chemical oxygen demand; MLVSS, mixed liquor volatile suspended solids; N, nitrogen; NH_4^+-N, ammonia nitrogen; N_2O, Nitrous oxide; O_2, oxygen; P, phosphorus; PAOs, Polyphosphate-accumulating organisms; SBR, Sequencing batch reactor; TN, total nitrogen.

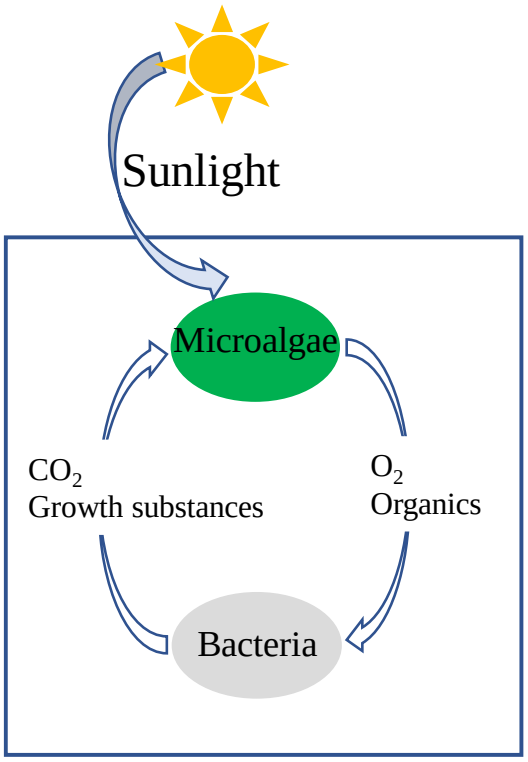

Fig. 1-1 Interaction and substances exchange between microalgae and bacteria in algal-bacterial consortia.

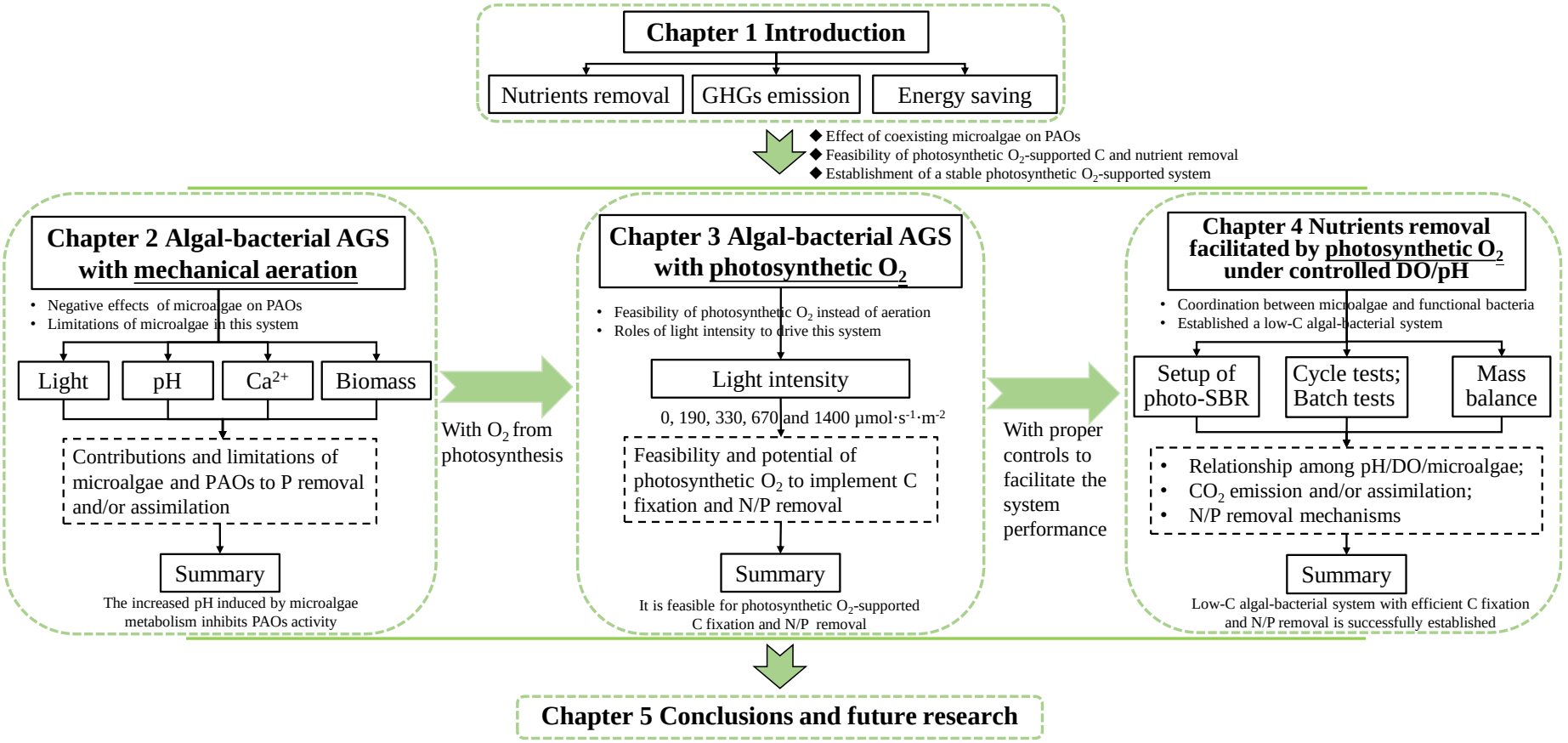

Fig. 1-2 Framework of this dissertation. AGS, aerobic granular sludge; P, phosphorus; N, nitrogen; DO, dissolved oxygen.

Chapter 2 Insight into aerobic phosphorus removal from wastewater in algal-bacterial aerobic granular sludge system

2.1 Background

Although the application of algal-bacterial consortia (not in granules) in wastewater treatment has been extensively studied since the 1950s (Ramanan et al., 2016), the emerging algal-bacterial AGS is just at its early development stage since its first report (Huang et al., 2015). Still, little information is available on the mechanisms of P removal in the algal-bacterial AGS system. In the bacterial AGS system, enrichment of PAOs in granules is still the main and effective way to achieve highly efficient P removal through the alternating operation of anaerobic/aeration periods (de Kreuk et al., 2005). However, the compact granular structure, as the most prominent feature, leads to local DO and pH gradients due to the mass transfer limitation (Mañas et al., 2011; de Sousa Rollemberg et al., 2018). The coexisting microalgae may supply extra O_2 for P uptake by PAOs and alleviate the limitation of O_2 mass transfer in granules besides the P assimilation (Ji et al., 2020a; Lemaire et al., 2008). On the contrary, photosynthesis by microalgae tends to elevate pH which not only promotes P precipitation but also influences the activity of PAOs (Oehmen et al., 2005). Thus there has been a dispute on P removal in algal-bacterial AGS. Huang et al. (2015) first reported the appearance of algal-bacterial AGS developed from CAS when exposed to natural sunlight, in which P removal and PAOs activity were inhibited along with the granule formation. However, a slight improvement by 5.4% on P removal was detected in algal-bacterial AGS developed from CAS under artificial light conditions, in which PAOs activity was assumed to increase due to the coexisting microalgae with *Chlorophyceae* dominated (> 60%) (Zhang et al., 2018). Meng et al. (2019) observed a significantly promoted P removal through increasing light density in algal-bacterial AGS system with pH controlled at 7.4 - 8.4. They attributed the enhanced P removal to the enhanced microalgae growth since PAOs were at a very low level signaled by no P release during the anoxic phase. Most recently, Wang et al. (2021) pointed out that the coexisting microalgae may significantly influence P release by PAOs under a high light intensity of 81 klux (1458 $\mu mol \cdot m^{-2} \cdot s^{-1}$) during the non-aeration phase although an enhanced P removal was detected in the algal-bacterial AGS system. In addition, Ji et al. (2020b) achieved 84% removal of influent P by using a non-aerated microalgal-bacterial AGS system, in which > 70% removal was contributed by the formation of polyphosphates in microalgae. Up to now, however, the interaction between microalgae and PAOs on aerobic P uptake and the mechanisms still remain

unclear in algal-bacterial AGS.

Therefore, this Chapter aimed to investigate the behavior of the coexisting microalgae during the aerobic phase and clarify the effects of microalgae growth, PAOs, and chemical precipitation on P removal in the algal-bacterial AGS naturally developed from bacterial AGS. Besides, the rate-controlling step of P uptake was also analyzed to further shed light on the P uptake mechanisms. In this study, it is hypothesized that (1) the main P removal mechanisms are microalgae growth, PAOs uptake, and chemical precipitation in algal-bacterial AGS, (2) the effect of microalgae growth is negligible under no light condition, and (3) the effect of chemical precipitation could be minimized through lowering liquid pH and/or eliminating ions that can precipitate P.

2.2 Materials and methods

2.2.1 Algal-bacterial AGS, synthetic wastewater, and synthetic P-rich solution

The algal-bacterial AGS was naturally developed from the bacterial AGS under the artificial light condition in a mother photo-SBR with a working volume of 16 L, which has been continuously operated for more than 2 years at an operation cycle of 6 h (with approximately alternative 2 h non-aeration and 4 h aeration) in the laboratory. The HRT and sludge retention time (SRT) were about 12 h and 32 d, respectively. The other operational conditions have been detailed in a previous study (Wang et al., 2022a). The granular structure of the algal-bacterial granules was shown in Fig. 2-1.

The same synthetic wastewater as fed to the mother photo-SBR was used in the batch tests in this study, which was prepared with tap water and chemicals including (per liter) 300 mg chemical oxygen demand (COD, CH_3COONa as the sole carbon source), 30 mg NH_4^+-N (NH_4Cl), 5 mg PO_4^{3-}-P (KH_2PO_4), 5 mg Mg^{2+} ($MgSO_4 \cdot 7H_2O$), 10 mg Ca^{2+} ($CaCl_2 \cdot 2H_2O$), 0.25 mg Fe^{2+} ($FeSO_4 \cdot 7H_2O$), 100 mg $NaHCO_3$ and 1 mL trace elements solution.

The modified synthetic wastewater containing no metal ions that can precipitate phosphate easily was also prepared for the batch tests, in which (1) deionized water (DW) instead of tap water was used, (2) the concentrations of COD, P, and NH_4^+-N were halved, and (3) Ca^{2+}, Fe^{2+}, and trace metals were not added to minimize P precipitation.

According to the obtained P-rich liquid from the anaerobic treatment of sampled algal-bacterial AGS (please refer to Chapters 2.2.2 and 2.3.1 for the details), the synthetic P-rich solution called as the artificial anaerobically released P liquid was prepared by using DW and chemicals including (per liter) 44 mg PO_4^{3-}-P (KH_2PO_4) close to the P concentration in the

actually obtained P-rich liquid, 15 mg NH_4^+-N (NH_4Cl), 5 mg Mg^{2+} ($MgSO_4 \cdot 7H_2O$), and 100 mg $NaHCO_3$. Also, Ca^{2+}, Fe^{2+}, and trace metals were not added to minimize P precipitation. In order to avoid the effect of pH variation on algal-bacterial granules, before the experiments the liquid pH was adjusted to 8.6 which was the same as the pH of the sampled granules at the end of aeration in the mother photo-SBR.

2.2.2 Batch experiments

The algal-bacterial granules used for the batch tests were sampled from the mother photo-SBR at the end of the aeration phase. As shown in Fig. 2-2 and Table 2-1, Batch Test 1 was performed to investigate the typical profile of aerobic P uptake by algal-bacterial AGS. The contributions of microalgae growth, chemical precipitation and PAOs alone to P removal were investigated by Batch Tests 2, 3 and 4, respectively. Batch Test 5 as a supplementary of Batch Test 2 was performed to check microalgae growth with granules as the sole substrate. Among these tests, the effects of microalgae growth and chemical precipitation were minimized by controlling light intensity at 0 $\mu mol \cdot m^{-2} \cdot s^{-1}$ and removing metal ions (except Mg^{2+}) that can precipitate with P from liquid, respectively. And the effect of PAOs was minimized by using granules at the end of the aeration phase from the mother photo-SBR (i.e., the granules have completed aerobic P uptake during one anaerobic/aerobic cycle).

The sampled granules were subjected to an anaerobic process in the presence of synthetic and modified (with no Ca^{2+}, Fe^{2+}, and trace metals) wastewaters to assess the anaerobic P release. The detailed anaerobic process was conducted as follows: Firstly, the sampled 1 L mixed liquor suspended granules from the mother photo-SBR were filtered, then all the granules (approximately 54 g in wet weight) were added to a 1 L beaker. Secondly, 0.47 L filter liquor plus 0.47 L synthetic wastewater were fed to the granules during Batch Test 1 (while 0.95 L modified synthetic wastewater was used during Batch Test 4) for anaerobic P release. In each test beaker, the granules were mixed by an arm stirring (Fine FL-135N, Japan) for 2 h under no light condition, and the pH was maintained at 7.4 by a pH controller (NPH-6900, Japan) with 0.1 mol/L HCl (with pH fluctuation < 0.1) to minimize P precipitation. After anaerobic P release, the solid (granules) and liquid (namely, P-rich liquid) were separated via the glass microfiber filter. The P-rich liquid obtained by using the synthetic wastewater (not modified wastewater) was used for Batch Test 3. The granules not treated by the anaerobic process were used in Batch Tests 2 and 5. In this study, the wet granules after filtration via the glass microfiber filter (934-AH, Whatman) were about 52 - 56 g per liter, and the dry weight (mg) based on mixed liquor suspended solids (MLSS) per unit wet weight (g) after filtration was determined as 95.6 ± 4.5

mg/g (or 4.9 - 5.4 g-MLSS/L in the test beakers).

As for the batch experiments, four or five plastic transparent cylindrical reactors with an inner diameter of 5 cm and a height of 15 cm each were used for the batch tests, in which air was provided by an air pump (AK-40, KOSHIN, Japan) from the bottom of the reactors at an aeration flowrate of 0.35 L/min, i.e., 0.3 cm/s in terms of air uplift velocity as the same as the mother photo-SBR. All the experiments were performed in triplicate.

(1) Batch Test 1: Typical aerobic P uptake under different light illuminance

Based on the pre-experiments, 10.8 g granules (wet weight) treated by the anaerobic process and 189.2 mL of the obtained P-rich liquid were added into each reactor for a 4 h aerobic P uptake test. Each reactor was operated under the designed light intensity, *i.e.*, 0, 90, 280, and 560 $\mu mol \cdot m^{-2} \cdot s^{-1}$, respectively. The maximum intensity applied in this study is the average illumination inside the test reactor, which is equivalent to the light intensity of the sunny days during winter in the test area. During the test period, the pH and DO were monitored but not controlled. µmol·m-2·s-1, µmol·m-2·s-1

(2) Batch Test 2: P uptake by microalgae alone under different light illuminance

Batch Test 2 was performed for 48 h to obtain detectable differences in granule properties before and after the test under the different light intensities (0, 90, 280, and 560 $\mu mol \cdot m^{-2} \cdot s^{-1}$, respectively). The liquid pH was controlled at 8.6 by the pH controller with 0.1 mol/L NaOH to simulate the pH condition during the aeration phase in the mother photo-SBR. 10.8 g wet granules not treated by the anaerobic process and 189.2 mL of the prepared synthetic P-rich solution in Chapter 2.2.1 instead of the actually obtained P-rich liquid (from anaerobic P release) were used in this batch test to minimize the effect of PAOs, P precipitation, and soluble microbial products (SMP). Before the tests, the granules were washed with the synthetic P-rich solution to minimize the effect of gradient diffusion of P into granules.

(3) Batch Test 3: Chemical deposition of anaerobically released P at different pHs

200 mL of the P-rich liquid as same as that in Batch Test 1 was transferred into each test reactor for chemical P precipitation tests under no light condition. The initial pHs were adjusted to 7.4, 8.2, 9.0, and 9.8 with 0.1 moL/L HCl or 1.0 moL/L NaOH, respectively. The pH values were set according to the pH range obtained from Batch Test 1.

(4) Batch Test 4: P uptake by PAOs under different pH conditions

Restated, to minimize the effect of P precipitation on aerobic P uptake by PAOs, the anaerobic P release was conducted by using the modified synthetic wastewater (with no addition of Ca^{2+}, Fe^{2+}, and trace metals) under pH7.4 in this batch test. 10.8 g wet granules and

189.2 mL of the obtained P-rich liquid were added into each reactor for aerobic P uptake under no light conditions. The pHs in the five test reactors were controlled at 7.4, 8.0, 8.6, 9.2, and 9.8, respectively by the pH controller with 0.1 mol/L HCl or NaOH during the entire aeration period.

(5) Batch Test 5: Growth of microalgae with granules as the sole substrate

10.8 g wet granules from the mother photo-SBR at the end of aeration were cultivated in 189.2 mL DW under 280 $\mu mol \cdot m^{-2} \cdot s^{-1}$ illumination for 48 h, in which the granules were the only materials (or substrates) with no control of pH.

2.2.3 Calculations and data analysis

In the Batch Tests (2) and (4), considering the change of volume due to the evaporation and/or the addition of NaOH or HCl for pH control, the concentration of PO_4^{3-}-P measured was corrected according to Eq. (2-1),

$$C_{cP} = \frac{C_{iCl,Na}}{C_{mCl,Na}} C_{mP} \quad (2\text{-}1)$$

where C_{cP}, C_{mP}, and $C_{mCl,Na}$ are the corrected PO_4^{3-}-P concentration, the measured PO_4^{3-}-P, and the measured ion Cl^- or Na^+ concentration at *t* h, respectively. The $C_{iCl,Na}$ is the initial Cl^- or Na^+ ion concentration (at 0 h), namely the Cl^- or Na^+ ion concentration before the pH adjustment.

The pseudo-first order (PFO, Eq. (2-2)), pseudo-second order (PSO, Eq. (2-3)), and intra-particle diffusion (IPD, Eq. (2-4)) models were used to understand the kinetics and reveal the rate-controlling step of P uptake, in which the nonlinear fitting method was used to analyze datum through the "Solver add-in" on the excel application of Microsoft Office 365. In addition, the chi-square (χ^2) value was calculated to identify the best-fit model, in which a low χ^2 value denotes little difference between the experimental and model data (Tran et al., 2017).

$$PFO\ model: q_t = q_e(1 - e^{-k_1 t}) \quad (2\text{-}2)$$

$$PSO\ model: q_t = q_e^2\ k_2\ t/(1 + q_e k_2\ t) \quad (2\text{-}3)$$

$$IPD\ model: q_t = k_p\sqrt{t} + C \quad (2\text{-}4)$$

where q_e (mg/g-MLVSS) and q_t (mg/g-MLVSS) are the amounts of the removed P from liquid at equilibrium and sampling time *t* (min), respectively; k_1 (1/min), k_2 (g/(min·mg)) and k_p ($mg/(min^{0.5} \cdot g)$) are the rate constants of the PFO, PSO and IPD models, respectively; C (mg/g) is a constant relating to the thickness of the boundary layer.

One-way analysis of variance (ANOVA) was performed by using IBM SPSS Statistics 27. The statistically significant difference was assumed at $p < 0.05$.

2.2.4 Analytical methods

Mixed liquor (volatile) suspended solids (ML(V)SS) and chlorophyll-*a* (Chl-*a*) content were determined according to the standard methods (APHA, 2012). The pH and DO in the liquid were measured by the pH controller and the DO meter (DO-31P, DKK-TOA, Japan), respectively. The concentrations of acetate, PO_4^{3-}, NO_2^- and NO_3^-, Cl^-, Na^+, NH_4^+, K^+, Mg^{2+}, and Ca^{2+} in the liquid were quantified by Ion Chromatography (SHIMADZU, Japan) after samples being filtered through 0.22 μm membrane filters (Wang et al., 2021). Dissolved total carbon (DTC), dissolved inorganic carbon (DIC), and dissolved organic carbon (DOC) in the liquid were measured by the TOC detector (TOC-VCSN, SHIMADZU, Japan) equipped with an autosampler (ASI-V, SHIMADZU, Japan). The EPS were extracted by using a heating method and then determined with the colorimetric methods, and microalgal taxonomy was analyzed according to a previous study (Wang et al., 2021): after being crushed and centrifuged, the liquid was used for the analysis of LB-EPS, and the residual sludge was re-suspended and treated at 80°C for 30 min for quantification of TB-EPS. Briefly, the total DNA extraction from granules was performed by using the PowerMax ®Soil Kit (QIAGEN GmbH, Germany). The hypervariable regions of the microalgal 23S rRNA gene and the bacterial 16S rRNA gene were amplified with the specific primer pairs (microalgae: P23SrV-1F 5'-GGACAGAAAGACCCTATGAA-3' and P23SrV-1R 5'-TCAGCCTGTTATC CCTAGAG-3'; Bacteria: 338F 5' -ACTCCTACGGGAGGCAGCA-3' and 806R 5'-GGACTACHVGGGTWTCTAAT-3'). High-throughput sequencing was performed on the PCR products after purification and quantification on the Illumina MiSeq PE300 platform. The microbiome sequencing data were analyzed on the free online platform of Majorbio Cloud Platform (www.majorbio.com).

2.3 Results and discussion

2.3.1 Anaerobic P release from algal-bacterial AGS

Anaerobic P release was assessed under no light, pH 7.4, and addition of synthetic wastewater. It was observed that the DO concentration decreased rapidly to below 0.2 mg/L within 5 min and was stably maintained at a very low level (Fig. 2-3). During the initial 30 min, P concentration linearly rose at a P release rate of about 16.24 ± 0.91 mg/(g-MLVSS·h), much higher than 0.22 - 7.90 mg/(g-VSS·h) obtained from WWTPs (Zhang et al., 2011). This observation indicated that the activity of PAOs was well remained at a relatively high level in the algal-bacterial AGS. During the later period of the anaerobic phase, the P concentration

slightly increased and finally reached approximately 44 mg/L. The obtained P concentration was slightly higher than other reported concentrations (19 - 40 mg/L) of algal-bacterial and bacterial AGS systems (Wang et al., 2021), but significantly lower than that (120 mg/L) as Zhang and coworkers (2015) reported in the bacterial AGS system for enhanced biological P removal. Being similar to the observations by Zhang et al. (2015) and Wang et al. (2021), Ca^{2+} concentration was not decreased during the anaerobic P release period (data not shown), indicating no Ca-P precipitates formation under the test pH 7.4 condition. In this study, the top 3 microalgal taxonomies were identified as *unclassified_p__Cyanobacteria* (15%), *Trebouxiophyceae* (3%), and *Betaproteobacteria* (0.06%), with the top 3 bacterial taxonomies being *Alphaproteobacteria* (53%), *Gammaproteobacteria* (17%), and *Bacteroidia* (13%) at class level, respectively (Fig. 2-4). At family level, the identified taxa with photosynthesis property were Leptolyngbyaceae (15%), *Chlorellaceae* (3%), and *Pseudanabaenaceae* (0.1%) (Fig. 2-4). The less relative abundance of *Actinobacteria* (1%) and *Betaproteobacteria* (0.06%) may be the major PAOs in the algal-bacterial AGS (Nancharaiah et al., 2016). These results imply that PAOs play important roles in P removal in this mature algal-bacterial AGS system, especially under no light conditions.

2.3.2 Aerobic P uptake by algal-bacterial AGS under different test conditions

(1) Typical aerobic P removal by algal-bacterial granules (Batch Test 1)

During the aerobic P uptake period (Fig. 2-5A), the P concentration in the liquid sharply dropped from the initial 44 mg/L to 11 - 16 mg/L at the 90th min, then gradually decreased to 5.4 - 6.7 mg/L at the end of the test under different light intensities. All the experimental results were well fitted to the three models with $R^2 \geq 0.9$, in which the PFO model with a relatively lower χ^2 value showed higher suitability. Among the three kinetic models, the IPD model is capable to predict the rate-controlling step and reveal sorption mechanisms. In this study, the IPD model reflected two linear regions at 5 - 90 min and 90 - 240 min, respectively (Table 2-2, and Fig. 2-5B), indicating a diffusion rate-controlling process with two-step mechanisms. The P uptake by the algal-bacterial granules is essentially an active bioaccumulation process under the aerobic phase during wastewater treatment with alternating anaerobic/aerobic processes, which differs from the mass transfer of particle adsorption processes initiated from the outside of particles. It is proposed that the mass transfer of PO_4^{3-} mainly follows the consecutive five stages including bulk diffusion, film diffusion, IPD, surface attachment on cells (PAOs), and active transport across the membrane (Chojnacka, 2010; Tran et al., 2017). Among the 5 stages, bulk diffusion and surface attachment are generally very quick (Mohan et al., 2004; Tran et al.,

2017); and the film diffusion may dominate the system under poor mixing with small particle size and diluted adsorbate concentration (Mohan et al., 2004). In this study, the rate-controlling step could be ascribed to the IPD since the test system was well mixed due to the aeration. On the other hand, the mass diffusion in different size pores may result in multi-linearity in the IPD model (Allen et al., 1989; Sun and Yang, 2003). Yang et al. (2020) found that the algal-bacterial AGS possesses high porosity including micropores and macropores, thus the two linear regions may be associated with the macropore and micropore diffusion, respectively. During the 5 - 90 min aeration, PO_4^{3-} inside the granules may rapidly attach on the surface of cells and transfer to the cells (PAOs) binding on the macropores and micropores. Firstly, the macropore diffusion or the first linear step dominated the P removal process, accounting for 64 - 75% of total P removal. As macropore diffusion diminished, the PO_4^{3-} ions slowly transferred to the surface of cells via micropores, or the second linear region (90 - 240 min) appeared. As seen, chemical precipitation needs to be considered as one of the main driving forces for P removal under 280 and 560 $\mu mol \cdot m^{-2} \cdot s^{-1}$ conditions due to the high pH values and decreased Ca^{2+} concentration (Figs. 2-5C and D). However, there is no significant difference ($p > 0.05$) in P concentrations under the different light conditions tested in this study (Fig. 2-5A) although the P removal driving force changed, which can be explained by the same rate-controlling step of IPD. Seen from Table 2-2, the P uptake process during the last 150 min aeration was relatively slow due to the much lower k_p values, leading to a high P concentration remaining in the liquid at the end of the experiment. Minimization of IPD limitation may improve P removal in the algal-bacterial AGS.

Interestingly, with the increase of the illuminance from 0 to 560 $\mu mol \cdot m^{-2} \cdot s^{-1}$, the photosynthetic O_2 production by microalgae was promoted as the DO concentration was increased from 8.07 to 8.29 mg/L with DIC being decreased from 32.63 ± 0.78 to 17.72 ± 0.20 mg/L at the end of the test (Fig. 2-5E). Taking the no significant change in P uptake into consideration, this observation suggests that the promoted microalgae metabolism may contribute little to P removal in the algal-bacterial AGS system under the test conditions. However, much difference was noticed in the liquid pH under the different light intensities, among which a stronger light intensity resulted in a higher liquid pH. At the end of the test, the liquid pH increased from pH 8.7 under the 0 $\mu mol \cdot m^{-2} \cdot s^{-1}$ condition to pH 9.8 under the 560 $\mu mol \cdot m^{-2} \cdot s^{-1}$ condition (Fig. 2-5C). In addition, NO_3^--N was detected about 9 - 10 mg/L while NH_4^+-N and NO_2^--N were not detectable under all the test conditions. This observation implies that the conversion (nitrification or assimilation) of nitrogen was not a key factor for the

different pH variations. In these tests, except for the different light intensities applied, the other operating conditions were the same for the four reactors. Therefore, the different results can be attributable to the different photosynthetic efficiency in each reactor. HCO_3^- ions are the main inorganic sources for microalgae growth under weak alkaline conditions (Gonçalves et al., 2017). According to Eq. (2-5), the bulk liquid pH would be elevated if more CO_2 are used by microalgae under a stronger light intensity condition. (Gonçalves et al., 2017). According to Eq. (2-5), the bulk liquid pH would be elevated if more CO_2 are used by microalgae under a stronger light intensity condition.

$$HCO_3^- = CO_2 + OH^- \quad (2\text{-}5)$$

This speculation was also supported by the decreased DIC concentration in the liquid with the increase of light illuminance (Fig. 2-5E). The much low DIC concentration in the liquid under high light intensity directly indicated the potential of algal-bacterial AGS for reduction of CO_2 emissions. In addition, it was noticed that the variation of DOC concentration in the liquid was not significant, implying that the organics probably generated by microalgae might be attached on the granules instead of being released into the liquid.

Along with the increase of liquid pH under stronger light illumination, a more decrease in Ca^{2+} concentration in the liquid was detected. Under 0 and 90 $\mu mol \cdot m^{-2} \cdot s^{-1}$ conditions, the decrease of Ca^{2+} concentration was not so significant as the liquid pH was lower than 8.9. This observation is in agreement with Zhang et al. (2018) who noticed little chemical P removal occurred when pH < 9.0. However, under the 280 or 560 $\mu mol \cdot m^{-2} \cdot s^{-1}$ conditions, the decrease of Ca^{2+} concentration was noticeable, especially under 560 $\mu mol \cdot m^{-2} \cdot s^{-1}$ condition with a resultant liquid pH much > 9 (Figs. 2-5C and D), clearly indicating the formation of Ca-P precipitates. The increased pH and possible P precipitation make aerobic P removal by PAOs or microalgae more complex in the algal-bacterial AGS system. In the following experiments, it was attempted to figure out the contributions of microalgae growth, chemical precipitation, and PAOs to P removal individually in the algal-bacterial AGS system.

(2) Aerobic P uptake by microalgae (Batch Test 2)

As illustrated in Fig. 2-6A, during the initial 4 h, the P concentration was gradually increased to 55.77 ± 7.36 mg/L under the light condition of 560 $\mu mol \cdot m^{-2} \cdot s^{-1}$, while it was maintained almost unchanged under lower illumination conditions. As mentioned before, no Ca^{2+}, Fe^{2+} and trace metals that can precipitate P were added in the synthetic wastewater applied. These results indicated that the coexisting microalgae cannot effectively lower the P concentration in the liquid but were capable to help release P from granules into the liquid in

the algal-bacterial AGS system. On the other hand, the unchanged P concentration implied that the contribution of adsorption (irrespective of the chemical, physical or biological one) is not significant to P removal in the algal-bacterial AGS system. During the subsequent 44 h aerobic process, the P concentration in the liquid was not decreased but gradually increased under all the test light intensities. Moreover, a higher light intensity induced more P release, and the P concentration was detected up to 132.88 ± 4.29 mg/L after operation for 48 h under the 560 $\mu mol \cdot m^{-2} \cdot s^{-1}$ condition, in which approximately half of P in granules were released. As pointed out by Lopez et al. (2006), the internal storage products (polyP, poly-β-hydroxyalkanoates (PHAs) and glycogen) of PAOs may be utilized by cells to generate maintenance energy during long-time starvation in the AS process, which may account for the release of P under no light condition. On the other hand, the higher light intensity may induce a stronger alkaline condition locally in granules due to the high photosynthetic efficiency, which was supported by the less NaOH requirement for pH maintenance under the high light intensity conditions (Fig. 2-6B). Taking the simultaneous release of K^+ and Mg^{2+} ions along with P release (data not shown) into consideration, it was deduced that polyP may be hydrolyzed as a protective response to the alkaline stress (Pick et al., 1990).

It was worth mentioning that Chl-*a* content in granules varied from the initial 5.09 ± 0.23 to 4.65 ± 0.19, 6.42 ± 0.17, 6.10 ± 0.05, and 4.97 ± 0.10 mg/g-MLVSS under 0, 90, 280, and 560 $\mu mol \cdot m^{-2} \cdot s^{-1}$, respectively. Namely, Chl-*a* content as the main index for microalgae biomass reflected a decreasing trend under the strongest light condition in this study, most probably attributable to the photoprotection in response to photoinhibition under that strong light intensity. The photoinhibition of microalgae can generally reduce the photosynthetic capacity under an intense illumination condition. In response to photoinhibition, microalgae may reduce their chlorophylls content as a protection mechanism to maintain the photosystem structure (Giacometti and Morosinotto, 2013; Sousa et al., 2013). Interestingly, with the increase of light intensity, the increase of MLVSS was detectable (Fig. 2-6C), and the NaOH consumption for maintaining pH decreased (Fig. 2-6B), suggesting that the utilization of inorganic carbon by microalgae was not declined under the inhibited synthesis of Chl-*a* or reduced Chl-*a* content in the case of strong light conditions.

(3) Aerobic P removal via chemical precipitation (Batch Test 3)

The contribution of chemical precipitation to P removal may occur when pH is higher than 8.0 in microalgae systems (Gonçalves et al., 2017) It was found that the pH was higher than 8.0 in the algal-bacterial AGS system even under no light conditions (Fig. 2-5C). During the

chemical P precipitation tests, irrespective of the lower pH of < 9 in which P precipitation may not occur (Zhang et al., 2018), P and Ca^{2+} were simultaneously decreased in the bulk liquid with the gradual increase of pH (Figs. 2-7) resulting from aeration under the initial pH of 7.4 and 8.2 conditions. When the initial pH was adjusted to 9.0 or 9.8, P was rapidly precipitated with Ca^{2+} and Mg^{2+} during the pH adjustment period. During the subsequent aeration period, the P concentration presented a slight increase which may be attributed to the decreased pH in the liquid (Fig. 2-7B). In the Ca^{2+}-, Mg^{2+}-, P-containing solution, $Ca_5(PO_4)_3OH$, $Ca_3(PO_4)_2$, $MgHPO_4 \cdot 3H_2O$, and $Mg_3(PO_4)_2 \cdot 8H_2O$ may be the main precipitates at pH 9 - 11 (Çelen et al., 2007). As expected, strong linear correlation relationships of P against Ca^{2+} ($R^2 = 0.9829$) and Mg^{2+} ($R^2 = 0.8950$) were obtained under all test pH conditions (Figs. 2-7E and F), with molar ratios of $\Delta Ca/\Delta P = 1.0457$ and $\Delta Mg/\Delta P = 0.5232$. On the other hand, the composition of the actual P-rich liquid was complex. A slight decrease (1 - 2 mg/L) in NH_4^+-N indicated the possible formation of struvite, and SMP or LB-EPS may aggregate with Ca-P precipitates as seed crystals and adsorb more P. However, the EPS content was very low in the P-rich liquids, and no significant difference was detected before and after precipitation. Therefore, the roles played by SMP may be more significant during a long-term operation rather than the short-term tests in this study. Considering the P removal amount via precipitation in the whole aerobic P removal (Figs. 2-7), it was inferred that the P removal by PAOs might be inhibited to some extent under a strong illuminance.

(4) Aerobic P uptake by PAOs (Batch Test 4)

After minimizing the effects of microalgae and P precipitation on P removal, pH reflected a great impact on aerobic P uptake by PAOs as shown in Fig. 2-8A. The P uptake efficiency was significantly enhanced from 87% to 98% when the liquid pH was increased from 7.4 to 8.0, while it was decreased to 87% when the pH was further elevated to 8.6. The P uptake efficiency by the algal-bacterial AGS was deteriorated to 41% with the liquid pH being further increased to 9.8. Moreover, a strongly negative and linear relationship ($R^2 = 0.9723$) was observed between P uptake efficiency and pH ranging from 8.0 to 9.8 (Fig. 2-8A). Oehmen et al. (2005) noted that a high external pH of approximately 8 (including anaerobic phase and aerobic phase) was beneficial for PAOs over glycogen-accumulating organisms (GAOs), resulting in a higher P removal compared to the pH control at neutral in the CAS-based enhanced P removal systems. In addition, similar to the observation in this study, they also noticed a slight decrease in P uptake rate when the external pH was increased from 8.0 to 8.5 in the batch experiments. This phenomenon suggests that the bioactivities of PAOs would be adversely impacted under higher

pH > 8.6 conditions like pH 9.2 and pH 9.8 in this study, which was supported by the IPD kinetic fitting results (Fig. 2-8B). In the tests, the P removal process can be still well fitted by the PFO and PSO models with high R^2 > 0.9 at pH 7.4 - 9.2, with slight deterioration being observed at pH 9.8 (Table 2-3). The IPD model fitting showed higher suitability under all the test pH conditions in terms of the χ^2 value. There are two linear regions under pH 7.4, 8.0, and 8.6 conditions (Fig. 2-8B). k_p was determined as 0.8871 mg/(min$^{0.5}$·g) within 5 - 90 min under the best pH 8.0 condition, which was higher than those obtained under other conditions. The increase of pH may greatly lower the activity of PAOs, the main contributors to P removal under the test conditions, leading to a lower inner driving force for P uptake by the granules. Thus, the rate constant k_p decreased with the increase of pH from 8.0 to 9.8 (Table 2-3). Especially, micropore diffusion became not significant when the pH was elevated up to 9.2, resulting in one linear region during the whole P removal process. Furthermore, it was speculated that the P removal was not limited by diffusion due to the lower activity of PO_4^{3-} transport across the membrane by PAOs under high pH conditions (pH 9.2 and 9.8). This finding was also supported by the worse fitting results from the PFO and PSO models under high pH conditions, suggesting the change of P removal mechanisms.

2.3.3 Contribution of the coexisting microalgae to aerobic P uptake

In this study, the positive contribution of microalgae assimilation to a lower effluent P concentration was not detected irrespective of different light conditions. In addition, no direct evidence was found to support the P assimilation by the coexisting microalgae from the bulk liquid. The bacterial AGS is generally rich in P content ranging between 19 and 150 mg/g (Cassidy and Belia, 2005; Lin et al., 2003). The total P content in the algal-bacterial AGS was about 37.10 ± 0.16 mg/g-MLSS in this study, slightly higher than the P content in the algal-bacterial granules reported by Zhao et al. (2018). Therefore, the coexisting microalgae might prefer to utilize the local P in the solid (granules) for their growth under the test conditions in the algal-bacterial AGS. This was supported by Batch Test 5, in which Chl-*a* content in the granules was detected to increase by 9 ± 2% in DW accompanied with the release of P from the solid part. However, the sources of P utilized by microalgae may be dependent on carbon/nitrogen availability, light intensity and availability, and/or microbial communities, which needs more in-depth research. It was worth mentioning that the removal of total inorganic nitrogen was not enhanced with the increase of light intensity in this study, while its potential for CO_2 emission reduction was significant.

On the other hand, the contribution of chemical P precipitation cannot be ignored, which

may become a primary P removal pathway under high pH conditions. In this study, the contribution of chemical precipitation on P removal was estimated up to 45% during the aerobic P removal phase under 560 $\mu mol \cdot m^{-2} \cdot s^{-1}$ condition. In the bacterial AGS system, nitrification and aerobic P uptake may result in pH decrease during the aerobic phase, while aeration might increase the liquid pH due to the stripping. However, in the algal-bacterial AGS system, microalgae metabolism may trigger a high pH in the bulk liquid via consuming inorganic C, which would finally weaken the carbonate buffer system. As a response, bacteria may produce some organic acids to resist the high alkaline condition. Moreover, the variation of the microbial community should be considered during the long-term operation of the system. On the other hand, the inhibition to PAOs activity under a high pH condition may lead to less CO_2 release, which possibly further increases liquid pH under the strong light condition. Although pH can be controlled lower than 9 through lowering light intensity, the pH inside the granules tends to be higher than that in the bulk liquid (Lemaire et al., 2008). Furthermore, excessive precipitates in granules are not beneficial for granular stability and activity (Lee et al., 2010). Considering the long-term stable operation and sustainability of the algal-bacterial AGS process, the system pH should be maintained at an appropriate level (pH 8.0 in this study). In this context, the introduction of CO_2 containing exhaust gas to buffer pH and sequester CO_2 may be a promising way.

The expected promotion on P uptake by PAOs via photosynthetic O_2 was not highlighted in this study, mainly attributable to the aeration operation. In this study, the DO concentration reached 8.7 mg/L at an aeration flowrate of 0.35 L/min under no light condition (Fig. 2-5C), which is enough for aerobic P uptake or nitrification. Thus, the effect of photosynthetic O_2 was not significant in this study. More in-depth studies are needed on the photosynthetic O_2 as an alternative to the aeration. On the other hand, aeration is an effective way to provide shear force for the stable granule structure while mechanical mixing seems not so efficient for granulation (Lee et al., 2010). Ji et al. (2020b) reported a good P removal performance in a non-aerated microalgal-bacterial granular system during a short-term test. However, they didn't address the contribution of chemical P precipitation and granular stability. Therefore, the balance point among pH, light intensity, aeration intensity, etc. should be researched in the followed-up experiments, which is vital for the design and operation of the algal-bacterial AGS system for its practical application.

It is worth noting that the kinetic process of P uptake is controlled by IPD including macropore and micropore diffusion, in which more than half of P can be quickly removed

during the macropore diffusion stage. In order to enhance P removal in the granule system, how to improve the IPD becomes crucial. In this study, the average diameter of the test granules was about 1.59 ± 0.37 mm, much larger than the minimum value of granules (0.2 mm) (de Kreuk et al., 2007). Therefore, it's possible to enhance P uptake by cultivating relatively smaller granules that can reduce the impact on the IPD (Mohan et al., 2004). On the other hand, partial separation of anaerobically released P is another option to enhance P uptake, which is expected to effectively remove the residual P during the macropore diffusion control stage and mitigate the influence of the slow micropore diffusion. A previous study (Wang et al., 2022a) reported that the successful and effective P removal can be achieved during the initial 2 h aeration when the Phostrip was applied in the algal-bacterial AGS-based photo-SBR.

2.4 Summary

The kinetic process of aerobic P removal by algal-bacterial AGS was somewhat similar to particle adsorption process, which was controlled by macropore and micropore diffusion along with the aeration. In this work, no direct evidence was found to support P assimilation by the coexisting microalgae from the bulk liquid. Strong metabolism of microalgae would elevate liquid pH even to 9.8 under 560 $\mu mol \cdot m^{-2} \cdot s^{-1}$. The high pH condition would enhance P removal through chemical precipitation. As well, it was verified that the high pH has strong negative effects on PAOs activity. Therefore, to coordinate PAOs and microalgae, the liquid pH should be carefully controlled in the next studies.

Meanwhile, this part study also found that the role of photosynthetic O_2 was not highlighted in the external O_2-supported system, in which aeration will rapidly strip O_2 and CO_2 out from the reactor. Actually, the exchange of O_2 and CO_2 between microalgae and bacteria was weakened in this system. Therefore, the photosynthetic O_2-supported system should be better for the development of algal-bacterial AGS.

Table 2-1 Operational conditions for the five batch tests in this study.

Batch test	Treatment on granules	Bulk liquor used for test	Illumination ($\mu mol \cdot m^{-2} \cdot s^{-1}$)	pH control
1	Anaerobic P release treatment with synthetic wastewater	Actual P-rich liquid	0, 90, 280, 560	No control
2	No treatment on granules	Synthetic P-rich solution with no ions and SMP that can precipitate P	0, 90, 280, 560	Maintained at pH 8.6
3	No granules	Actual P-rich liquid	0	Initial pH controlled at pH 7.4, 8.2, 9.0, and 9.8, respectively
4	Anaerobic P release treatment with the modified synthetic wastewater	Actual P-rich liquid	0	Maintained at pH 7.4, 8.0, 8.6, 9.2, and 9.8, respectively.
5	No treatment on granules	Deionized water	280	No control

Note: The test granules were sampled from the mother PSBR at the end of aeration phase. SMP, soluble microbial products.

Table 2-2 The nonlinear fitting parameters of PFO, PSO and IPD models under different light intensities.

Model	Light condition ($\mu mol \cdot m^{-2} \cdot s^{-1}$)	R^2		q_e (mg/g)	k_1 (1/min)	k_2 (g/(min·mg))	k_p (mg/($min^{0.5}$·g))		C (mg/g)		χ^2	
		5 - 90 min	90 - 240 min				5 - 90 min	90 - 240 min	5 - 90 min	90 - 240 min	5 - 90 min	90 - 240 min
IPD	0	0.9923	0.9728	-	-	-	0.7876	0.2323	-1.4654	3.9377	0.2456	0.0047
	90	0.9952	0.9630	-	-	-	0.8012	0.2214	-1.5300	4.0969	0.1659	0.0058
	280	0.9912	0.9700	-	-	-	0.7183	0.2843	-1.1359	2.8947	0.0426	0.0082
	560	0.9937	0.8987	-	-	-	0.7380	0.2422	-1.2795	3.7702	0.1595	0.0211
PFO	0	0.9965		7.6605	0.0156	-	-	-	-	-	0.0664	
	90	0.9964		7.6504	0.0159	-	-	-	-	-	0.0912	
	280	0.9976		7.1880	0.0164	-	-	-	-	-	0.0286	
	560	0.9976		7.7012	0.0148	-	-	-	-	-	0.0357	
PSO	0	0.9887		10.0561	-	0.0014	-	-	-	-	0.1994	
	90	0.9878		10.0164	-	0.0014	-	-	-	-	0.2492	
	280	0.9958		9.2880	-	0.0017	-	-	-	-	0.0953	
	560	0.9902		10.1760	-	0.0013	-	-	-	-	0.1296	

Note: IPD, intra-particle diffusion; PFO, pseudo-first order; PSO, pseudo-second order.

Table 2-3 The nonlinear fitting parameters of PFO, PSO and IPD models under different pH conditions.

Model	Test pH condition	R^2		q_e (mg/g)	k_1 (1/min)	k_2 (g/(min·mg))	k_p (mg/(min$^{0.5}$·g))		C (mg/g)		χ^2	
		5 - 90 min	90 - 240 min				5 - 90 min	90 - 240 min	5 - 90 min	90 - 240 min	5 - 90 min	90 - 240 min
IPD	pH 7.4	0.9933	0.9352	-	-	-	0.8090	0.1508	-1.1612	4.9916	0.0343	0.0050
	pH 8.0	0.9802	0.9724	-	-	-	0.8871	0.1481	-0.7332	6.2091	0.1470	0.0016
	pH 8.6	0.9870	0.9881	-	-	-	0.7608	0.2393	-1.2711	3.7648	0.2976	0.0022
	pH 9.2	0.9881		-	-	-	0.3337		-0.0659		0.0993	
	pH 9.8	0.9898		-	-	-	0.1793		0.8289		0.0285	
PFO	pH 7.4	0.9982		7.2859	0.0211	-	-	-	-	-	0.0292	
	pH 8.0	0.9924		8.3467	0.0245		-	-	-	-	0.1539	
	pH 8.6	0.9960		7.5239	0.0161	-	-	-	-	-	0.1076	
	pH 9.2	0.9752		5.0872	0.0116	-	-	-	-	-	1.1166	
	pH 9.8	0.7967		3.0626	0.0332	-	-	-	-	-	1.1409	
PSO	pH 7.4	0.9874		9.0623	-	0.0023	-	-	-	-	0.1869	
	pH 8.0	0.9881		10.0898	-	0.0026	-	-	-	-	0.1663	
	pH 8.6	0.9898		9.8029	-	0.0015	-	-	-	-	0.1787	
	pH 9.2	0.9810		6.7980		0.0015	-	-	-	-	0.7647	
	pH 9.8	0.8990		3.4784	-	0.0131	-	-	-	-	0.4419	

Note: IPD, intra-particle diffusion; PFO, pseudo-first order; PSO, pseudo-second order.

Fig. 2-1 Morphology of algal-bacterial AGS. AGS, aerobic granular sludge.

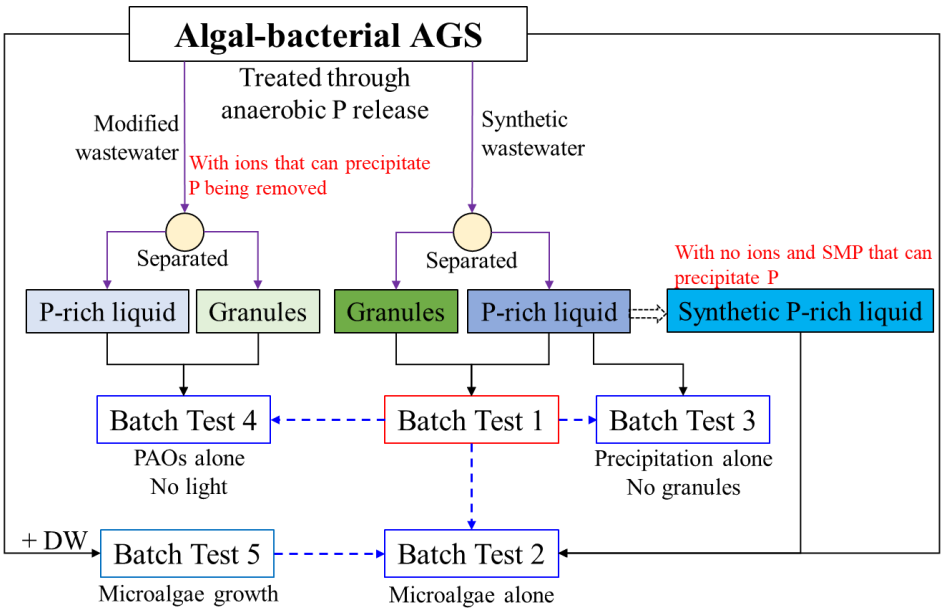

Fig. 2-2 Granules and wastewater applied for the five batch tests with MLSS of 4.9 - 5.4 g/L in this study. The blue dash lines are used to show the relationships between five batch tests. AGS, aerobic granular sludge; DW, deionized water; MLSS, mixed liquor suspended solids; P, phosphorus; PAOs, polyphosphate-accumulating organisms; SMP, soluble microbial products.

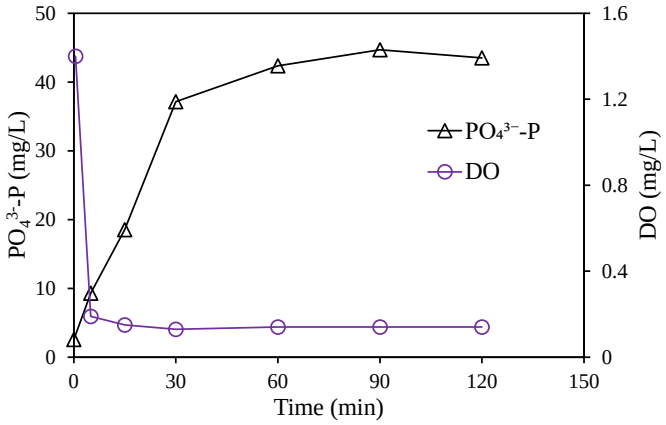

Fig. 2-3 Profiles of P release and DO level during anaerobic P release at pH 7.4 under no light condition. DO, dissolved oxygen.

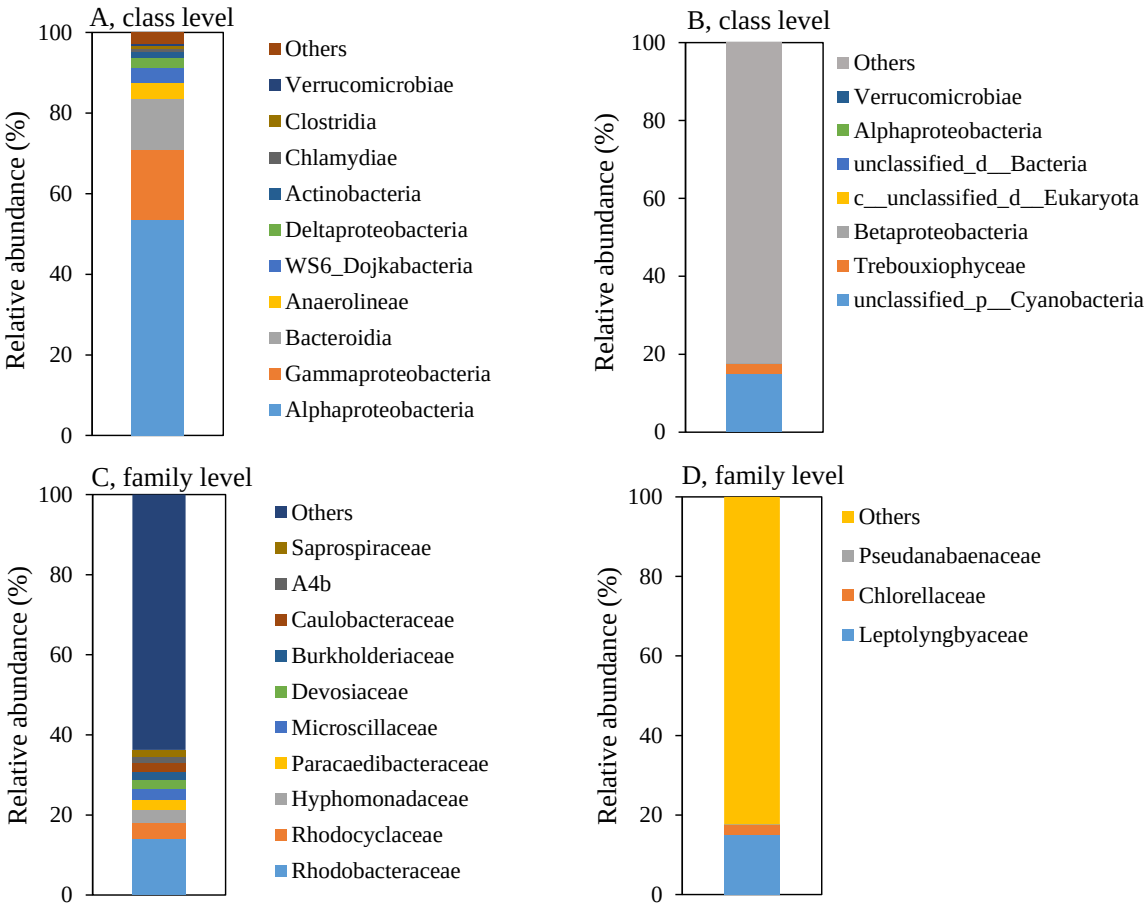

Fig. 2-4 Classification of top bacterial taxonomies (A and C) and algal taxonomies (B and D) at class and family levels.

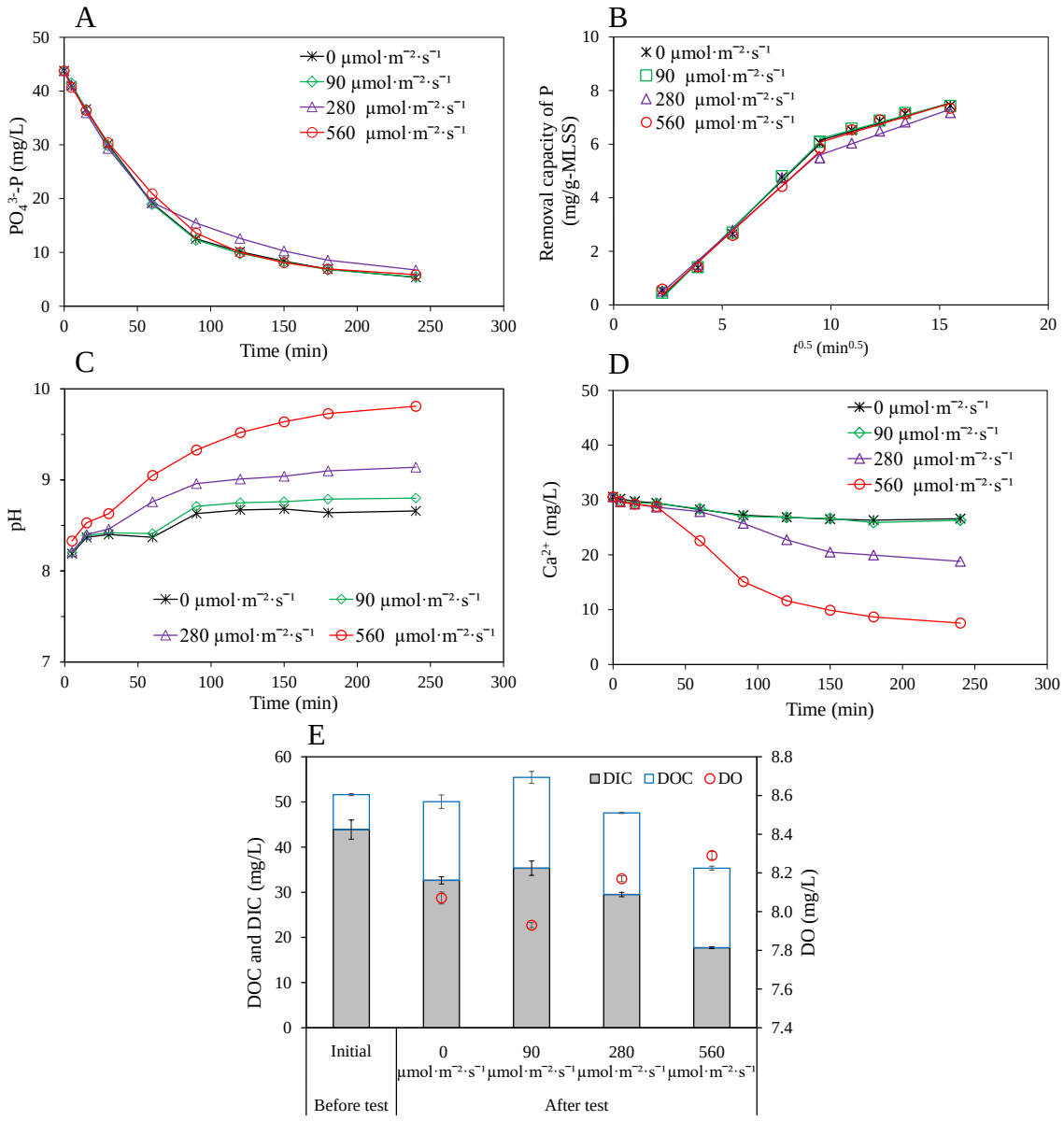

Fig. 2-5 Profiles of P concentration (A), pH (C) and Ca^{2+} concentration (D) during the aerobic P uptake by both PAOs and microalgae in the algal-bacterial AGS right after anaerobic P release (Batch Test 1). B and E illustrate multistep fitting curves of IPD model of the kinetic process of P removal and the variations of DIC, TOC and DO in the liquid before and after the test under different light illuminance, respectively. IPD, intra-particle diffusion; DO, dissolved oxygen; DOC, total dissolved organic carbon; DIC, inorganic carbon.

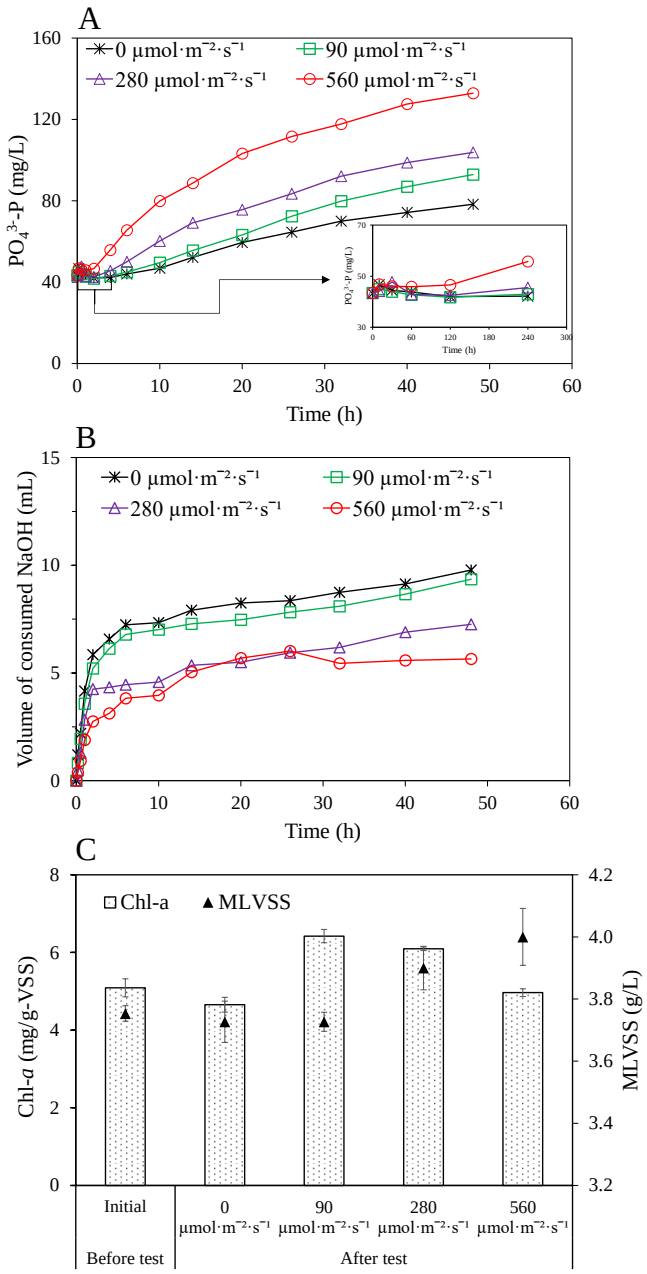

Fig. 2-6 Profiles of P concentration during the 48-h aerobic operation of the algal-bacterial AGS sampled at the end of aerobic phase (A); consumption in volume of 0.1 mol/L NaOH for pH maintaining at 8.6 with the operation (B); and the variations of Chl-*a* content and MLVSS before and after the test (C) (Batch Test 2). MLVSS, mixed liquor volatile suspended solids.

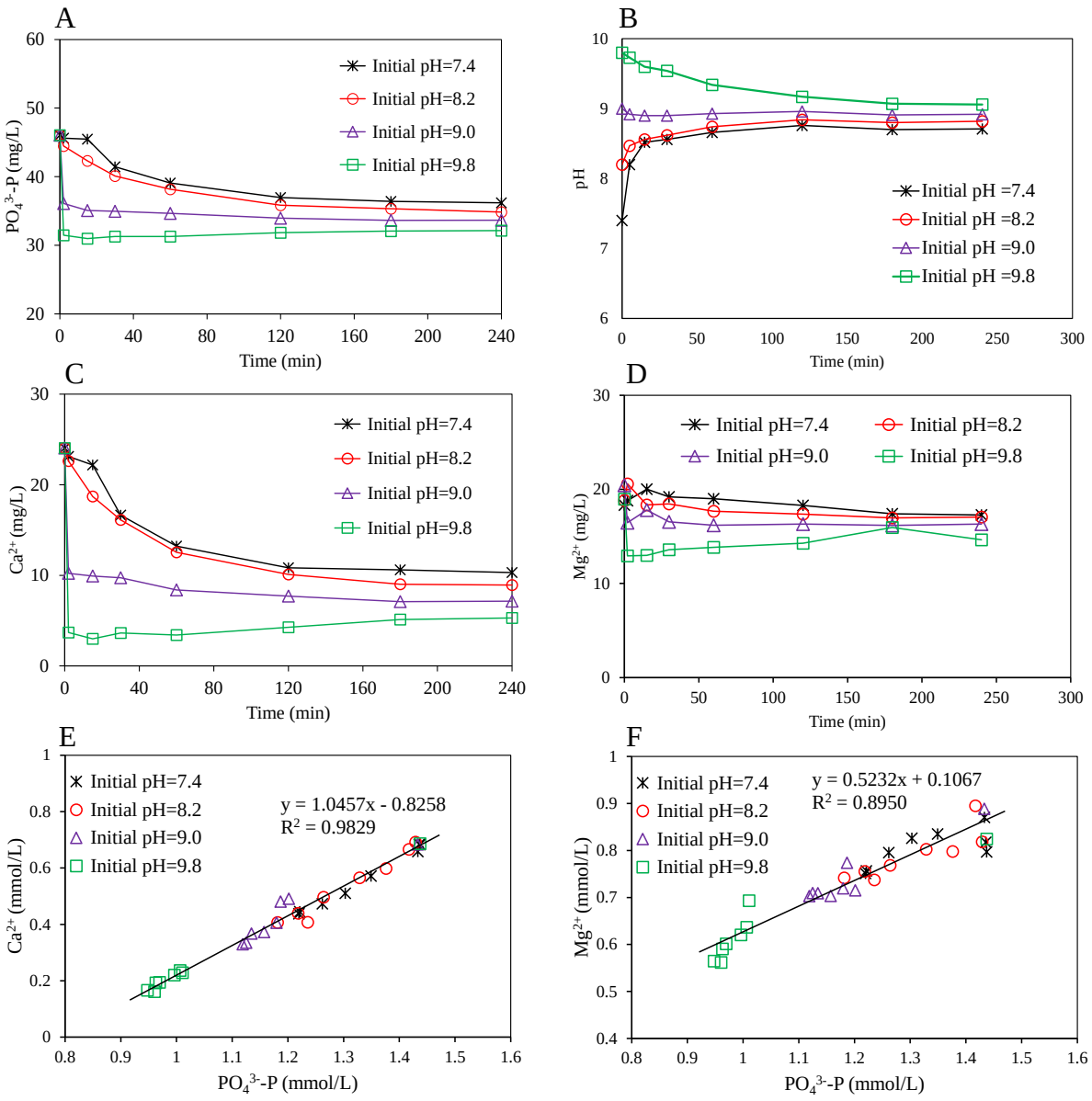

Fig. 2-7 Profiles of P concentration (A), pH (B), Ca^{2+} (C) and Mg^{2+} (D) ion concentrations under different initial pHs; and the linear relationships of PO_4^{3-}-P against Ca^{2+} (E) and Mg^{2+} (F) concentrations in the P-rich liquid during chemical P precipitation (Batch Test 3).

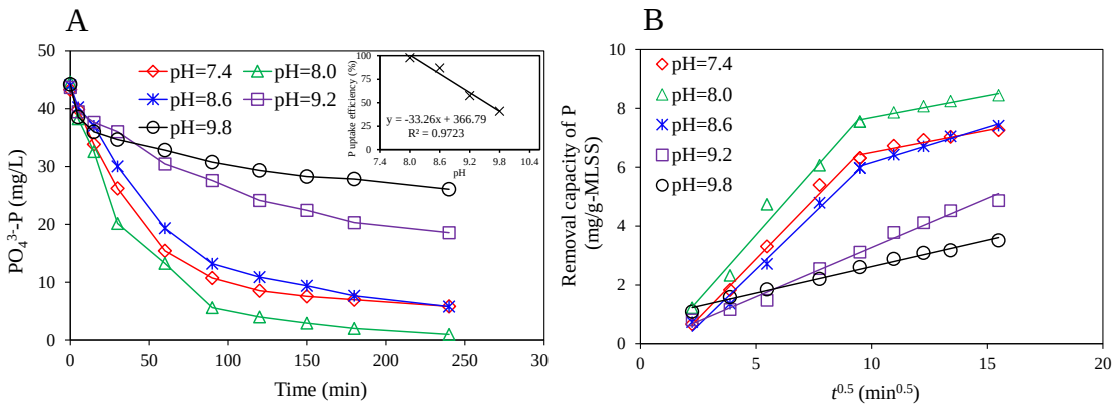

Fig. 2-8 Impact of pH on aerobic P uptake by algal-bacterial AGS fed with the modified synthetic wastewater under no light condition (A, Batch Test 4), and the corresponding IPD model fitting (B). The inset was the relationship between P uptake efficiency and pH increase from 8.0 to 9.8. AGS, aerobic granular sludge; IPD, intra-particle diffusion.

Chapter 3 Feasibility of photosynthetic O_2 as an alternative of aeration to drive the algal-bacterial AGS system

3.1 Background

As illustrated in Chapter 2, the photosynthesis is possibly a better O_2 supply way in the algal-bacterial system compared to aeration. Such operation can maximize function of photosynthetic O_2 by microalgae and extend gas retention time in liquid for adequate substance exchange between microalgae and bacteria.

As mentioned in Chapter 1.5.1, light intensity is the most essential factor to fulfill the functions of microalgae. An appropriate increase in light intensity to 200 - 400 $\mu mol \cdot m^{-2} \cdot s^{-1}$can increase microalgal activity (Muñoz and Guieysse, 2006). On the other hand, photoinhibition may occur under a stronger light condition. As noticed by Meng et al. (2019), a light intensity > 90 $\mu mol \cdot m^{-2} \cdot s^{-1}$ can yield enough O_2 and create aerobic/anaerobic zones inside the granules, while illumination ≥ 180 $\mu mol \cdot m^{-2} \cdot s^{-1}$ may inhibit nitrite oxidizing bacteria (NOB) with resultant nitrite accumulation in the reactor. Some similar negative effects were also noticed under natural sunlight conditions (Huang et al., 2015). However, other researchers reported stable nutrients removal performance under a stronger light intensity such as 280 klux (probably ≥ 200 $\mu mol \cdot m^{-2} \cdot s^{-1}$) (Wang et al., 2022a) and 500 $\mu mol \cdot m^{-2} \cdot s^{-1}$ (Trebuch et al., 2020). Most of the above algal-bacterial AGS systems were operated under an additional mechanical or air-bubbling aeration. Most of the above algal-bacterial AGS systems were operated under an additional mechanical or air bubbling aeration.

In general, the photosynthetic O_2-supported algal-bacterial AGS system requires a stronger light intensity as no additional mechanical aeration is provided. Ji et al. (2020a) tested a photosynthetic O_2-supported algal-bacterial system at 200 $\mu mol \cdot m^{-2} \cdot s^{-1}$, achieving enhanced N/P removal. Abouhend et al. (2018) realized photosynthetic O_2-supported nitrification at 150 $\mu mol \cdot m^{-2} \cdot s^{-1}$ in an algal-bacterial granule system. Up to the present, still, very limited information is available on the crucial roles of light intensity in the algal-bacterial AGS supported by photosynthetic O_2, let alone how to select an appropriate light intensity for a designated algal-bacterial AGS system.

This Chapter aimed to systematically investigate the effects of light intensity varying from 0 to 1400 $\mu mol \cdot m^{-2} \cdot s^{-1}$ on photosynthetic O_2 production, liquid pH, C and O_2 exchange, nutrients removal in the photosynthetic O_2-supported algal-bacterial AGS system with pH control. In addition, the responses of major ions involving in this system were first disclosed.

3.2 Materials and methods

3.2.1 Seed granules and synthetic wastewater

The seed algal-bacterial AGS were collected from a long-term operated mother photo-SBR treating synthetic domestic wastewater mainly consisting of 300 mg/L COD with CH_3COONa as the sole carbon source, 30 mg/L NH_4^+-N (NH_4Cl) and 5mg/L PO_4^{3-}-P (KH_2PO_4). It has been stably operated for 4 years with a working volume of 16 L and an operation cycle of about 2 h non-aeration and 4 h aeration. The other operational parameters for this mother photo-SBR including light intensity can be found in a previous study (Wang et al., 2022a).

Considering the volumetric exchange ratio of 50% applied to the mother photo-SBR and possible influencing substances (especially DIC) in tap water, the synthetic wastewater was correspondingly modified for the batch tests in this study. In the following batch tests, the influent COD, N and P were halved with Milli-Q water being used for its preparation.

3.2.2 Batch experiments

The algal-bacterial granules used for batch experiments were sampled from the mother photo-SBR at the end of aeration phase. After being harvested via glass microfiber filtration and washed with Milli-Q for three times, 40 g wet granules were added to a 500 mL glass beaker and mixed with 460 mL synthetic wastewater. During the whole batch test period, an arm stirring (Fine FL-135 N, Japan) at 100 rpm was used to suspend all the granules. After 50 min no light period (anaerobic phase), illumination was provided for 190 min by an LED light (NLSS20C, NIKKI, Japan) from the right upper side of the beaker with the light intensity on the water surface controlled at 0, 190, 330, 670 and 1400 $\mu mol \cdot m^{-2} \cdot s^{-1}$, respectively. During the no light and illumination phases, pH was controlled ≤ 8.0 by a pH controller (NPH-6900, Nissin Rika, Japan) using 0.1 mol/L HCl; at the same time DO was not controlled but monitored with a DO meter (HQ40d, HACH, USA). The MLSS and MLVSS concentrations in the batch tests were about 5.2 g/L and 4.1 g/L, similar to that in the mother photo-SBR. Average values from duplicate tests were presented in this study.

3.2.3 Analytical methods

The morphology of granules was obtained by using Leica M205 C Microscope (Leica Microsystems, Switzerland) and their average diameter was analyzed using ImageJ 1.53a. The existing form of P in algal-bacterial AGS was extracted and quantified following the Standards, Measurements and Testing (SMT) Programme (Ruban et al., 1999). The pigment contents in granules were extracted and quantified by using the methanol method (Pancha et al., 2014).

The other analytical methods were same as described in Chapter 2.2.4.

3.3 Results and discussion

3.3.1 Characteristics of the test granules

The test algal-bacterial AGS with compact structure and brown-green color had an average diameter of 0.69 ± 0.21 mm (Table 3-1), within the reported range of 0.2 - 5 mm (de Sousa Rollemberg et al., 2018). The granules contained a higher EPS content when compared to bacterial AGS (Wang et al., 2021), about 45 mg/g-MLVSS of polysaccharides (PS) and 190 mg/g-MLVSS of proteins (PN). In addition, the granules had a high P content of 32.3 mg/g-MLSS, in which the bioavailable P was about 30.6 mg/g-MLSS with a P bioavailability of 95%. The contents of microalgae or phototrophic bacteria in the granules were estimated by Chl-*a*, Chl-*b*, and carotenoid, about 5.9 mg/g-MLVSS, 1.0 mg/g-MLVSS, and 1.8 mg/g-MLVSS, respectively. The detected Chl-*a* content in the biomass was similar to that from a SBR with air bubbling (Wang et al., 2022b).

3.3.2 Effects of light intensity on DO and pH variations

Significant differences in DO concentration and pH value can be noticed during the illumination phase under different light intensities (Fig. 3-1). The DO concentration remained at nearly zero while pH exhibited a decreasing trend under no light condition, indicating little effect of ambient air on the bulk liquor DO level in this open algal-bacterial system. When a weak light of 190 $\mu mol \cdot m^{-2} \cdot s^{-1}$ was supplied, an insignificant DO elevation was detected at the end of illumination phase. While an obvious accumulation of photosynthetic O_2 was noticed at 330 $\mu mol \cdot m^{-2} \cdot s^{-1}$, resulting in a DO of 2 mg/L at the end of illumination phase; this DO level can be elevated up to 11 and 16 mg/L when the light intensity was further increased to 670 and 1400 $\mu mol \cdot m^{-2} \cdot s^{-1}$, respectively, which demonstrated a linearly increasing trend during the last 1 h. This observation agree with the previously reported mixed culture of nitrifiers and microalgae (Karya et al., 2013). As noticed, the increase of DO was limited (< 0.5 mg/L) during the initial 100 min illumination irrespective of the different stronger light intensities applied in this study. The limited DO increase during the initial 100 min illumination is probably attributable to the rapid consumption of photosynthetic O_2 by nutrient removal process.

Microalgae can utilize inorganic C including CO_2 and HCO_3^- in the liquid, resulting in the increase in liquid pH. Thus, microalgae photosynthesis inevitably elevates the liquid pH. As shown in Figs. 3-1B and C, the liquid pH started to increase once illumination was initiated, while it kept relatively stable under no light condition. Although aerobic P uptake and

nitrification are pH-decreasing processes according to N/P removal chemical reactions (Cheremisinoff, 1996; Smolders et al., 1995), some photosynthesis-induced pH increase dominated the liquid pH in this study. The liquid pH was detected to slowly rise to the set value of 8.0 under a light intensity of 190 μmol·m^{-2}·s^{-1}, which became faster with the increase of light intensity, in agreement with the changes in liquid DO (Fig. 3-1A). Since the granule functionality is closely associated with the bulk pH as shown in Chapter 2, a careful attention should be paid to pH control in this kind of photo-driven system. Seen from Fig. 3-1C, in order to well maintain the liquid pH, the acid solution (0.1 M HCl used in this study) was automatically injected to the system, indicated by the increase of Cl^- concentration in the bulk liquid. As shown, a higher light intensity suggests a more consumption of chemicals. Therefore, the cost of acid addition or alternative(s) for controlling the system pH needs to be further considered for a better design and practical application of this algal-bacterial system, targeting its sustainable management.

3.3.3 Effects of light intensity on nutrients removal

(1) C removal

During the no light period, the DOC concentration rapidly decreased due to the removal of acetate (Figs. 3-2A and C). During the illumination phase, the DOC concentration remained relatively stable under the different test light intensities, but it was not reduced to near zero, possibly indicates that some dissolved organics were formed under these conditions. Meanwhile, a slight increase in DIC was detected, attributable to anaerobic degradation of acetate by PAOs (Smolders et al., 1994). Although some DOC may be photosynthetically produced, it was not reflected in this study. In this photosynthetic O_2-supported system, some exchange of CO_2 and O_2 between microalgae and bacteria inevitably occurred. In this study, in order to clearly explain the exchange mechanisms in the liquid, photosynthetic quotient (PQ, mol O_2 produced/mol CO_2 fixed) and respiratory quotient (RQ, mol CO_2 produced/mol O_2 consumed) were adopted. For these two quotients, PQ > 1 (RQ < 1) may denote more reduced end compounds from photosynthesis or respiration (such as lipids); PQ = 1 (RQ = 1) indicates carbohydrates; and PQ < 1 (RQ > 1) suggests more oxidized compounds (such as some organic acids) in the biomass (Burris, 1981). As illustrated in Fig. 3-2B, all the DIC concentrations remained relatively stable under no light condition, implying that the exchange of O_2 and CO_2 between the liquid and ambient air may be negligible. During the light period, the DIC concentration didn't vary significantly in the initial 70 - 120 min irrespective of the increase of light intensity from 190 to 1400 μmol·m^{-2}·s^{-1}; while photosynthesis did occur as the liquid pH

was detected to increase obviously (Figs. 3-1B and C), which implied some balance between the consumption and output of inorganic C by photosynthetic organisms and bacteria. Taking little O_2 accumulation in the liquid into consideration, that is, the photosynthetically produced O_2 was immediately consumed by bacteria, it was thus inferred that the PQ was almost equal to 1/RQ under this condition. On the other hand, acetate was almost uptaken by PAOs (Fig. 3-2C) during the no light period (anaerobic phase), and PHAs (RQ < 1) may be the main metabolized substances during the oxic phase. Meng et al. (2019) detected an increased lipid content in granules during the development of algal-bacterial AGS. It was thus inferred that lipids may be the main photosynthetic product in this study, which needs further confirmation in the followed-up experiments. When the light intensity was increased to 330 $\mu mol \cdot m^{-2} \cdot s^{-1}$, the DIC concentration remained almost unchanged in the initial 100 min illumination and then slightly decreased during the subsequent period. This observation indicates that the bacterial respiration rate might decrease after 100 min illumination, possibly resulting from less available PHAs. When the light intensity was further increased to 670 $\mu mol \cdot m^{-2} \cdot s^{-1}$ and 1400 $\mu mol \cdot m^{-2} \cdot s^{-1}$, the DIC concentration was reduced by about 16% and 36%, respectively; while the duration of stable DIC concentration was shortened to 80 min under 670 $\mu mol \cdot m^{-2} \cdot s^{-1}$, which was not further shortened under 1400 $\mu mol \cdot m^{-2} \cdot s^{-1}$. This observation implies that the low microalgae content (indicated by a low Chl-*a* content) in the algal-bacterial granules may limit the photosynthetic rate. However, photoinhibition was excluded since a higher O_2 accumulation and pH increase were detected during the illumination period when increasing the light intensity (Figs. 3-1A and B). Therefore, to achieve a highly efficient CO_2 and O_2 exchange between microalgae and bacteria, a higher microalgae content should be maintained in the granules besides a suitable light intensity.

(2) N and P removal

As shown in Fig. 3-3A, a large amount of PO_4^{3-}-P was released during the no light period (anaerobic phase), corresponding to the rapid decrease of acetate (Fig. 3-2C). Such a phenomenon was due to hydrolysis of polyphosphates by PAOs, in which acetate was uptaken and converted into PHAs for aerobic P uptake (Wang et al., 2021). After the 50 min no light period, the liquid P concentration was detected relatively stable under no light condition, further confirming the negligible effect of O_2 from ambient air on the system. Although the DO concentration was lower than 0.5 mg/L during the initial 100 min illumination under all the test light conditions, the removal of P started once the illumination was initiated, indicating photosynthetic O_2 may facilitate P uptake. Clearly seen from Figs. 3-1A and 3-3A,

photosynthetic O_2 plays a crucial role in P uptake in this system. The P uptake rate was about 2.8 $mg \cdot g^{-1} \cdot h^{-1}$ under 190 $\mu mol \cdot m^{-2} \cdot s^{-1}$, which was increased to 3.8 $mg \cdot g^{-1} \cdot h^{-1}$ under 330 $\mu mol \cdot m^{-2} \cdot s^{-1}$, and reached the maximum 4.0 $mg \cdot g^{-1} \cdot h^{-1}$ under 670 and 1400 $\mu mol \cdot m^{-2} \cdot s^{-1}$, respectively. It is worth mentioning that the P uptake rate was not further increased when the light intensity was increased from 670 to 1400 $\mu mol \cdot m^{-2} \cdot s^{-1}$, while the system photosynthesis efficiency continued to increase as seen from the increase in DO concentration and liquid pH. Results from Chapter 2 find that P uptake is controlled by intraparticle diffusion in the algal-bacterial AGS. Therefore, the P uptake rate in this study was possibly limited by intraparticle diffusion under enough O_2 supply conditions. Another explanation may be due to the low microalgae content in the test algal-bacterial AGS. Although > 90% of released P can be removed under illumination at 330 - 1400 $\mu mol \cdot m^{-2} \cdot s^{-1}$, the net P removal efficiency in these batch tests were not desirable, possibly due to the sudden change of O_2 supply way from air-bubbling to photosynthetic O_2.

Similar to P removal, NH_4^+-N removal was observed under different light conditions, about 60% under 190 $\mu mol \cdot m^{-2} \cdot s^{-1}$ and nearly 100% under 330, 670, and 1400 $\mu mol \cdot m^{-2} \cdot s^{-1}$ (Fig. 3-3B). Meanwhile, along with NH_4^+-N removal, the accumulation of NO_3^-N while no NO_2^-N accumulation was detected under all the test light conditions (Figs. 3-3C and D). In previous studies, photosynthetic O_2-supported nitrification has been observed in different algal-bacterial consortia, including the mixed culture of microalgae and nitrifier (Karya et al., 2013), and algal-bacterial AGS (Abouhend et al., 2018). Nitrification may also function well at a low DO concentration of 0.5 mg/L (How et al., 2018). It is speculated that the photosynthetic O_2-supported algal-bacterial AGS system may favor the denitrification process (Abouhend et al., 2018). In the batch tests, a stable and low nitrification efficiency of 52 – 58% under 300-1400 $\mu mol \cdot m^{-2} \cdot s^{-1}$. According to the ratio of sum of NO_3^--N and NO_2^--N concentrations detected to NH_4^+-N concentration removed, also indicates simultaneous nitrification and denitrification. In addition, the contribution of microalgal assimilation to NH_4^+-N removal can't be excluded in this kind of system. However, its contribution may be limited considering the stable nitrification efficiency under 330 - 1400 $\mu mol \cdot m^{-2} \cdot s^{-1}$ and the short test duration of 190 min illumination. It is worth noting that the nitrification efficiency was about 15% under 190 $\mu mol \cdot m^{-2} \cdot s^{-1}$, meaning that more of the removed NH_4^+-N were not oxidized. This low efficiency can be hardly attributed to microalgal assimilation since a higher light intensity did not further decrease the nitrification efficiency. Bassin et al. (2011) pointed out that NH_4^+-N can be reversibly adsorbed on granules. Considering the rapid decrease and increase in NH_4^+-N concentrations in the initial

30 min of the anaerobic phase (Fig. 3-3B), it was thus inferred that some NH_4^+-N might be adsorbed on the granules but not nitrified or assimilated due to the fact of limited photogenetic O_2 production detected (Fig. 3-1A).

In the course of rapid N/P removal during the initial 100 min illumination, accumulation of photosynthetic O_2 was not significant. After this period, namely, after 60 - 90% of P and NH_4^+-N being removed, the O_2 demand by nitrifier and PAOs declined, leading to the accelerated accumulation of photosynthetic O_2. Therefore, DO can be utilized as an important indicator for a real-time monitoring and controlling of nutrients removal in this system. In addition, an appropriate light strategy via photosynthetic O_2 feedback can also save light energy input.

3.3.4 Effects of light intensity on the changes of main ions involved

The concentrations of main ions including Na^+, K^+, Mg^{2+}, Ca^{2+}, and SO_4^{2-} were also monitored in this algal-bacterial AGS system. There was no significant change in Na^+ and SO_4^{2-} concentrations during the no light and illumination periods. K^+ and Mg^{2+} as counterions of polyphosphates were released and uptaken along with the anaerobic release and aerobic uptake of PO_4^{3-} under all the test light conditions (Figs. 3-4A and C). This observation further confirmed that PAOs accounted for aerobic P uptake and anaerobic acetate removal. Meanwhile, both K^+ and Mg^{2+} showed an excellent linear relationship ($R^2 > 0.97$) with PO_4^{3-} during the illumination period. Polyphosphate is known to have an assumed stoichiometry of $(K_{0.33}Mg_{0.33}PO_3)_n$ (Barat et al., 2005). In this study, the $\Delta K/\Delta P$ molar ratios were calculated as 0.24, 0.30, 0.31, and 0.22 under 190, 330, 670, and 1400 $\mu mol \cdot m^{-2} \cdot s^{-1}$, respectively (Fig. 3-4B). The low value under 190 $\mu mol \cdot m^{-2} \cdot s^{-1}$ is probably attributable to the relatively low pH value than other light intensity conditions, while the low value under 1400 $\mu mol \cdot m^{-2} \cdot s^{-1}$ may be due to microalgae absorption of K^+. On the other hand, the $\Delta Mg/\Delta P$ molar ratios under the different test light intensities were about 0.30 - 0.33 (Fig. 3-4D) slightly deviated from the theoretical value. Mg^{2+} is a key element for chlorophyll synthesis (Ermis et al., 2020). The different light intensities applied did not bring about a significant difference in the $\Delta Mg/\Delta P$ molar ratios, although photosynthesis efficiency was observed different under different light intensities according to the DO production (Fig. 3-1A). This observation suggests the contribution of microalgae to P removal may be limited, and PAOs are still the major contributor to P removal under the test light conditions in this study. Such a stable $\Delta Mg/\Delta P$ molar ratio is different from the finding by Wang et al. (2021) in a mechanically aerated algal-bacterial AGS reactor with

uncontrolled pH. In their system both ΔK/ΔP and ΔMg/ΔP molar ratios increased with the increase of light intensity. Such differences may come from the different operational conditions including bulk pH, O_2 supply means, wastewater compositions, etc.

Interestingly, Ca^{2+} concentration was also detected to increase and decrease with the release and uptake of PO_4^{3-} in the batch tests (Fig. 3-4E). Furthermore, similar with K^+ and Mg^{2+}, Ca^{2+} showed a linear dependence on PO_4^{3-}, with $R^2 > 0.97$ and ΔCa/ΔP molar ratio = 0.07 – 0.08 under the different light intensity conditions. Ca^{2+} is generally not a counterion of polyphosphate (Schönborn et al., 2001). The low pH ≤ 8.0 adopted in this study excluded the possibility of Ca-P precipitation. Recently, Wang et al. (2023a) revealed that Ca^{2+} can exchange with Mg^{2+} during the anaerobic P release process in a bacterial AGS system. The exchange of Ca^{2+} and Mg^{2+} is thus a reasonable way to account for the release and uptake of Ca^{2+}, which may explain the slight deviation of ΔMg/ΔP molar ratios from the theoretical value. If Ca^{2+} and Mg^{2+} were considered together, the molar (ΔCa + ΔMg)/ΔP ratio was found to be about 0.36–0.39, slightly higher than 0.33. Such results imply some unclear factors influencing the release and uptake of Ca^{2+}, which needs in-depth investigation.

3.3.5 Implications and future prospects

As illustrated in Fig. 3-5, one of the major benefits brought about by photosynthetic O_2 is energy saving, namely eliminating the mechanical aeration, the most energy-intensive unit in WWTPs (Vergara-Araya et al., 2021). The reduction of C emission is another promising benefit of this system considering the increasing pressure on global warming. In addition, the highly valuable biomass resulting from the coexisting microalgae may provide some considerable values. On the other hand, this photo-driven system also brings costs from the mechanical stirring and light illumination. The former is believed more economic when compared to the mechanical aeration, while the latter should not be ignored since a relatively high light input is required in this system. To cope with this light cost issue, natural light can be properly introduced to this system thus reducing the artificial light input. Obviously, in this algal-bacterial AGS system, illumination on the one hand can facilitate C fixation and biomass production, which on the other hand may increase operational cost due to more chemicals consumption for pH control if a stronger light intensity is adopted. Thus, the selection of a suitable light intensity is crucial for meeting various targets of the system. Interestingly, the net removal of DIC indicates that the system can utilize extra CO_2 while CO_2 as acid gas may be used to neutralize the increased liquid pH, which would be promising to enhance CO_2 utilization

and reduce chemicals consumption.

3.4 Summary

Aerobic N/P removal can be simultaneously driven by photosynthetic O_2 under 190-1400 $\mu mol \cdot m^{-2} \cdot s^{-1}$ in the algal-bacterial AGS system. Efficient N/P removal and C fixation were achieved under 670 – 1400 $\mu mol \cdot m^{-2} \cdot s^{-1}$. The O_2 supply by photosynthesis showed little effect on major ions except for K^+ in the pH-controlled system. However, a stronger light intensity not only means higher energy cost but also induces higher liquid pH and O_2 accumulation. In this photo-driven system, the costs brought about by chemicals addition/light input and the benefits from C fixation/nutrient removal and aeration saving should be carefully considered for a sustainable algal-bacterial granule system.

Light intensity brings both benefits and costs to this system. Currently these benefits and costs are hardly unified and quantified. However, the selection of appropriate light intensity can be decided on individual research objective. For example, if photosynthetic O_2-supported N/P removal via bacteria is targeted, a low illumination (670 $\mu mol \cdot m^{-2} \cdot s^{-1}$ in this study) is recommended. On the other hand, if C fixation is the target, a stronger light intensity is more promising.

Table 3-1 Properties of the test algal-bacterial AGS.

Diameter (mm)	Pigments (mg/g-MLVSS)			EPS (mg/g-MLVSS)		P fractionation (mg/g-MLSS)				
	Chl-*a*	Chl-*b*	Carotenoid	PN	PS	TP	OP	IP	NAIP	AP
0.69 ± 0.21	5.9	1.0	1.8	190	45	32.3	1.2	30.9	29.4	0.6

Note: EPS, extracellular polymeric substances; ML(V)SS, mixed liquor (volatile) suspended solids; PN, proteins; PS, polysaccharides. TP, OP, IP, NAIP, and AP denote total P, organic P, inorganic P, non-apatite inorganic P, and apatite P, respectively.

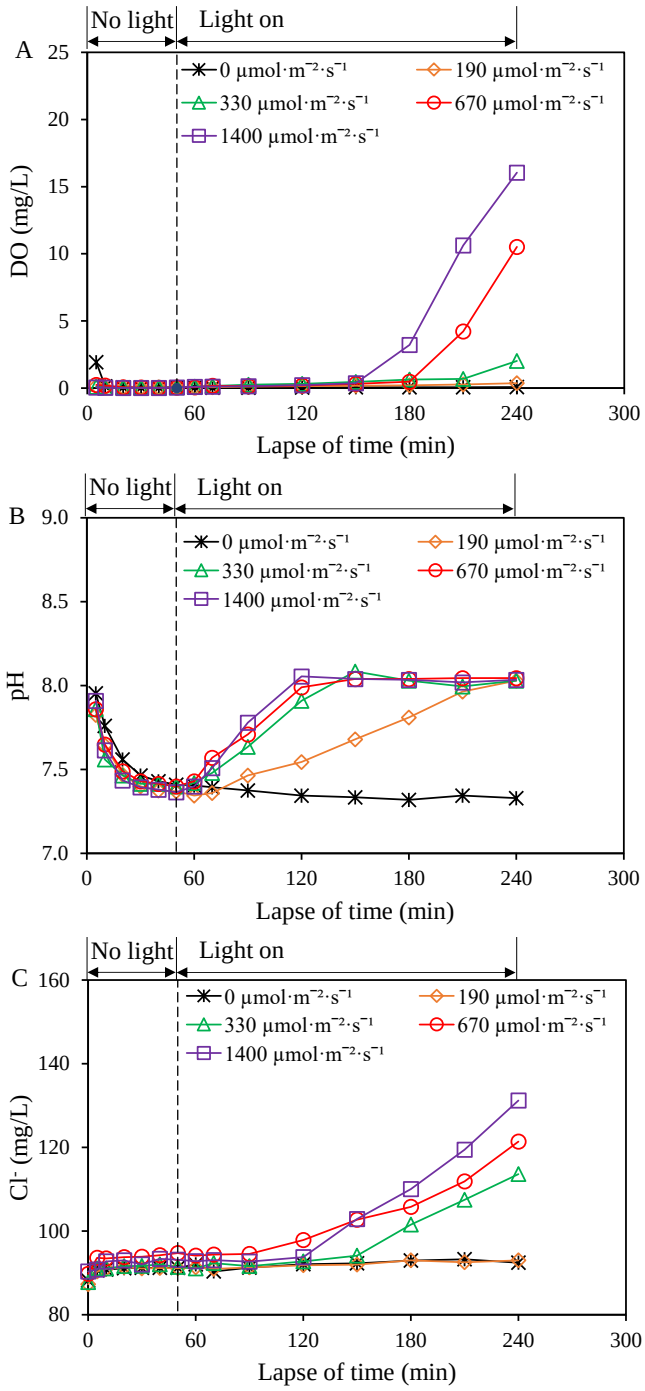

Fig. 3-1 Profiles of DO (A), pH (B), and Cl^- (C) during the 50 min no light and 190 min light-on periods under different light intensities. The increase of Cl^- concentration was resulted from the addition of 0.1 mol/L HCl for pH control. DO, dissolved oxygen.

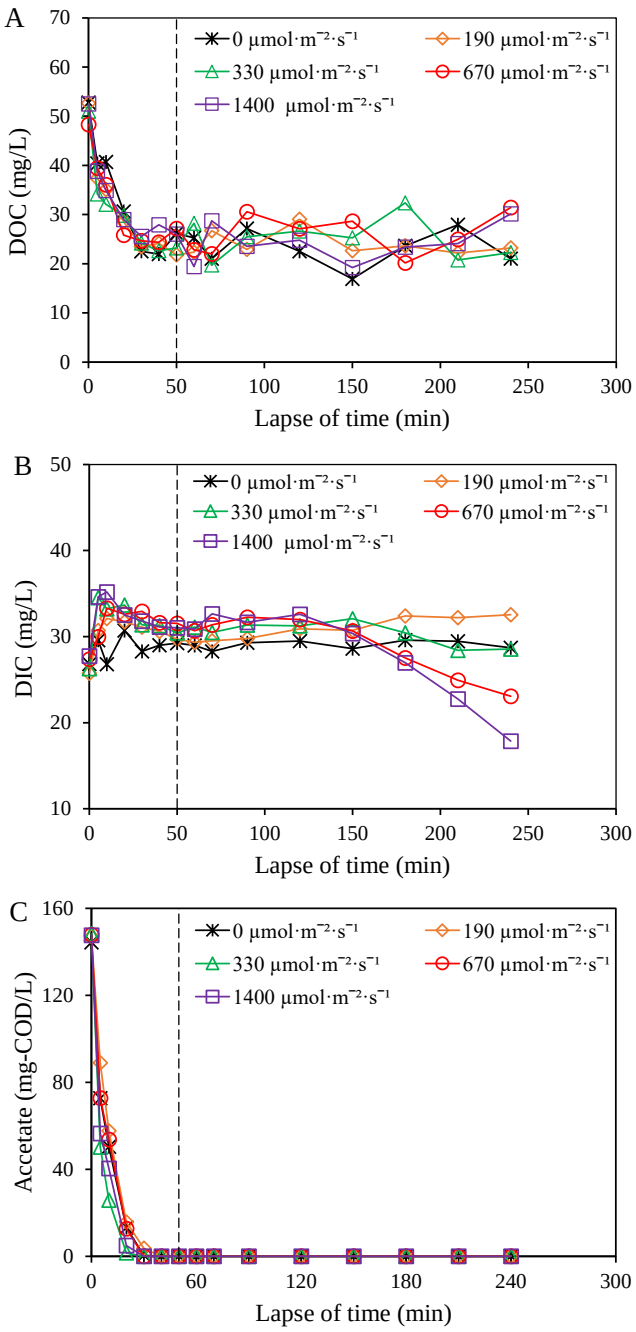

Fig. 3-2 Profiles of DOC (A), DIC (B), and acetate (C) concentrations during the test periods under different light intensities. mg-COD/L means that the acetate concentrations are expressed as chemical oxygen demand (COD) equivalent. DOC, dissolved organic carbon; DIC, Dissolved inorganic carbon.

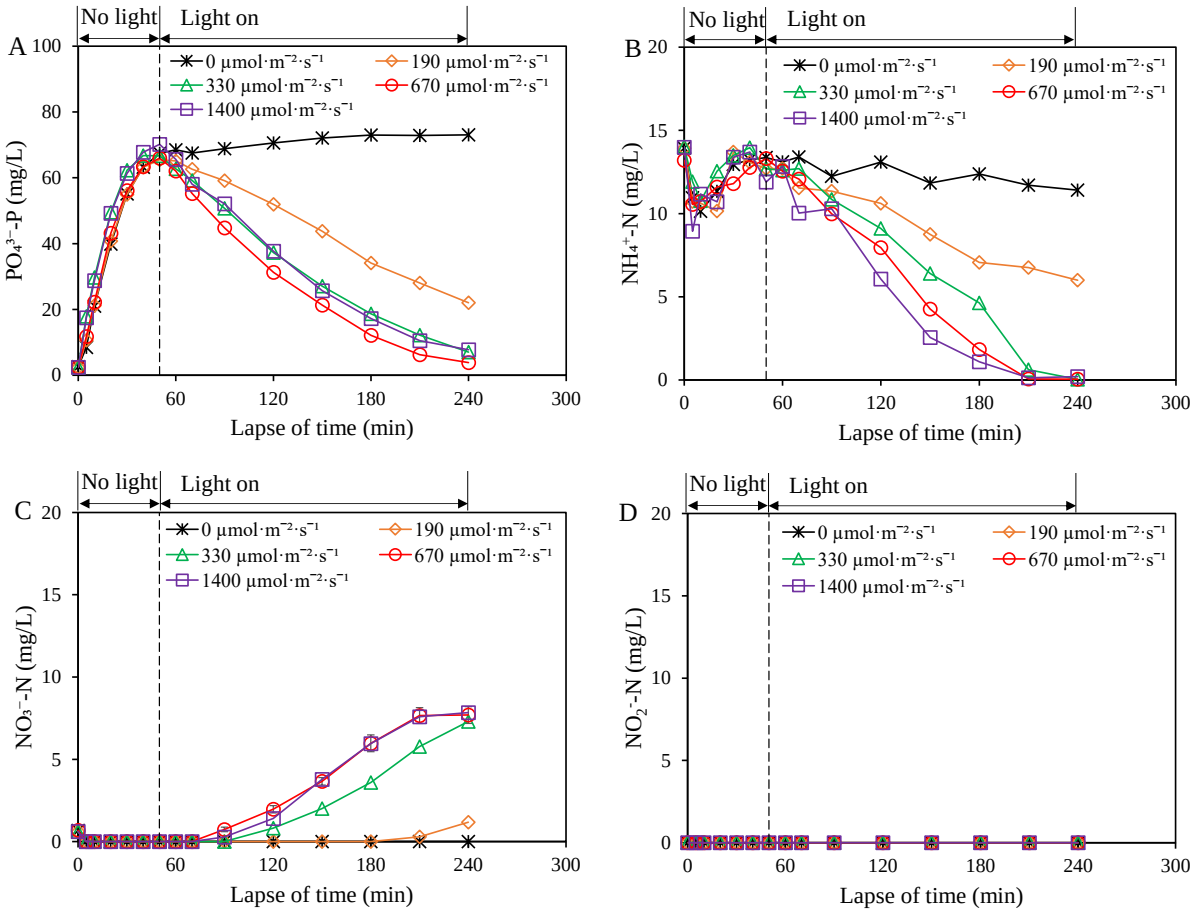

Fig. 3-3 Profiles of PO_4^{3-}-P (A), NH_4^+-N (B), NO_3^--N (C), and NO_2^--N (D) concentrations during the test periods under different light intensities.

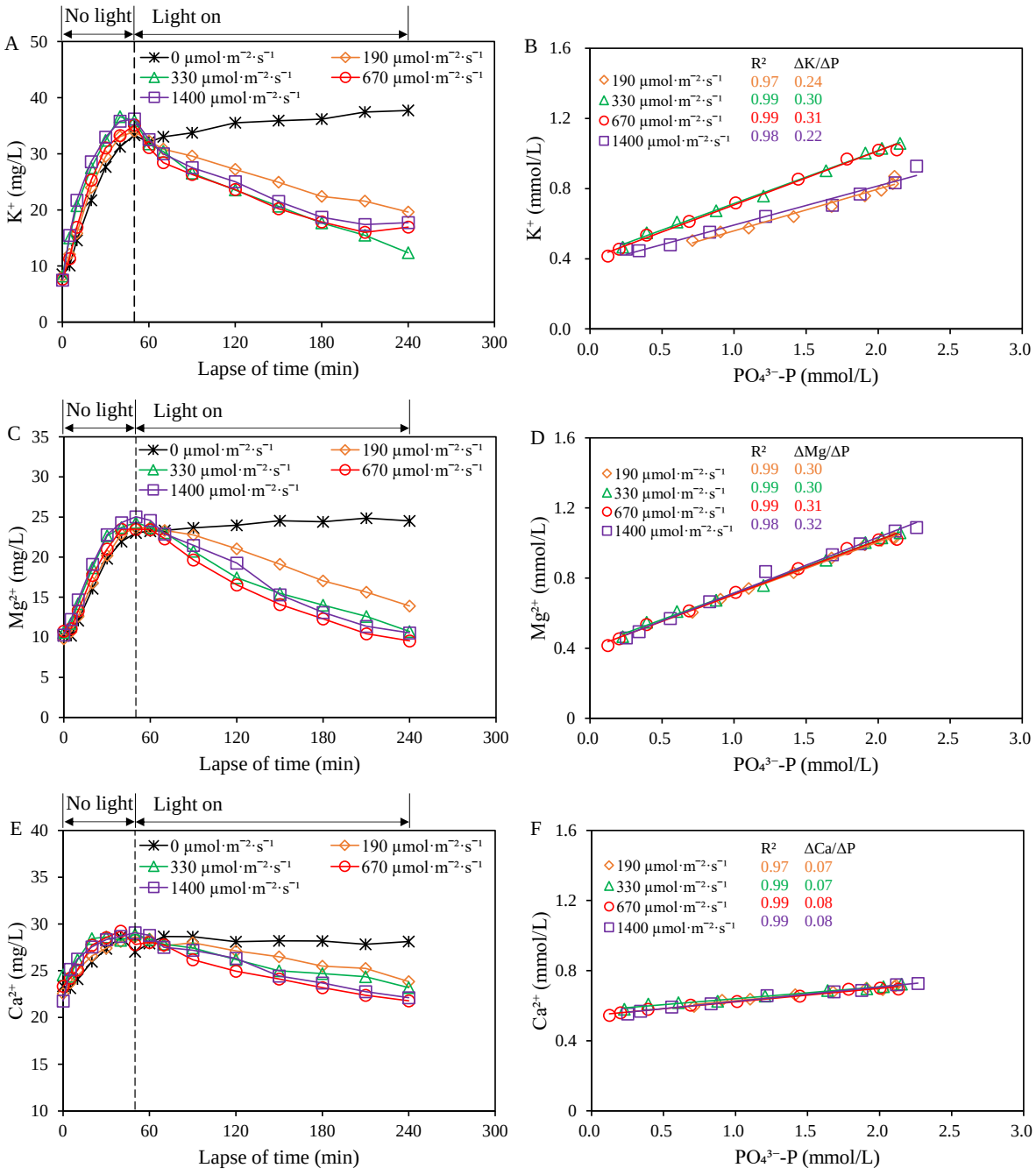

Fig. 3-4 Profiles of K^+ (A), Mg^{2+} (C), and Ca^{2+} (E) concentration under different light intensities, and plots of K^+ (B), Mg^{2+} (D) and Ca^{2+} (F) against PO_4^{3-}-P during the test period.

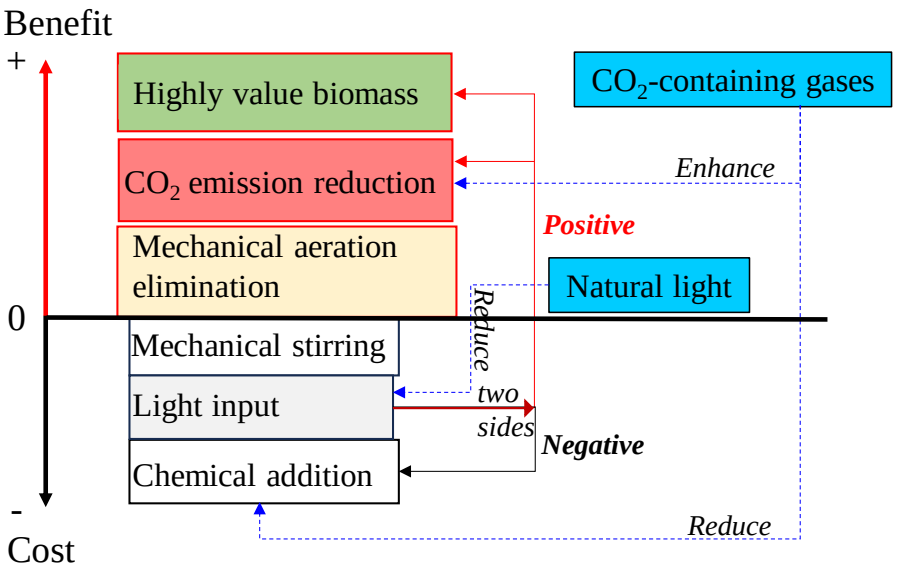

Fig. 3-5 Schematic benefits and costs due to application of photosynthetic O_2 instead of mechanical aeration in the algal-bacterial AGS system.

Chapter 4 Highly efficient nutrients removal facilitated by photosynthetic O_2 under controlled DO/pH from algal-bacterial aerobic granular sludge

4.1 Background

As illustrated in Chapter 1, good coordination between microalgae and functional bacteria can favor the sustainable O&M of algal-bacterial AGS systems. Results from Chapter 3 indicated the feasibility of C fixation and photosynthetic O_2-supported N/P removal by nitrifiers and PAOs. However, little information is available on long-term performance of this kind system with appropriate design.

In the photosynthetic O_2-supported algal-bacterial AGS system, the growth of microalgae can impact two critical parameters, namely DO concentration and pH, that are closely associated with the activities of functional bacteria under uncontrolled conditions. Therefore, this study was designed to coordinate microalgae with functional bacteria for simultaneously high efficiencies of N/P removals and C fixation in algal-bacterial AGS by adopting the following strategies: (1) pH control for enhanced growth of the functional bacteria; (2) DO control to eliminate adverse impacts of high DO concentration on phototrophs and functional bacteria for reduced light energy consumption; and (3) a shorter oxic phase to promote simultaneous nitrification and denitrification for improved N removal and reduced energy consumption. In this study, batch cycle tests, mass balance analysis, and microbial community analysis were also conducted to shed light on the mechanisms involved in C/N/P removal and the C and O_2 mass exchanges between microalgae and bacteria.

4.2 Materials and methods

4.2.1 Experimental setup of photo-SBR

The experimental photo-SBR was a glass beaker (AS ONE, Japan) with a working volume of 1.0 L (10.4 cm in inner diameter and 15.1 cm in height). Two LED lights (NLSS20C, NIKKI, Japan) were placed opposite at the right and left sides to provide a photon flux density of about 480 $\mu mol \cdot s^{-1} \cdot m^{-2}$ (about 28 klux) at the beaker wall. An overhead stirrer (OS20-S, DLAB, China) was operated at 150 rpm to ensure the mature granules in suspension in the beaker during the anaerobic and oxic phases. A pH controller (NPH-6900, Nissin Rika, Japan) was used to monitor and control the bulk pH by automatically adding 0.5 mol/L HCl when the bulk pH rose above the setpoint pH. The bulk DO concentration was also monitored and/or controlled by a DO controller (HI8410, Hanna Instruments, USA) connected to the two LED lights that were

automatically switched on or off at the DO level below or above the set range.

4.2.2 Operation of the photo-SBR

In a pre-experiment, the impact of atmospheric O_2 on aerobic P uptake and nitrification was evaluated using this open photo-SBR under the same operating conditions described in Chapter 4.2.1. The DO concentration remained below 0.1 mg/L after a one-hour anaerobic phase. The concentrations of P and NH_4^+-N were detected almost unchanged during a subsequent three-hour test period under no illumination and mechanical aeration (air bubbling). These results indicate that atmospheric O_2 had minimal influence on this open system under the operational conditions applied.

As shown in Table 4-1, the whole study comprised three Stages. During Stage I, according to the nutrient removal profiles from the pre-experiment, the open photo-SBR was operated at a 4-h cycle consisting of 50 min anaerobic phase (including 5 min feeding), 170 min illumination phase (oxic phase), 3 min settling, 5 min discharging, and 12 min idling. Among them, anaerobic, oxic, and idling durations were set to allow completely anaerobic P release, aerobic NH_4^+-N and P removal, and residual O_2 removal, respectively. The bulk pH was controlled at ≤ 8.0 during the illumination period, facilitating the activities of PAOs (Chapter 2.3.2). DO was monitored but not controlled during Stage I, and the VER was controlled at 50% (HRT=8 h). During Stage II, a feedback loop "Microalgae → Light → O_2 → DO controller → Light → Microalgae" was constructed through the DO controller to stabilize the growth of microalgae and reduce input illumination/energy consumption. The LED lights were switched on via the DO controller at DO < 3 mg/L, which were switched off at DO > 4 mg/L during the illumination phase. During Stage III, under the controlled bulk pH and DO concentration conditions, the cycle time was optimized for a higher wastewater treatment efficiency and capacity, in which the oxic and idling periods were decreased to 115 min and 7 min, respectively, leading to a shorter cycle time of 3 h (HRT = 6 h) with the other operational parameters being unchanged. The SRT was not controlled in this study, estimated as 28, 10, or 14 days during Stages I, II, or III, respectively, according to the discharged effluent biomass and sampled sludge for analysis (averagely 10 mL/d). It was worth mentioning that the operation of algal-bacteria AGS was not stopped after the experiments in this study because this proposed system was then used to examine other impact factors and some interesting phenomena to better its design and sustainable operation.

The seed algal-bacterial AGS was sampled from a mother photo-SBR treating synthetic domestic wastewater, which has been stably operated for 4 years in the laboratory. The synthetic

wastewater (pH ~ 7.4) was prepared with tap water and chemicals as previously (Wang et al., 2021). During the whole test period, the average concentrations of the primary influent nutrients and ions were as follows: DOC (with CH_3COONa as the sole organic carbon), 91.05 ± 4.22 mg/L; DIC, 27.19 ± 1.65 mg/L; TP (KH_2PO_4), 4.77 ± 0.18 mg/L; TN (NH_4Cl), 30.57 ± 1.63 mg/L; K^+, 11.74 ± 1.09 mg/L; Mg^{2+}, 11.43 ± 0.36 mg/L; Ca^{2+}, 22.89 ± 0.69 mg/L; Na^+, 158.30 ± 5.00 mg/L; Cl^-, 131.59 ± 7.13 mg/L; SO_4^{2-}, 50.25 ± 1.22 mg/L; and Fe^{2+}, 0.24 ± 0.02 mg/L.

4.2.3 Cycle and batch tests

(1) General cycle tests

During the test period, two consecutive cycle tests were performed every 2 - 4 days to check the reactor performance, with average values being reported. In addition, a 1:1 (v/v) mixture solution of influent (synthetic wastewater) and effluent from the previous cycle was used as the sample at zero min during the cycle tests.

(2) Batch tests

In the batch tests, aeration, instead of photosynthetic O_2 to maintain DO concentration at 3 - 4 mg/L, was performed to illuminate the role of phototrophic organisms. The lights were switched off during the oxic phase, but an air pump aerated the bulk liquor at a low aeration rate of 0.3 L/min. Other parameters, including stirring, were the same as the cycle tests in Chapter 4.2.3-(1).

(3) Mass balance analysis of C, N, and P

In order to analyze the fates of influent C, N, and P, mass balance analysis was performed during the stable operation from days 31 to 43. During this period, the sampled effluents were centrifuged. The liquid was used to analyze soluble C/N/P concentrations, and the solid was collected and stored at -18°C for further quantification of C/N/P contents in the effluent biomass. In addition, the granular C/N/P contents were also quantified from the sampled granules. The released C and N were calculated by subtracting C and N in the liquid and solid portions from the total input C and N amounts.

4.2.4 Calculations and statistical analysis

(1) Calculations

The calculations of (1) total emitted C or N (mg/(g-MLVSS·d)) and assimilated C or N in biomass (mg/(g-MLVSS·d)), (2) the molar ratios of ΔP/ΔC, ΔK/ΔP, ΔMg/ΔP, or ΔCa/ΔP for estimation of PAOs activity (Acevedo et al., 2012), (3) P release or uptake rates (mg/(g-MLVSS·h)), and (4) nitrification efficiency (%) were described in detail as following,

1) In the case of open systems, the total emitted C or N (T_{emi}, mg/g-MLVSS·d) and total

assimilated C or N in biomass (T_{ass} mg/g-MLVSS·d) were calculated as follows.

$$T_{emi} = T_{inf} - T_{ass} - T^{l}_{eff} \quad (4\text{-}1)$$

$$T_{ass} = T_{gro} + T_{dis} + T^{b}_{eff} \quad (4\text{-}2)$$

where T_{inf}, T^{l}_{eff}, T^{b}_{eff}, T_{gro}, and T_{dis} (unit: mg/g-MLVSS·d) are the average influent TC or TN, liquid effluent TC or TN, effluent biomass TC or TN, grown biomass TC or TN in the reactor, and the manually discharged granular biomass TC or TN, respectively.

2) The molar ratio of ΔP/ΔC, ΔK/ΔP, ΔMg/ΔP, or ΔCa/ΔP was calculated to characterize PAOs performance (Acevedo et al., 2012), which was the absolute slope value of the linear fitting obtained through plotting P concentration against 2 times acetate concentration in the initial 30 min no-light period (molar ΔP/ΔC ratio), or plotting K, Mg or Ca concentration against P concentration during the whole cycle test (molar ΔK/ΔP, ΔMg/ΔP, or ΔCa/ΔP ratio). In addition, the kinetic process of P release or uptake was quantified by Eq. (4-3),

$$P\ release\ or\ uprate\ rate\ (mg/(g-MLVSS\cdot h)) = \frac{Slope_{P-t}}{M} \quad (4\text{-}3)$$

where M is the biomass concentration (g-MLVSS/L), and $slope_{P\text{-}t}$ is the absolute slope value of P (mg/L) against time (h) within the initial 30 min of the non-illumination phase (P release) or the initial 70 min of the illumination phase (P uptake), respectively.

3) Nitrification efficiency was calculated according to Arun et al. (2021) as shown in Eq. (4-4).

$$Nitrification\ efficiency\ (\%) = \frac{Max\ NO_x^- - N}{NH_4^+ - N} \times 100 \quad (4\text{-}4)$$

where the maximum NO_x^--N is the maximum sum of NO_2^--N and NO_3^--N concentrations, and NH_4^+-N is the removed NH_4^+-N during the cycle test.

4) Calculation of power consumption for illumination

The average light intensity was about 28 klux (about 480 μmol·s^{-1}·m^{-2}) received by reactor wall. Considering the surface area of the reactor wall, the power (P, W) of lights required by light intensity was calculated as follows (RapidTable),

$$P(W) = E \times A / \eta \quad (4\text{-}5)$$

where E is the light intensity (lux), A is the square aera (m^2), and η is luminous efficacy (lm/W). In this study, E and A were 28 klux (about 480 μmol·s^{-1}·m^{-2}) and 0.0385 m^2, and η was assumed to be 90 lm/W for the LED lights. The average light on duration was 92 min every cycle during last 10 days. Finally, 36.73 kWh/m^3 was required for wastewater treatment.

(2) Statistical analysis

Paired- samples T-Test was adopted to analyze the statistical difference of datum using IBM SPSS Statistics 27. $p < 0.05$ was assumed as statistically significant difference. The linear correction coefficient was also calculated.

(3) Analytical methods

Total P and N in liquid were measured with the standard methods (APHA, 2012) after the samples were completely oxidized with persulfate. The total C and N in solid was determined by an elemental analyzer (UNICUBE, Elementar, Germany). The extraction and quantification methods of pigment contents in granules were same as those described in Chapter 3.2.3.

The Lab-Aid824s DNA Extraction kit (ZEESAN) extracted total DNA from freeze-dried sludge samples. A 2-step tailed PCR method was used to amplify 16S rRNA and 18S rRNA gene fragments from the extracted DNA using primers of 338F/806R and 1422f/1642r, respectively. The verified amplicons were subjected to paired-end sequencing on the Illumina MiSeq sequencing platform at Bioengineering Lab Co. Ltd. (Japan). The raw reads have been deposited in the NCBI Sequence Read Archive (SRA) database (Accession Number: PRJNA957041).

Other parameters have been described in Chapters 2.2.4 and 3.2.3.

4.3 Results and discussion

4.3.1 Changes in granule properties

(1) Biomass concentration, pigments, and EPS

The results shown in Fig. 4-1A indicate a rapid increase in MLVSS from 5.1 ± 0.1 g/L on day 1 to 7.1 ± 0.1 g/L on day 7 during Stage I, accompanied by a corresponding increase in Chl-*a* content from 5.3 ± 0.1 to 7.4 ± 0.5 mg/g-MLVSS (Fig. 4-1B). During Stage II, however, the MLVSS decreased to 5.1 ± 0.4 g/L (Fig. 4-1A). In contrast, the Chl-*a* content continued to increase to 12.0 ± 0.4 mg/g-MLVSS on day 13 (Fig. 4-1B), probably due to high effluent biomass and decreased inhibition of controlled DO on the growth of phototrophic organisms. In Stage III, both MLSS and MLVSS showed an upward trend, while the effluent biomass decreased and then remained stable, achieving a biomass yield of about 0.64 g-MLVSS/g-COD during the last 12 days. Despite the reduced illumination time as a result of the shortened cycle time and controlled DO, a high Chl-*a* content of 11.1 ± 0.9 mg/g-MLVSS was maintained (Fig. 4-1B). This content is significantly higher than those of algal-bacterial AGS developed under mechanical aeration conditions (He et al., 2018a; Wang et al., 2022b), but close to those of

algal-bacterial AGS developed under non-aeration conditions(Ji and Liu, 2022; J. Wang et al., 2020; Zhao et al., 2019). Additionally, the trend in Chl-*b* content was similar to that of Chl-*a* (Fig. 4-1B), while the carotenoid content showed a slight increase during Stages I and II and decreased during Stage III (Fig. 4-1B). This observation may suggest no photoinhibition to microalgae in this system, as a high carotenoid content with low Chl-*a* content is generally considered a sign of photoinhibition (Sousa et al., 2013). The variation of EPS and their components, PS and PN, are associated with the changes in granular stability. Both PS and PN contents decreased during Stage I (Fig. 4-2), which can be attributed to the rapidly growing biomass. However, they gradually increased during Stage II, which may imply that the granular stability deteriorated to some extent during Stage I while recovered during Stage II, in agreement with the variations of effluent biomass concentration (Fig. 4-1A).

(2) Granule morphology

The seed algal-bacterial AGS was nearly spherical with a compact structure and smooth surface, entangled with green microalgae and surrounded by some filamentous organisms (Fig. 4-3). The average diameter of seed granules was 1.24 ± 0.59 mm, and about 44% were smaller than 1.00 mm. Along with the operation, the granules became brushier with more significant amounts of green matter, which was also indicated by the increment of Chl-*a* content. On day 31, some brown matter appeared and intertwined with the filamentous organisms, which promoted the growth of some small new granules, increasing the percentage of granules with a diameter of < 1.00 mm. The newly grown granules were cylindrical, different from the spherical granules sampled from the mother photo-SBR, probably due to the stirring operation.

(3) Microbial community

Fig. 4-4 shows that the relative abundances of major functional bacteria kept well during the test period in this photo-SBR. *Nitrosomonadaceae* (1 - 2%) and *Nitrospiraceae* (9 - 10%), the frequently reported ammonia-oxidizing bacteria (AOB) and NOB (He et al., 2018b), remained relatively stable during the entire period, suggesting a stable nitrification process. The genera *Paracoccus* and *Pseudomonas* as typical denitrifying bacteria were detected but presented a low relative abundance of < 0.04% in this system, thus the enriched *Zoogloea* and *Acinetobacter* possibly contributed to denitrification (Rajta et al., 2020). The typical PAOs like the genus *Candidatus Accumulibacter* (Oehmen et al., 2007) were also detected at a relative abundance of 3 - 4%. These data imply the stable nutrient removal performance by the functional bacteria.

The identified eukaryotic microalgae were class Trebouxiophyceae, but their relative

abundance decreased from 7% on day 1 to 4 % on day 43 (Fig. 4-4D). Thus, the increased Chl-*a/b* and carotenoid contents (Fig. 4-1B) were probably attributable to the growth of photosynthetic bacteria, including genera *Arthronema*, *Leptolyngbya*, *Rhodobacter*, and *Oscillochloris* (Fig. 4-4C). Besides the genera *Arthronema* and *Leptolyngbya* of Cyanobacteria, the genus *Thiothrix* of Proteobacteria possibly contributed to the filamentous structure of algal-bacterial granules.

4.3.2 Changes of DO and pH, and their control strategies

During the operation of Stage I, a significant amount of photosynthetic O_2 production was detected during the illumination phase (Figs. 4-5A and C), which is sufficient for both aerobic P uptake and nitrification. The DO profile was characterized as three steps during the light-on period of Stage I: (1) DO concentration rapidly rose after initializing the illumination (Step 1); (2) DO reached a stable concentration (Step 2), during which the generated O_2 was consumed by aerobic P uptake, nitrification and/or other aerobic reactions as discussed in Chapters 4.3.4 and 4.3.5 (Please note that the DO concentration was elevated by 1 - 3 mg/L along with the operation (Fig. 4-5A), possibly resulting from the increased Chl-*a* content); and (3) at Step 3, the DO concentration linearly increased to a level up to supersaturation. In this step, the photosynthetic O_2 was much more than the O_2 consumption needed by the system. Such a too-high DO concentration may affect P uptake by PAOs (Carvalheira et al., 2014) and N removal by denitrifiers (Mosquera-Corral et al., 2005). Thus, the DO concentration in the subsequent oxic phases during Stages II and III was controlled at 3 - 4 mg/L via the DO controller and LED lights on/off, which was set slightly higher than the stable DO concentration (Step 2) at the end of Stage I, as a higher DO concentration may allow microalgae to fix more inorganic C. During Stages II and III, the DO concentration increased faster to the set DO range (3 - 4 mg/L) in Step 1 (Fig. 4-5C) than in Stage I due to their higher Chl-*a* contents. With adequate DO control, some balance might be established among Chl-*a* content, DO concentration, and illumination. As such, the increased Chl-*a* content promotes photosynthetic O_2 production to increase DO; the rapid increase of DO activates the DO controller to switch off the LED lights, limiting the phototrophs growth (increase in Chl-*a* content). This resulted in a relatively stable Chl-*a* content during Stage III (Fig. 4-1B).

During the anaerobic phase, the pH slightly decreased (Fig. 4-5D), probably due to the combined effects of influent wastewater and anaerobic decomposition. Once the illumination was initiated, the pH linearly rose to the controlling point of 8.0 due to CO_2 consumption by photosynthesis. During Stages I and II, the time needed for pH rising to the setpoint (pH 8.0)

were gradually shortened (Fig. 4-5D), owing to the increased phototrophs growth indicated by Chl-*a* content. During Stage III, the principal pH rise was completed in 30 min (Figs. 4-5D), attributable to the granules' relatively stable and high Chl-*a* content (Figs. 4-1B). Then the pH gradually decreased with DO fluctuations after reaching the set DO. In this proposed system, the illumination phase is dominated by three biological reactions: photosynthesis by phototrophs, aerobic P removal by PAOs, and (de)nitrification by (de)nitrifiers, respectively (Fig. 4-4). For simplicity, microbial assimilation was not taken into consideration in these bioreactions. The following reactions summarize the major biological processes as described by Gerardi (1997) and Smolders et al. (1995).

$$\text{Photosynthesis: } CO_2 + H_2O \rightarrow CH_2O + O_2 \quad (4\text{-}6)$$

$$\text{P uptake: } 0.87CH_{1.5}O_{0.5} + O_2 + 3.23\,H_3PO_4 \rightarrow 3.23HPO_3 + 0.87CO_2 + 3.87\,H_2O \quad (4\text{-}7)$$

$$\text{Nitrification: } 0.5NH_4^+ + O_2 \rightarrow 0.5NO_3^- + H^+ + 0.5H_2O \quad (4\text{-}8)$$

$$\text{Denitrification: } 0.625\,CH_2O + 0.5\,NO_3^- + 0.5\,H^+ \rightarrow 0.25\,N_2 + 0.625CO_2 + 0.875\,H_2O \quad (4\text{-}9)$$

P uptake and nitrification are pH-decreasing processes, while photosynthesis and denitrification are pH-increasing processes. Seen from the above reactions, one mmol CO_2 corresponds to one mmol O_2 production during photosynthesis; One mmol O_2 utilized by nitrifiers can generate one mmol H^+ or 0.87 mmol CO_2 by PAOs. If all the produced NO_3^- is denitrified, one mmol O_2 consumed would produce 0.50 mmol H^+ and 0.63 mmol CO_2. In this reaction, the contribution of produced protons is much more significant than CO_2, considering the very low dissociation constant of carbonic acid, $pK_{a1} = 6.37$ (25°C). Therefore, the decrease in pH is mainly attributable to nitrogen removal during the illumination phase. Restated, in the present photo-SBR system, the increased pH by photosynthesis based on the unit O_2 produced was lower than the decreased pH by nutrient removal based on the unit O_2 utilized. As such, if the pH controller controlled the LED lights to maintain liquid pH, the DO increase by photosynthesis based on a unit pH elevated will be higher than the DO decrease by nutrients removal based on a unit pH decreased, which has been supported by an increasing DO concentration during the oxic phase.

4.3.3 C removal

(1) Changes in C species and their removal

The photo-SBR system demonstrated an excellent and stable DOC removal efficiency of 90 ± 3% during the entire test period (Fig. 4-6A). The average effluent DOC was 8.95 ± 2.78 mg/L, close to the effluents from bacterial or algal-bacteria AGS systems (Zhao et al., 2018). This observation is attributable to the dissolved organic substances excreted by the coexisting

microalgae and/or bacteria since the sole organic carbon (sodium acetate) was largely removed within the initial 30 min during the anaerobic phase (Figs. 4-6C and E). During Stages I and II, the effluent DIC concentration remained low at 17.44 ± 3.56 mg/L, lower than the influent DIC concentration. When the illumination duration was shortened during Stage III, the effluent DIC concentration slightly increased, very close to the influent DIC, suggesting less contribution of microalgae to the DIC removal.

Under the mechanical aeration operation, an insignificant increase of DIC was detected (Fig. 4-6D), in which DIC from acetate degradation may be stripped into the air by aeration operation. In the photosynthetic O_2 condition, the DIC concentration decreased during the illumination period (Fig. 4-6C), demonstrating the great potential of the algal-bacterial AGS system for GHGs emission reduction.

(2) C assimilation and CO_2 emission reduction

As expected, the TC content in granules increased from 405.7 mg/g-MLVSS on day 1 to 460.3 mg/g-MLVSS on day 43. The average C assimilation rate was 35.03 mg/(g-MLVSS·d) during the last 12 days (Table 4-2). To estimate the contribution of phototrophs to C fixation in the algal-bacterial AGS, an empirically stoichiometric formula of $CH_{1.78}O_{0.36}N_{0.12}P_{0.01}$ (Boelee et al., 2014) for phototrophs and a ratio of 56.31 mg-MLVSS/mg-Chl-*a* (Samiotis et al., 2021) were used. As shown in Table 4-2, the contribution of phototrophic organisms to C sequestration was about 23.28 mg/(g-MLVSS·d), with a CO_2 fixation capacity of 85.36 mg-CO_2/(g-MLVSS·d), which accounted for about 66% of total C assimilation by the algal-bacterial AGS, higher than 46% in an algal-bacterial system as shown in Table 4-3.

The CO_2 emission from this algal-bacterial granule system was only 0.25 kg-CO_2/kg-COD (without consideration of other direct and indirect CO_2 emissions), much lower than 74 - 80 kg-CO_2/kg-COD in AS based SBR system (Lee et al., 2008), and also lower than 0.58, 0.68, 0.76, and 0.97 kg-CO_2/kg-COD from the four full-scale A^2O, AO, oxidation ditch, and SBR-based WWTPs (Bao et al., 2015), indicating its great potential of reducing GHGs emission. It was estimated that 14% of input DTC was released, while the biomass assimilated 52% of input DTC. In this study, the contribution of microalgae to C fixation was limited due to the short illumination duration of 80 - 104 min under the DO control strategy applied. In order to achieve more reduction of CO_2 emission from this photo-SBR, the DO control range is a crucial factor which needs more in-depth studies.

4.3.4 N removal

(1) N removal and nitrification efficiency

As shown in Fig. 4-7, effective N removal was achieved through the photosynthetic O_2 supply. The effluent TN concentrations rapidly decreased during Stage I and kept relatively stable during Stage II, possibly associated with the relatively low DO concentration compared to the near-saturated DO concentration in the mother photo-SBR. The effluent NO_3^--N concentration followed the trend of the effluent TN, while the effluent NH_4^+-N and NO_2^--N concentrations were negligible during these two stages. As a result, the TN removal efficiency was increased from 62% on day 1 to 79 ± 2% during Stage II, with NH_4^+-N removal of nearly 100% during Stages I and II.

An interesting phenomenon was observed when the illumination duration was shortened during Stage III. The photo-SBR experienced a deterioration period and then recovery of N removal. The effluent NH_4^+-N concentration increased first and then decreased, while the effluent NO_3^--N concentration decreased first and remained low. In addition, the effluent NO_2^--N concentration slightly increased. As such, the NH_4^+-N removal efficiency dropped to 77% on day 27 and then recovered to nearly 100%, while TN removal efficiency kept at 81 ± 7% during Stage III.

A competitive NH_4^+-N removal rate was obtained during the entire test period (Fig. 4-6B), average 1.25 ± 0.30 mg/(g-MLVSS·h), much higher than 0.89 ± 0.05 mg/(g-MLVSS·h) of a bacterial AGS system under an aerobic/oxic/anoxic mode (He et al., 2016). On the other hand, the nitrification efficiency was almost halved from 68% to 35% during Stage I. It remained at 36 ± 2% and 20 ± 12%, respectively during Stages II and III, significantly lower than 80% by the mother photo-SBR. When taking the relatively stable TN removal efficiency into consideration, it can be inferred that more N might be emitted and/or assimilated in the biomass during the operation.

(2) Main contributors to N Removal

As illustrated in the cycle tests (Figs. 4-8A and B), NH_4^+-N removal was rapidly initiated once the LED lights switched on, while NO_3^--N was correspondingly produced during Stages I and II. In Stage I, N removal was completed in 2 h illumination, in correspondence with the stable DO concentration (Step 2 in Fig. 4-5C). The above results indicated a photosynthetic O_2 driving aerobic nitrification process, which was evidenced by the stable AOB and NOB abundance in granules (Fig. 4-4). On the other hand, the generated NO_3^--N and low NO_2^--N production cannot cover the decreased amount of NH_4^+-N. What is more, the effluent NO_3^--N

decreased with the operation. Such an increasing N loss may imply its complex N removal pathways including microbial assimilation, simultaneous nitrification and denitrification, anammox, and/or ammonia precipitation (such as struvite formation).

The TN content in the seed granules was about 92.0 mg/g-MLVSS, higher than 56.7 ± 11.3 mg/g in the AS (Chen et al., 2021) used for the initial seed sludge for granulation in the mother photo-SBR. In addition, the granular N content did not increase with the increase in Chl-*a* content, which was about 88.4 mg/g-MLVSS on day 31 and 91.4 mg/g-MLVSS on day 43. According to the N balance analysis (Table 4-2), approximately 44% of input N was assimilated in biomass compared to the maximum 20% by seed granules in the mother photo-SBR from their nitrification efficiency. Such assimilation was higher than AS-based SBR system while lower than other reported algal-bacterial systems (Table 4-3), possibly due to the high simultaneous nitrification/denitrification. This significant difference is attributable to the enhanced assimilation by phototrophic bacteria indicated by the increased Chl-*a* content (Fig. 4-1B) and enriched *Arthronema*, *Leptolyngbya*, *Rhodobacter*, and *Oscillochloris* (Fig. 4-4C). The N assimilation rate was about 7.55 mg-N/(g-MLVSS·d) in this study, lower than 11 - 37 mg-N/(g-MLVSS·d) by AS with enriched nitrogen-fixing bacteria treating thermomechanical pulping wastewater (Slade et al., 2003). The N assimilation rate of phototrophs was estimated as 3.26 mg-N/(g-MLVSS·d) (Table 4-2), indicating that bacteria in this system contributed about half of N assimilation. As illustrated in Fig. 4-8D, the photosynthetic O_2 can help remove N faster with a higher N removal efficiency when compared to the mechanical aeration, suggesting less contribution of nitrifiers to N removal in this algal-bacterial AGS system. However, a similar nitrification efficiency of 14% was observed under the two O_2 supply strategies, implying that the N species assimilated by phototrophs include both NH_4^+-N and NO_3^--N since whichever N species was utilized alone by phototrophs would contribute to their difference in nitrification efficiency (Fig. 4-8D).

Simultaneous nitrification and denitrification are considered other competitive contributors to N removal since about 42% of input N was emitted from the system according to the N balance analysis. Although a low NO_2^--N and NO_3^--N during NH_4^+-N removal process may imply the possibility of shortcut denitrification during Stage III, the enriched *Nitrospiraceae* directly indicated a stable nitrite-oxidizing process. Therefore, shortcut denitrification is not considered a major N emission pathway. The low DO concentration, increasing granular size (Fig. 4-3), and short oxic time may favor denitrification in the AGS systems (Abouhend et al., 2023; He et al., 2018b; Mosquera-Corral et al., 2005) probably

accounting for simultaneous nitrification and denitrification in the present system. On the other hand, the DOC concentrations during the illumination phase were statistically ($p < 0.05$) higher than those under the mechanical aeration condition (Figs. 4-6C and D), which may be utilized as carbon sources to some extent. Thus, the relatively high phototroph content and the photosynthetically produced DOC or organic matter may favor simultaneous nitrification and denitrification.

It is worth mentioning that the removal of NH_4^+-N by ammonia precipitation (struvite) was excluded since struvite is unsaturated under the low pH value ≤ 8.0 estimated by Visual MINTEQ 3.1 software. On the other hand, during the NH_4^+-N removal process, the set DO range of 3 - 4 mg/L still maintained an oxic condition with almost no NO_2^- accumulation (Fig. 4-8). In addition, the typical anammox bacteria, such as genera *Brocadia, Kuenenia, Anammoxoglobus, Jettenia,* and *Scalindua,* were not detected in the granules (Fig. 4-4). The anammox process is thus not considered as the primary N removal pathway in this study.

4.3.5 P removal

(1) P removal efficiency and removal rate

A highly efficient P removal was achieved through photosynthetic O_2 production that supports aerobic P uptake. During Stage I, the TP removal efficiency rapidly increased from 42% on day 1 to 98% on day 7 (Fig. 4-9A), indicating that the algal-bacterial AGS quickly adapted to the new environment under the adopted pH control strategy. The controlled DO and shortened illumination time also showed little adverse impact on TP removal efficiency, which remained at 97 ± 2% and 92 ± 8% during Stages II and III, respectively.

The P release and uptake functioned well during the test period (Figs. 4-9B and C). The P uptake process was completed within 2 h illumination during Stages II and III, corresponding to the stable DO concentration (Step 2 in Fig. 4-4C); during this period, the O_2 generated by microalgae was used for aerobic P uptake and nitrification. The P release rate of the seed granules was about 27.57 mg/(g-MLVSS·h), much higher than 2.87 ± 0.29 mg/(g-MLSS·h) from the bacterial AGS (He et al., 2016) and 16.24 ± 0.91 mg/(g-MLVSS·h) from the algal-bacterial AGS system under no pH control (Chapter 2.3.1). During Stage I, the P release rate decreased quickly to 16.55 mg/(g-MLVSS·h) on day 7, accompanied by the decrease of maximum P release; this decreasing trend continued during Stage II with a lower decrease rate till day 25 (Fig. 4-9B). Finally, the P release rate remained around 10.84 ± 0.41 mg/(g-MLVSS·h) during the subsequent operation. During Stages I and II, the growth of phototrophic bacteria and higher effluent biomass (Figs. 4-1A and Fig. 4-4) possibly led to the low granular

polyP content that accounts for the decrease in P release rate. This deduction is partially evidenced by the decrease in granular NAIP content (Fig. 4-10D). In contrast, the variation of P uptake rate was insignificant, averagely 7.18 ± 0.24 mg/(g-MLVSS·h) during the entire test period. As discussed in Chapter 2, aerobic P uptake is limited by intra-particle diffusion, including macropore and micropore diffusion in the algal-bacterial AGS. Luo et al. (2014) claimed that flocculent sludge had a higher surface area than AGS. According to the morphological changes of the algal-bacterial AGS (Fig. 4-3), the granules became more significant with more filamentous matter attached along with the operation. This morphological change may increase granular surface area and improve IPD limitation, maintaining the stable granular P uptake rate under the controlled DO/pH operation conditions.

(2) P removal pathway

All the plots of ΔP against ΔC achieved high linear correlation coefficients (R^2) (Fig. 4-10A). Similar to the changes in P release rate, the molar ΔP/ΔC ratio significantly decreased during Stages I and II, implying the decreased PAOs activity in the granules (Acevedo et al., 2012). During Stage III, the molar ΔP/ΔC ratio was 0.36 ± 0.03, lower than 0.48 - 0.80 for PAOs-enriched cultures but much higher than 0 - 0.02 for GAOs-enriched cultures (Acevedo et al., 2012). Meanwhile, the genus *Candidatus Accumulibacter* of PAOs slightly decreased from 4% on day 1 to 3% on day 43 (Fig. 4-4). This observation suggests that the PAOs primarily contributing to P removal were still active in the present study.

K^+ and Mg^{2+} as the counterions of PO_4^{3-} are known to participate in anaerobic hydrolysis and aerobic synthesis of polyP at an assumed stoichiometry of $(K_{0.33}Mg_{0.33}PO_3)_n$. The increase in phototrophs abundance may change their quantitative relationship. From the cycle tests, the molar ΔK/ΔP and ΔMg/ΔP ratios were relatively stable (Fig. 4-10B), averagely 0.23 ± 0.02 and 0.28 ± 0.03, lower than the theoretical value of 0.33. This observation may support P assimilation by phototrophic organisms that result in low ΔK/ΔP and ΔMg/ΔP ratios. According to the TP removal efficiency and the assumed stoichiometry of polyP, the maximum contributions of PAOs to K^+ and Mg^{2+} reduction can be up to 7% and 4%, respectively. The latter estimation is close to the measured Mg^{2+} reduction, about 4 ± 2%, except on day 1 (Fig. 4-10B), but the former significantly deviated from the measured K^+ reduction (24 ± 11%) except on day 1. Such a deviation is probably associated with active assimilation by phototrophic organisms that require more K^+, which needs further confirmation. In the case of Ca^{2+}, besides the low pH condition, its negligible reduction in concentration may exclude Ca-P precipitation from the P removal pathway.

Fig. 4-10C presents the apparent advantage of the photosynthetic O_2 on P removal compared to the mechanical aeration due to a higher P uptake rate detected in the former. However, similar molar ratios under the two O_2 supply strategies did not support the phototrophs' P assimilation. A previous study found that microalgal P assimilation during aerobic P uptake from the liquid was negligible in the algal-bacterial AGS system. P for microalgae growth was from the solid (granules) instead of the liquid. Generally, P assimilation by phototrophs requires a long HRT. The adopted short HRT of 6 h during Stage III in the present study may not highlight the contribution of assimilation. As shown in Table 4-2, according to the estimated contribution (0.60 mg/(g-MLSS·d)) of phototrophs to P assimilation, namely 0.1 mg/g-MLSS is required for each cycle. This value is significantly lower than the anaerobically released P (5.9 ± 1.1 mg/g-MLSS based on MLSS concentration during the last 12 days' operation). This study determined the P assimilation was about 86.7% of input P with a rate of 2.08 mg/(g-MLSS·d), which were competitive to AS, AGS, and Algal-bacterial systems as shown Table 4-3. As noted in Table 4-2, the measured output TP cannot cover the input TP, probably due to TP dissolution from the effluent biomass during the collection and storage stages (for final determination).

4.3.6 Energy consumption and implications

The energy requirement by the biological treatment (especially the aeration unit) generally accounts for 50 - 70% of the total operating costs in WWTPs (Vergara-Araya et al., 2021). According to the ideal mixing energy requirement of 1.5 W/m^3 and the mixing energy of 5 W/m^3 in an example WWTP (Vergara-Araya et al., 2021), the energy consumption for only mixing applied in this study was about 5.75 Wh/m^3 during the oxic phase, significantly lower than 180 - 800 Wh/m^3 for the commonly mechanical aeration operation (Silva and Rosa, 2021). This observation implies that only mixing instead of mechanical aeration to suspend algal-bacterial granules is economically feasible. However, the energy consumption by stirring should be carefully re-examined when the reactor system is scaled up since the energy consumption may not increase linearly with the increase in system treatment capacity. On the other hand, a high electricity consumption of 36.73 kWh/m^3 by the LED lights is required, which can be replaced by natural sunlight and designed correspondingly in the followed-up research works.

The algal-bacterial AGS system is promising for C fixation and CO_2 emission reduction from WWTPs, which successfully assimilated 52% of the total input C. The fixed C estimated by the assumed formula of phototrophs (Table 4-2) can be used to produce a maximum 55 mg-

O_2 per cycle, enough to complete the high O_2 requirement by the nitrification process (35 mg-O_2, assimilated N was not counted) and aerobic P uptake process (15 mg-O_2) according to Eqs. (4-2) and (4-3) and nutrient removal performance. This observation indicates that a higher C fixation could be achieved when treating wastewater with a higher NH_4^+-N concentration that requires more O_2. In addition, the DO control by switching on/off the light reduces illumination time from 115 min to 80 - 104 min, saving 10 - 30% of light energy requirement. As noted, compared to the energy-intensive mechanical aeration, the photosynthetic O_2 is more efficient for nutrients removal as the O_2 molecules generated by the coexisting microalgae inside or on the granule surface may avoid the resistance to gas diffusion and transfer from the gas phase to liquid phase and then into the granules.

4.4 Summary

The long-term feasibility of using photosynthetic O_2 from microalgae for simultaneous aerobic nitrification and P uptake by PAOs in an algal-bacterial AGS system has been demonstrated. A low CO_2 emission was achieved at 0.25 kg-CO_2/kg-COD. The energy consumption of 5.75 Wh/m^3 for mixing required only for the proposed system is more economical than that of mechanical aeration commonly used for AGS systems. Although the additional illumination cost by artificial lights was relatively high in this study, the DO control strategy involving switching the lights on and off could reduce light energy consumption by 10 - 30%.

In a short HRT of 6 h, the coexisting microalgae in algal-bacterial AGS could photosynthesize enough O_2 production to implement nitrification and aerobic P uptake. The system achieved a highly efficient TN removal of 81 ± 7 % with an N assimilation rate of 7.55 mg/(g-MLVSS·d), mainly due to microbial assimilation and simultaneous nitrification/denitrification under the test conditions. In the proposed pH/DO-controlled algal-bacterial AGS system, PAOs dominated P removal process and exhibited high activity, as indicated by a high P release rate of 10.84 ± 0.41 mg/(g-MLVSS·h), P uptake rate of 7.18 ± 0.24 mg/(g-MLVSS·h), and a molar $\Delta P/\Delta C$ ratio of 0.36 ± 0.03, resulting in TP removal greater than 92%.

Considering the scale-up and better O&M of the proposed algal-bacterial AGS system, more in-depth research is demanded. C/N/P assimilation and removal mechanisms, contributions of microalgae/phototrophs and bacteria, light system design, the sensitivity of

CO_2 emission to DO/pH control range, and influence of influent characteristics should be further explored during the long-term operation of the algal-bacterial AGS system.

Table 4-1 Experimental conditions during the three test stages.

	Duration	pH control	DO control (mg/L)	Cycle time (h)	Hydraulic Retention Time (HRT, h)
Stage I	Days 1 ~ 7(7 d)	≤ 8.0	No control	4	8
Stage II	Days 8 ~ 13 (6 d)	≤ 8.0	3~4 *	4	8
Stage III	Days 14 ~ 43 (30 d)	≤ 8.0	3~4 *	3	6

*The DO concentration may be a little bit lower than 3 mg/L during the increase period of DO by photosynthetic O_2 production due to the delayed response of the DO controller. Solids retention time (SRT) was not controlled during the test periods.

Table 4-2 Mass balance analyses of total C, N, and P during the last 12 days' operation.

Element	Input		Assimilated in biomass			Effluent liquid	Emission [a]	Contribution of microalgae [b]
	Total	Total organic	Grown	Discharged	Effluent			
C (mg/(g-MLVSS·d))	66.87	51.50	14.22	4.68	16.13	22.44	9.40	23.28
P (mg/(g-MLSS·d))	2.40	-	1.20	0.23	0.65	0.12	-	0.60
N (mg/(g-MLVSS·d))	17.29	-	3.22	0.90	3.43	2.50	7.24	3.26

[a] Calculated as ([Input] – [Fixed in biomass] – [Effluent liquid]). [b] Estimated according to an assumed stoichiometric formula ($CH_{1.78}O_{0.36}N_{0.12}P_{0.01}$) of microalgae (Boelee et al., 2014) and the ratio (56 g/g) of microalgae's MLVSS to Chl-*a* (Samiotis et al., 2021).

Table 4-3 Comparison of C, N, and P balance in different wastewater treatment processes.

Element	Sludge and reactor	Assimilated in biomass		Effluent liquid	Emission	References
		Bacteria	Microalgae			
C (%)	Algal-bacterial AGS, SBR	23	45	14	18	This study
	Algal-bacterial AGS, closed bottle	49	41	10	-	Ji et al. (2020a)
	Algal-bacterial AGS, SBR	90		4	6	Guo et al. (2021)
	AGS, SBR	51	-	5	44	Guo et al. (2021)
	AS, SBR	33~37	-	9	54~58	Lee et al. (2008)
N (%)	Algal-bacterial AGS, SBR	25	19	14	42	This study
	Algal-bacterial AGS, closed bottle	50	25	16	9	Ji et al. (2020a)
	Algal-bacterial AGS, SBR	92		8	-	Guo et al. (2021)
	AGS, SBR	62		8	30	Guo et al. (2021)
	AS, SBR	15~17	-	30~34	49~55	Lee et al. (2008)
P (%)	Algal-bacterial AGS, SBR	62	25	5	-	This study
	Algal-bacterial AGS, closed bottle	86		14	-	Ji et al. (2020b)
	Algal-bacterial AGS, SBR	97		3	-	Guo et al. (2021)
	AGS, SBR	94	-	6	-	Guo et al. (2021)
	AS, SBR	50~77	-	-	23~50	Lee et al. (2008)

Note: AGS, aerobic granular sludge; AS, activated sludge; C, carbon; N, nitrogen; P, phosphorus; SBR, sequencing batch reactor.

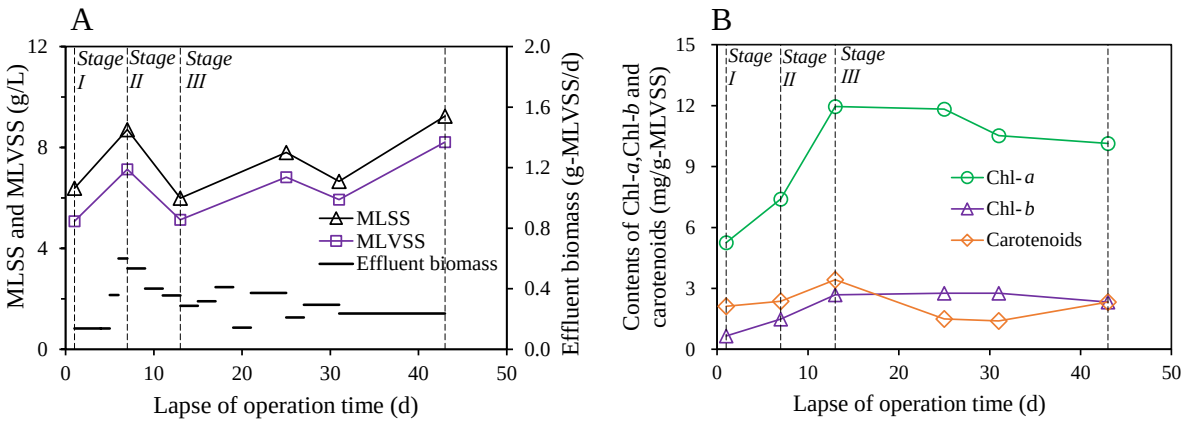

Fig. 4-1 Variations of biomass concentration (A) and pigments content (B) during the three operational stages. MLSS, mixed liquor suspended solids; MLVSS, Mixed liquor volatile suspended solids.

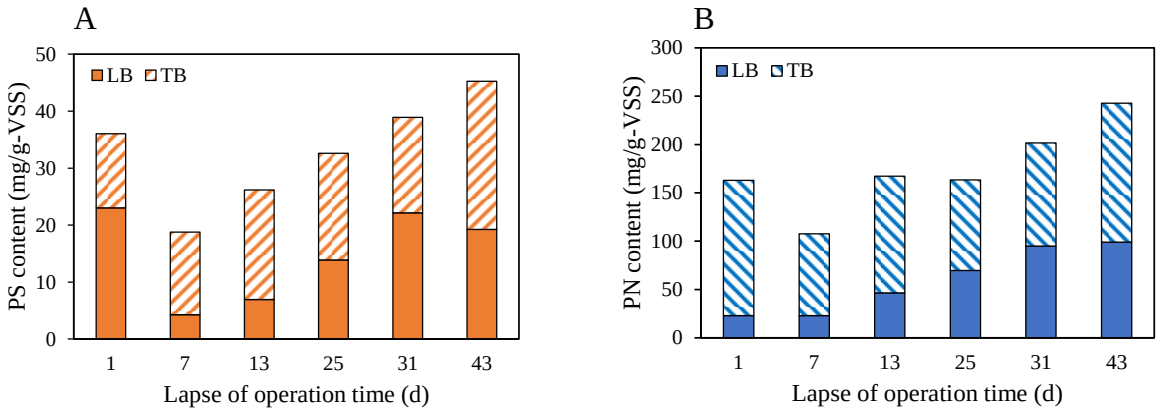

Fig. 4-2 Changes of granular polysaccharides (PS, A) and proteins (PN, B) in extracellular polymeric substances (EPS) during the three operational stages. LB, loosely bound; TB, tightly bound; VSS, volatile suspended solids.

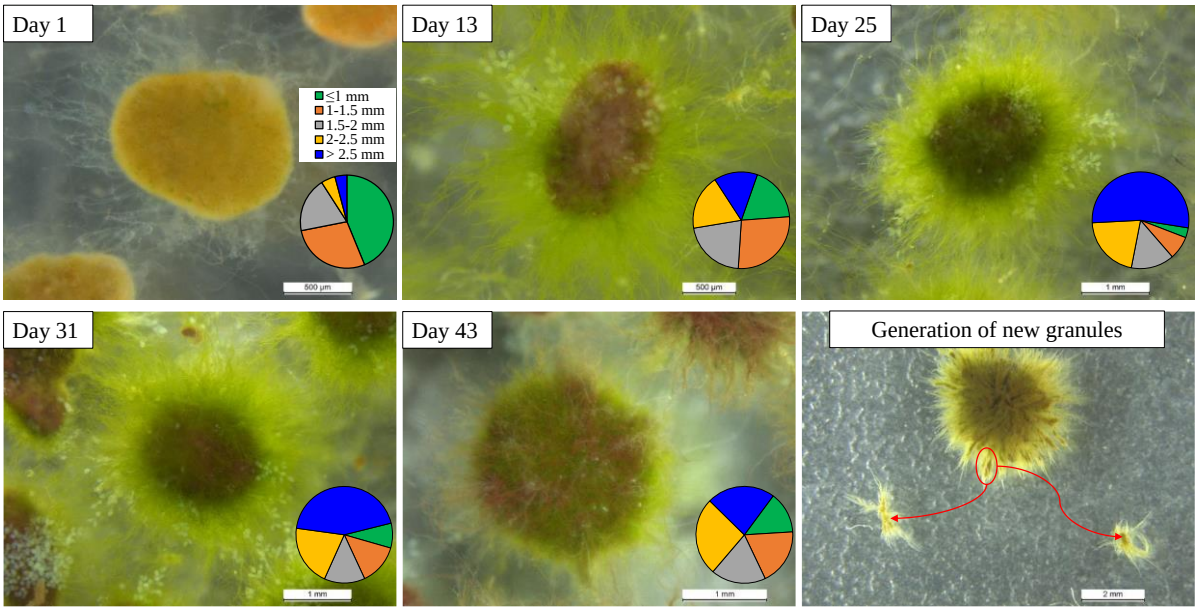

Fig. 4-3 Changes in morphology and diameter distribution (pie chart) of algal-bacterial AGS during the three operational stages.

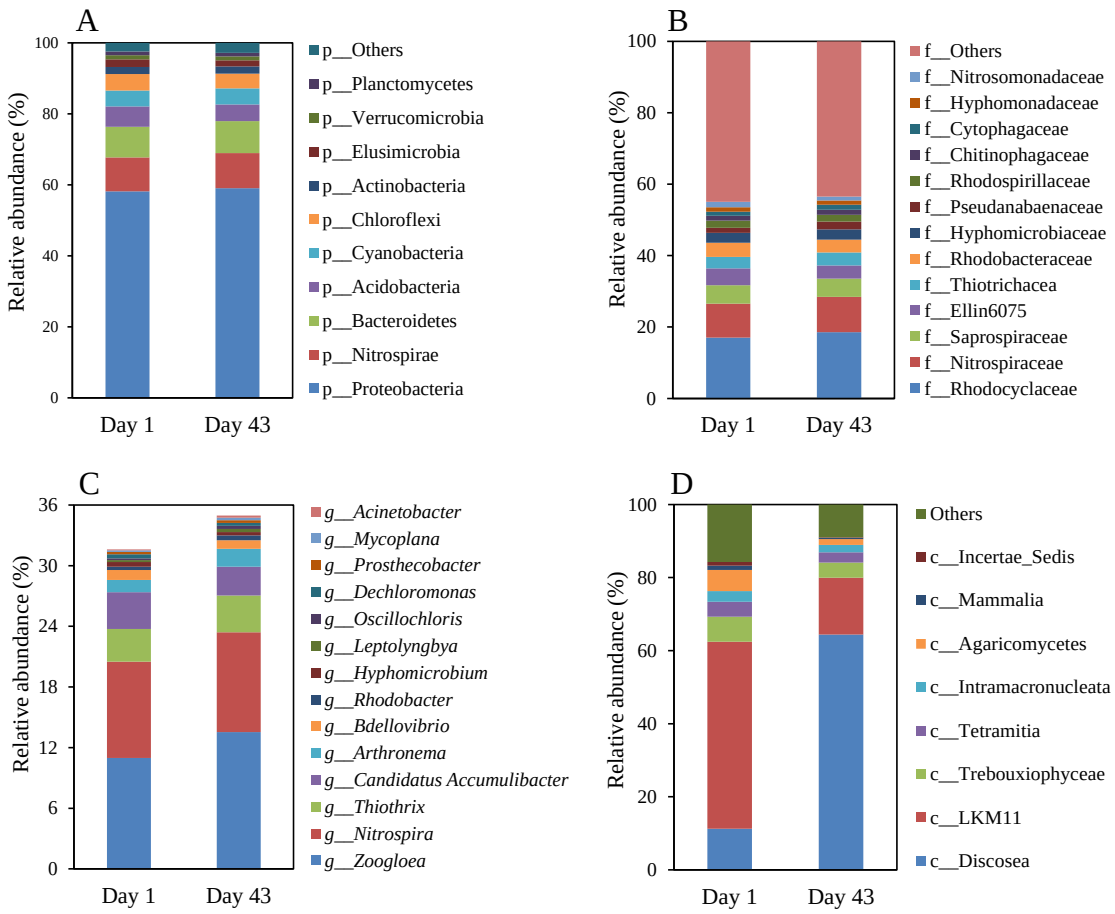

Fig. 4-4 Changes in microbial communities including prokaryotes at phylum (> 1%, A), family (> 1%, B), and genus (top 14 identified groups, C) levels in addition to eukaryotes (D) in the algal-bacterial aerobic granular sludge AGS on day 1 and day 43, respectively.

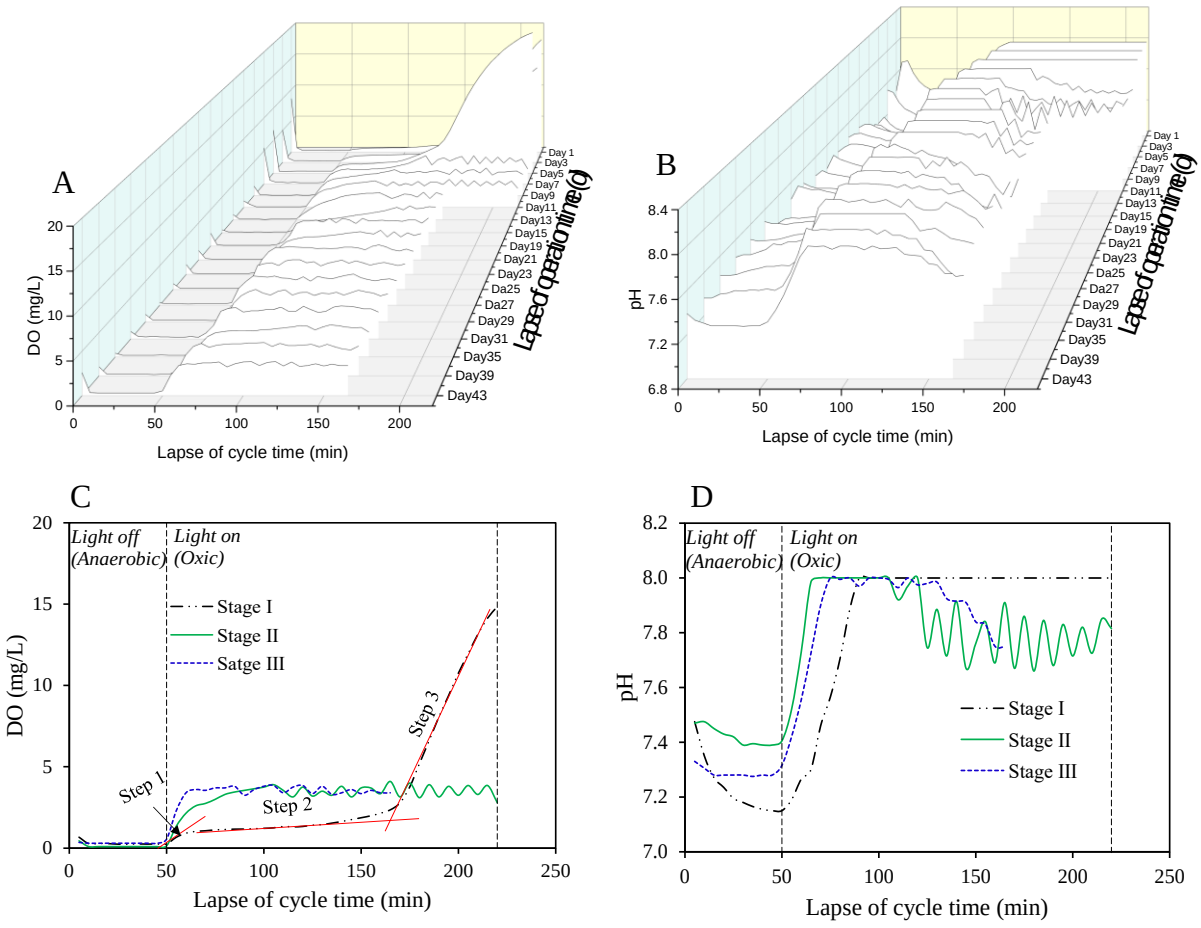

Fig. 4-5 DO (A and C) and pH (B and D) profiles during cycle tests during the three operational stages. DO, dissolved oxygen.

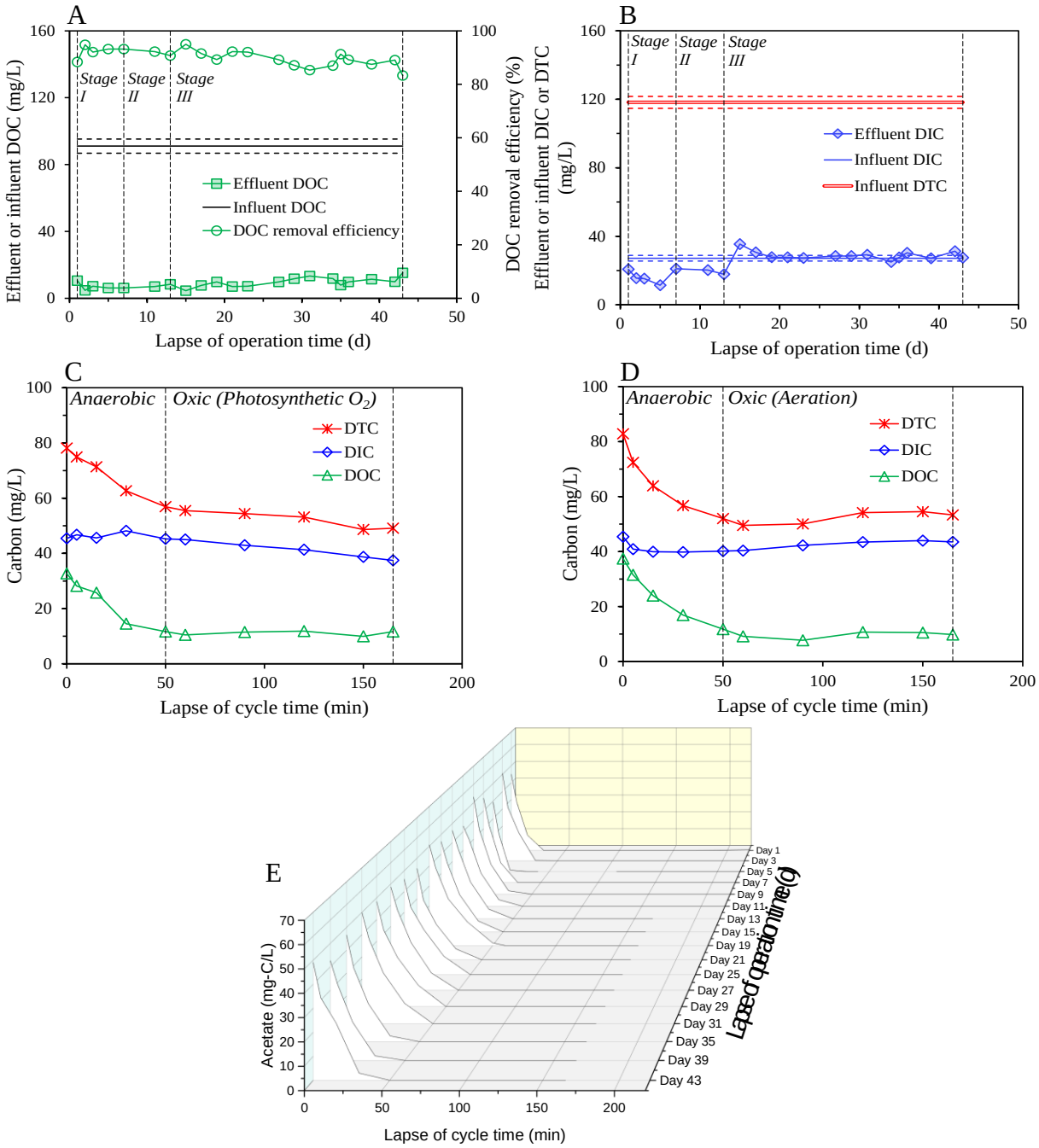

Fig. 4-6 Variations of DOC (A) and effluent DIC (B) concentrations during the three operational stages; typical dissolved C profiles with the oxic phase maintained by the photosynthetic O_2 (C) and the mechanical aeration (D) in the batch tests; and profiles of acetate (E) during cycle tests during the three operational stages. DIC, Dissolved inorganic carbon; DOC, dissolved organic carbon; DTC, dissolved total carbon.

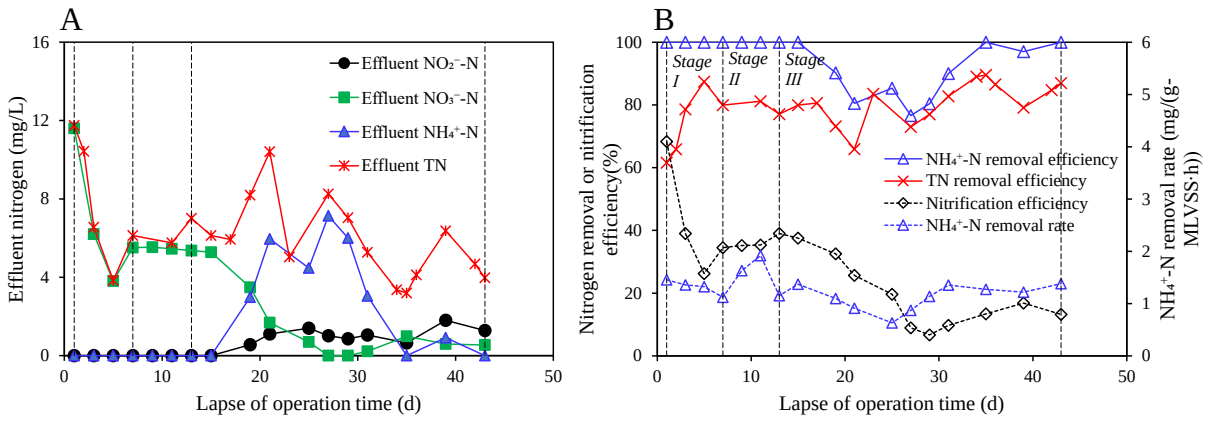

Fig. 4-7 Profiles of effluent nitrogen (A), nitrification efficiency, and nitrogen removal rate (B) during the three operational stages.

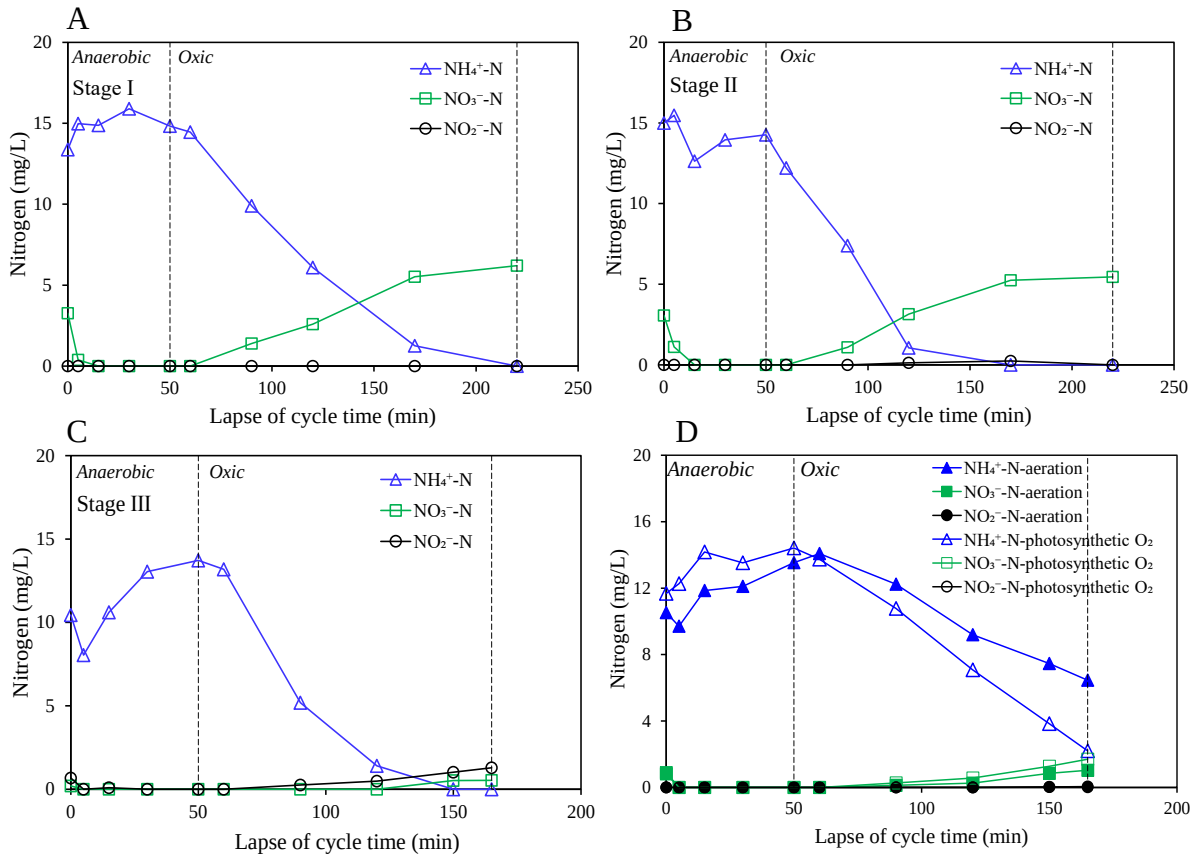

Fig. 4-8 Changes in N species during the cycle tests in Stages I (A), II (B), and III (C), and their comparative results from mechanical aeration and illumination conditions (D).

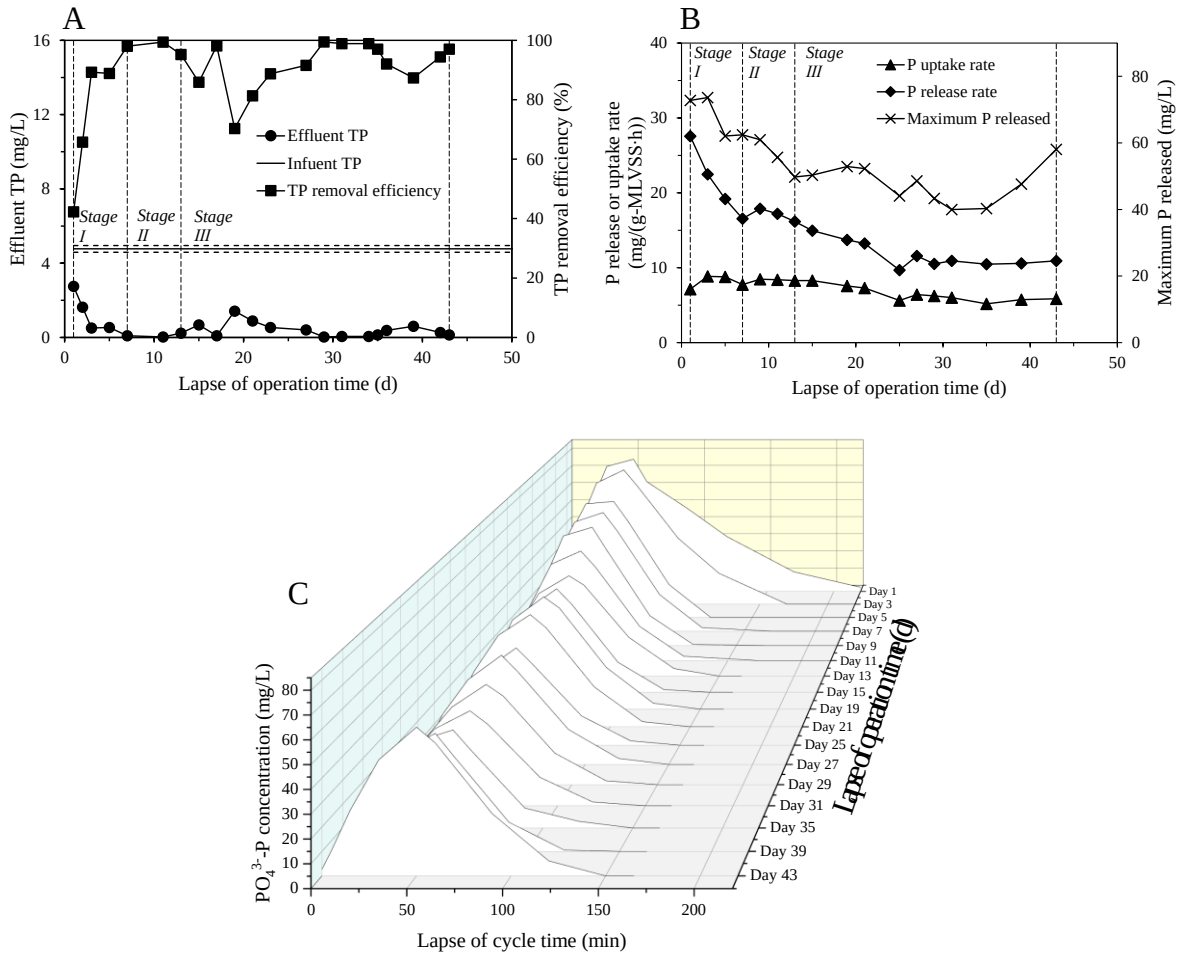

Fig. 4-9 Changes in effluent TP concentration and TP removal efficiency(A); P release and uptake during the three operational stages (B); and profiles of PO_4^{3-}-P during cycle tests during the three operational stages (C). TP, total phosphorus.

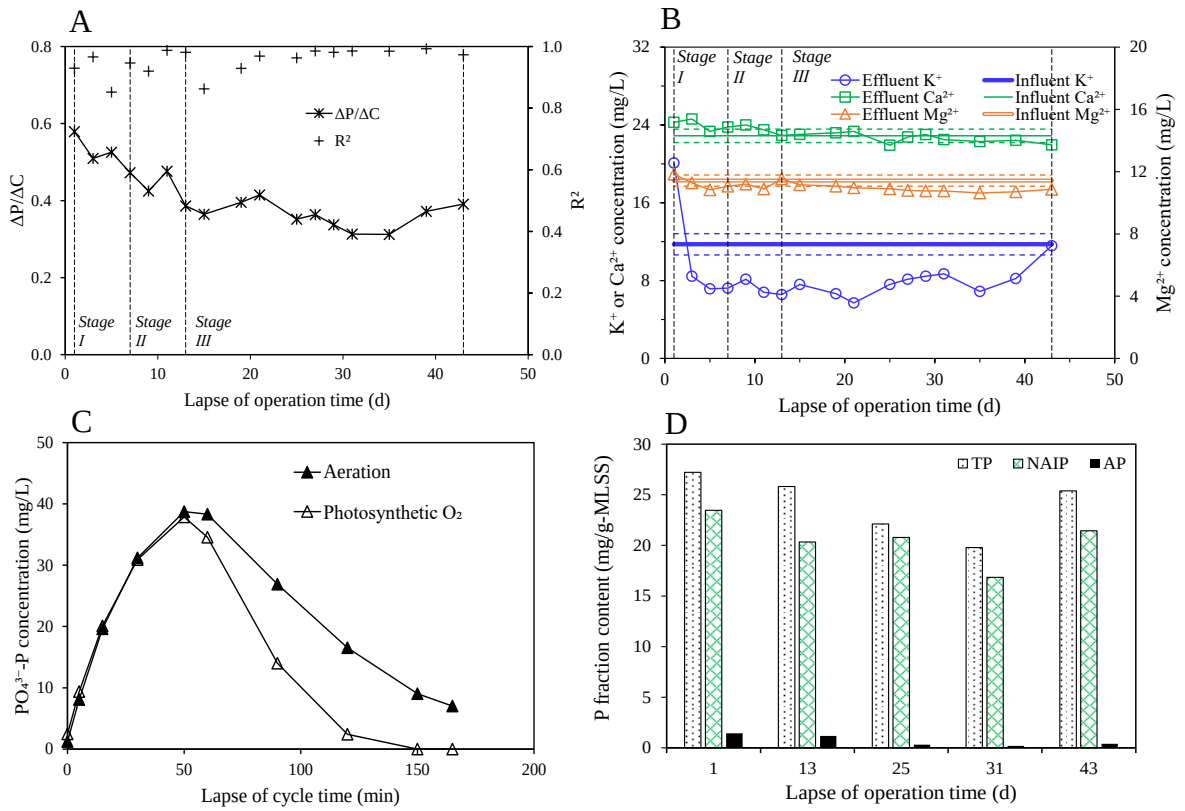

Fig. 4-10 Changes in molar ΔP/ΔC ratio and correlation coefficient (R^2) of ΔP against ΔC (A) and changes in effluent K, Mg and Ca concentrations (B) during the three operational stages; P profiles during the cycle tests using photosynthesis (Stage III) and mechanical aeration to supply O_2 (C); and changes in P fractionation in the granules during the test periods (D).

Chapter 5 Conclusions and future research perspectives

5.1 Conclusions

In this study, to coordinate microalgae and functional bacteria for a stable algal-bacterial AGS system with high organics and N/P removal, the interaction between microalgae and PAOs was for the first time considered the main factor that controls the impacts of microalgal growth on functional bacteria in the external O_2-supported algal-bacterial AGS system with mechanical aeration (Chapter 2). Then photosynthesis instead of aeration was proposed as a more efficient means for O_2 supply, which was confirmed in Chapter 3. Finally, a photosynthetic O_2-supported algal-bacterial AGS system with controlled pH and DO was established to implement highly efficient N/P removal and C fixation according to a feedback loop "Microalgae → Light → O_2 →DO controller → Light → Microalgae" (Chapter 4). All the above works from this study can be summarized as follows.

5.1.1 Contributions of microalgae, PAOs, and precipitation to aerobic P removal

In the external O_2-supported algal-bacterial AGS system, a strong illumination induced high pH in the bulk liquid due to the uptake of inorganic C by microalgae, in which chemical P precipitates were formed at a molar Ca/P ratio of 0.99 (Fig. 5-1). The chemical P precipitates indirectly induced by microalgae accounted for up to 48% of the total P removal from the bulk liquid under a light illuminance of 560 $\mu mol \cdot m^{-2} \cdot s^{-1}$ in comparison to almost no chemical P precipitates detected under no light condition. On the other hand, the contribution of microalgae growth to P removal from the bulk liquid was negligible. During the aerobic P uptake process, the evolution of P uptake was similar ($p > 0.05$) under different light illuminance (0, 90, 280 and 560 $\mu mol \cdot m^{-2} \cdot s^{-1}$), implying that P removal may not be promoted by the enhancement of microalgae growth. The coexisting microalgae significantly inhibited the P removal by PAOs through elevating the liquid pH thus weakening PAOs activity. The kinetic results indicate that aerobic P removal process in the algal-bacterial AGS system is somewhat similar to particle adsorption process, which is controlled by macropore and micropore diffusion along with the aeration (Fig. 5-1).

In addition, the mechanical aeration operation may strip CO_2 and O_2 out from the SBR and lead to a short contact time between gaseous and solid phases, thus limiting the substance exchange between microalgae and bacteria. More studies are thus recommended to improve substance exchange between microalgae and bacteria.

5.1.2 Feasibility of photosynthetic O_2-supported algal-bacterial AGS system

As shown in Chapter 2, the high liquid pH induced by microalgae photosynthesis may significantly affect the activity of PAOs. Meanwhile, the exchange of CO_2 and O_2 between microalgae and bacteria is inadequate under mechanical aeration. Therefore, photosynthesis instead of mechanical aeration was used to implement simultaneous nutrients removal in the algal-bacterial AGS with pH control.

According to the batch tests, aerobic N/P removal by nitrifiers and PAOs can be driven by only photosynthetic O_2 even at a low DO concentration < 0.5 mg/L under 190 – 1400 $\mu mol \cdot m^{-2} \cdot s^{-1}$ in the algal-bacterial AGS system (with no mechanical aeration). An obvious O_2 accumulation occurred after 60 - 90% nutrients being removed under 330 - 1400 $\mu mol \cdot m^{-2} \cdot s^{-1}$, and high ammonia removal, P uptake, and efficient DIC removal were achieved under 670 - 1400 $\mu mol \cdot m^{-2} \cdot s^{-1}$ (Fig. 5-2). On the other hand, photosynthesis as the O_2 supplier showed little effect on the changes of major ions except K^+. However, a stronger light intensity not only means a higher energy cost but also induces higher liquid pH and O_2 accumulation. Results from this study show that the costs brought about by chemicals addition/light input and the benefits from C fixation/nutrient removal and aeration saving should be carefully considered for a sustainable algal-bacterial granule system.

On the other hand, the photosynthetic O_2-supported system was only tested in a short-term operation. Thus the stability of granules and the whole system needs to be confirmed by a long-term operation, in which the mass C/N/P balance analyses can be conducted to reveal mechanisms involved.

5.1.3 Highly efficient nutrients removal by algal-bacterial AGS system

In this study, according to the results from Chapter 3, the photosynthetic O_2-supported algal-bacterial AGS system with pH/DO control was developed for efficient C assimilation and N/P removal during a long-time operation.

The photosynthetic O_2 produced by microalgae organisms maintained the DO level at 3 - 4 mg/L in the bulk liquid, and an LED light control system reduced 10 - 30% of light energy consumption. Results show that the biomass assimilated 52% of input DTC with a low CO_2 emission of 0.25 kg-CO_2/kg-COD, and the produced O_2 simultaneously facilitated aerobic nitrification and P uptake with the coexisting phototrophs serving as a C fixer and O_2 supplier (Fig. 5-3). This resulted in a stably high TN removal of 81 ± 7% and an N assimilation rate of 7.55 mg/(g-MLVSS·d) with enhanced microbial assimilation and simultaneous nitrification/denitrification. Good P removal of 92 - 98% was maintained during the test period

at a molar ΔP/ΔC ratio of 0.36 ± 0.03 and high P release and uptake rates of 10.84 ± 0.41 and 7.18 ± 0.24 mg/(g-MLVSS·h), respectively. In this system, photosynthetic O_2 was more advantageous for N and P removal than mechanical aeration. This proposed algal-bacterial AGS system can contribute to a better design and sustainable operation of WWTPs when algal-bacterial AGS is applied in practice.

This Chapter presented very interesting results, but also reveal some important factors (such as DO concentration, light strategy) on this system performance, which need to be further investigated.

5.2 Implications

To cope with global climate change, global efforts are being made to control C emissions resulting from human activity. For example, the government of China announced that C emission will peak in 2030 in China where C neutrality will be realized by 2060 (Liu et al., 2022). As well, Japan has declared that it will achieve C neutrality by 2050 (Ozawa et al., 2022). As reviewed in Chapter 1, the GHG emissions from WWTPs may account for 1 - 3% of total anthropogenic emissions. Thus, C emission reduction is an urgent issue in WWTPs. WWTPs as centralized treatment facilities have great prospects in C emission reduction. In view of the direct and indirect C emissions from WWTPs, this study established a low-carbon biological treatment system based on algal-bacterial AGS, in which microalgae and functional bacteria including PAOs and nitrifying/denitrifying microorganisms are well coordinated for efficient C fixation and nutrients removal under controlled DO/pH conditions. The reduction of C emissions from the biosystem can be implemented by (1) saving energy (with O_2 supply for aeration by photosynthetic O_2 instead of mechanical aeration) and (2) C fixation (microalgal photosynthesis). Results from this study show that this new biosystem can largely reduce CO_2 emissions compared with the bacterial AGS or CAS systems.

To sum up, this study provides an in-depth understanding of the symbiotic interaction between microalgae and bacteria. This proposed algal-bacterial AGS system can improve water quality and reduce CO_2 emissions, and thus contribute to achieving SDG 6 and C neutrality goals. Furthermore, it can contribute to the future design and sustainable operation of WWTPs, the development of C-neutral WWTP, and the transformation of WWTP from an energy consumer to an energy saver.

5.3 Future research

In this study, a "Microalgae → Light → O_2 →DO controller → Light → Microalgae" feedback loop was found and applied in the photosynthetic O_2-supported algal-bacterial AGS system. The results indicate that DO concentration plays a vital role in the coordination between microalgae and bacteria. Although the nutrients removal mechanism with DO concentration controlled at 3 - 4 mg/L has been confirmed in this study, the efficiency of IC fixation is not high enough as expected. Therefore, some further attempts should be followed to clarify the roles of DO concentration for a better design of algal-bacterial AGS based-WWTPs. Other aspects as follows are also important for the practical application of algal-bacterial AGS in real wastewater treatment.

(1) The light strategy and its layout in the system (like outside or inside the reactor system in addition to natural or artificial light source) need to be examined for further reducing C emissions;

(2) The emissions of other GHGs (especially N_2O) from this system should be investigated; and

(3) The system needs to be tested on real wastewaters.

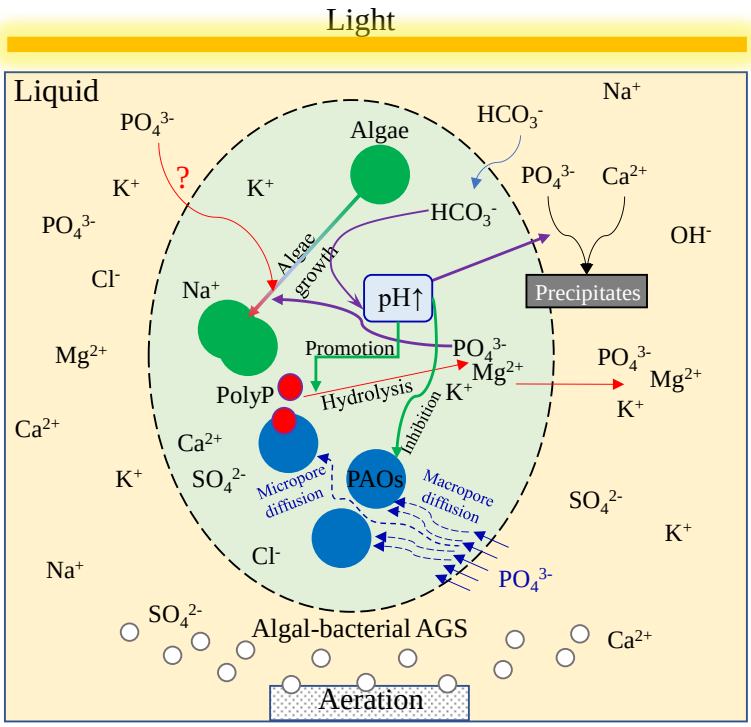

Fig. 5-1 The main ions and processes involved in algal-bacterial AGS focusing on aerobic P removal by the coexisting microalgae. AGS, aerobic granular sludge; PAOs, polyphosphate accumulating organisms.

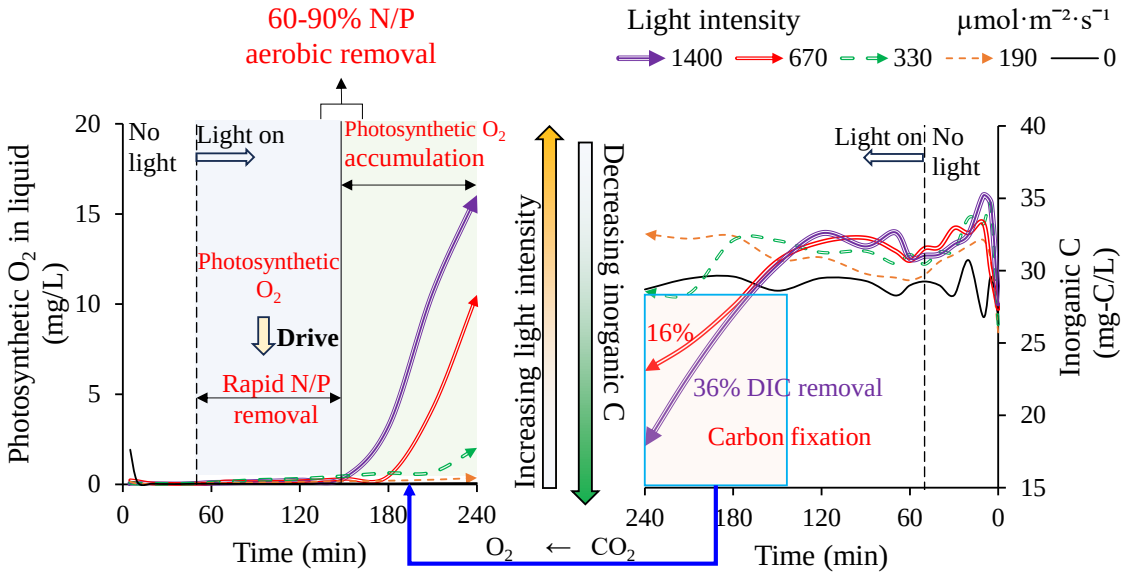

Fig. 5-2 Schematic of photosynthetic O_2-supported C fixation and N/P removal under different light intensities in algal-bacterial AGS system

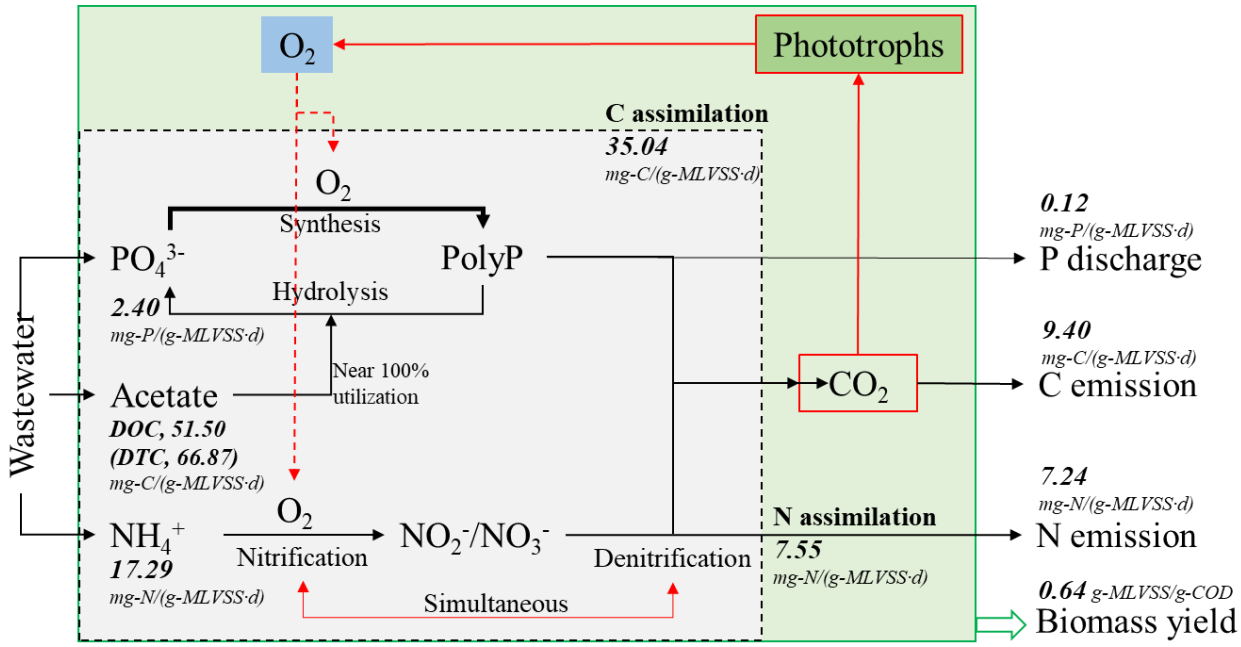

Fig. 5-3 Fates of C, N, and P in a well-established and photosynthetic O_2-suppotred algal-bacterial AGS system under controlled pH/DO conditions. PolyP, Polyphosphate.

References

Abouhend, A.S., Gikonyo, J.G., Patton, M., Butler, C.S., Tobiason, J., Park, C., 2023. Role of hydrodynamic shear in the oxygenic photogranule (OPG) wastewater treatment process. ACS ES&T Water 3, 659–668. https://doi.org/10.1021/acsestwater.2c00317

Abouhend, A.S., McNair, A., Kuo-Dahab, W.C., Watt, C., Butler, C.S., Milferstedt, K., Hamelin, J., Seo, J., Gikonyo, G.J., El-Moselhy, K.M., Park, C., 2018. The oxygenic photogranule process for aeration-free wastewater treatment. Environ. Sci. Technol. 52, 3503–3511. https://doi.org/10.1021/acs.est.8b00403

Acevedo, B., Oehmen, A., Carvalho, G., Seco, A., Borrás, L., Barat, R., 2012. Metabolic shift of polyphosphate-accumulating organisms with different levels of polyphosphate storage. Water Res. 46, 1889–1900. https://doi.org/10.1016/j.watres.2012.01.003

Adav, S.S., Lee, D.-J., Show, K.-Y., Tay, J.-H., 2008. Aerobic granular sludge: Recent advances. Biotechnol. Adv. 26, 411–423. https://doi.org/10.1016/j.biotechadv.2008.05.002

Allen, S.J., McKay, G., Khader, K.Y.H., 1989. Intraparticle diffusion of a basic dye during adsorption onto sphagnum peat. Environ. Pollut. 56, 39–50. https://doi.org/10.1016/0269-7491(89)90120-6

APHA, 2012. Standard methods for the examination of water and wastewater, American Public Health Association/American Water Work Association/Water Environment Federation, Washington, D.C., USA.

Arun, S., Ramasamy, S., Pakshirajan, K., 2021. Mechanistic insights into nitrification by microalgae-bacterial consortia in a photo-sequencing batch reactor under different light intensities. J. Clean. Prod. 321, 128752. https://doi.org/10.1016/j.jclepro.2021.128752

Bao, Z., Sun, S., Sun, D., 2015. Characteristics of direct CO_2 emissions in four full-scale wastewater treatment plants. Desalin. Water Treat. 54, 1070–1079. https://doi.org/10.1080/19443994.2014.940389

Barat, R., Montoya, T., Seco, A., Ferrer, J., 2005. The role of potassium, magnesium and calcium in the enhanced biological phosphorus removal treatment plants. Environ. Technol. 26, 983–992. https://doi.org/10.1080/09593332608618485

Barnard, J., Comeau, Y., 2014. Chapter 6 - Phosphorus removal in activated sludge, in: Jenkins, D. and Wanner, J. (Eds.), Activated Sludge - 100 Years and Counting, IWA Publications, pp. 93-115. https://doi.org/10.2166/9781780404943

Bassin, J.P., Pronk, M., Kraan, R., Kleerebezem, R., van Loosdrecht, M.C.M., 2011.

Ammonium adsorption in aerobic granular sludge, activated sludge and anammox granules. Water Res. 45, 5257–5265. https://doi.org/10.1016/j.watres.2011.07.034

Belloir, C., Stanford, C., Soares, A., 2015. Energy benchmarking in wastewater treatment plants: The importance of site operation and layout. Environ. Technol. (United Kingdom) 36, 260–269. https://doi.org/10.1080/09593330.2014.951403

Boelee, N.C., Temmink, H., Janssen, M., Buisman, C.J.N., Wijffels, R.H., 2014. Balancing the organic load and light supply in symbiotic microalgal-bacterial biofilm reactors treating synthetic municipal wastewater. Ecol. Eng. 64, 213–221. https://doi.org/10.1016/j.ecoleng.2013.12.035

Burris, J.E., 1981. Effects of oxygen and inorganic carbon concentrations on the photosynthetic quotients of marine algae. Mar. Biol. 65, 215–219. https://doi.org/10.1007/BF00397114

Cai, T., Park, S.Y., Li, Y., 2013. Nutrient recovery from wastewater streams by microalgae: Status and prospects. Renew. Sustain. Energy Rev. 19, 360–369. https://doi.org/10.1016/j.rser.2012.11.030

Campos, J.L., Valenzuela-Heredia, D., Pedrouso, A., Val del Río, A., Belmonte, M., Mosquera-Corral, A., 2016. Greenhouse gases emissions from wastewater treatment plants: minimization, treatment, and prevention. J. Chem. 2016, 3796352. https://doi.org/10.1155/2016/3796352

Capodaglio, A.G., Olsson, G., 2020. Energy issues in sustainable urban wastewater management: Use, demand reduction and recovery in the urban water cycle. Sustainability. 12, 266. https://doi.org/10.3390/su12010266

Carvalheira, M., Oehmen, A., Carvalho, G., Eusébio, M., Reis, M.A.M., 2014. The impact of aeration on the competition between polyphosphate accumulating organisms and glycogen accumulating organisms. Water Res. 66, 296–307. https://doi.org/10.1016/j.watres.2014.08.033

Cassidy, D.P., Belia, E., 2005. Nitrogen and phosphorus removal from an abattoir wastewater in a SBR with aerobic granular sludge. Water Res. 39, 4817–4823. https://doi.org/10.1016/j.watres.2005.09.025

Çelen, I., Buchanan, J.R., Burns, R.T., Bruce Robinson, R., Raj Raman, D., 2007. Using a chemical equilibrium model to predict amendments required to precipitate phosphorus as struvite in liquid swine manure. Water Res. 41, 1689–1696. https://doi.org/10.1016/j.watres.2007.01.018

Chen, M., Oshita, K., Mahzoun, Y., Takaoka, M., Fukutani, S., Shiota, K., 2021. Survey of

elemental composition in dewatered sludge in Japan. Sci. Total Environ. 752, 141857. https://doi.org/10.1016/j.scitotenv.2020.141857

Cheremisinoff, N.P. (Ed.), 1996. Chapter 4 - Nitrification and denitrification in the activated sludge process, in: Biotechnology for Waste and Wastewater Treatment. Noyes Publications, New Jersey, pp.151-188. https://doi.org/10.1016/B978-081551409-1.50006-6

Chojnacka, K., 2010. Biosorption and bioaccumulation – the prospects for practical applications. Environ. Int. 36, 299–307. https://doi.org/10.1016/J.ENVINT.2009.12.001

Crini, G., Lichtfouse, E., 2019. Advantages and disadvantages of techniques used for wastewater treatment. Environ. Chem. Lett. 17, 145–155. https://doi.org/10.1007/s10311-018-0785-9

Daudt, G.C., Magnus, B.S., Schambeck, C.M., Libardi, N.J., Da Costa, R.H.R., 2022. Assessment of nitrous oxide and carbon dioxide emissions and the carbon footprint in an aerobic granular sludge reactor treating domestic wastewater. Environ. Eng. Sci. 39, 561–572. https://doi.org/10.1089/ees.2021.0280

de Kreuk, M.K., Heijnen, J.J., van Loosdrecht, M.C.M., 2005. Simultaneous COD, nitrogen, and phosphate removal by aerobic granular sludge. Biotechnol. Bioeng. 90, 761–769. https://doi.org/10.1002/bit.20470

de Kreuk, M.K., Kishida, N., van Loosdrecht, M.C.M., 2007. Aerobic granular sludge - State of the art. Water Sci. Technol. 55, 75–81. https://doi.org/10.2166/wst.2007.244

de Sousa Rollemberg, S.L., Mendes Barros, A.R., Milen Firmino, P.I., Bezerra dos Santos, A., 2018. Aerobic granular sludge: Cultivation parameters and removal mechanisms. Bioresour. Technol. 270, 678–688. https://doi.org/10.1016/j.biortech.2018.08.130

Ermis, H., Guven-Gulhan, U., Cakir, T., Altinbas, M., 2020. Effect of iron and magnesium addition on population dynamics and high value product of microalgae grown in anaerobic liquid digestate. Sci. Rep. 10, 1–12. https://doi.org/10.1038/s41598-020-60622-1

Gandiglio, M., Lanzini, A., Soto, A., Leone, P., Santarelli, M., 2017. Enhancing the energy efficiency of wastewater treatment plants through co-digestion and fuel cell systems. Front. Environ. Sci. 5, 1–21. https://doi.org/10.3389/fenvs.2017.00070

Garcés-Pastor, S., Fletcher, W.J., Ryan, P.A., 2023. Ecological impacts of the industrial revolution in a lowland raised peat bog near Manchester, NW England. Ecol. Evol. 13, 1–22. https://doi.org/10.1002/ece3.9807

Giacometti, G.M., Morosinotto, T., 2013. Photoinhibition and photoprotection in plants, algae,

and cyanobacteria, In: Lennarz W.J. and Lane M. D. (Eds.), Encyclopedia of Biological Chemistry (2nd Edition). Academic Press. pp. 482-487. https://doi.org/10.1016/B978-0-12-378630-2.00229-2

Gonçalves, A.L., Pires, J.C.M., Simões, M., 2017. A review on the use of microalgal consortia for wastewater treatment. Algal Res. 24, 403–415. https://doi.org/10.1016/j.algal.2016.11.008

Guo, D., Zhang, X., Shi, Y., Cui, B., Fan, J., Ji, B., 2021. Microalgal-bacterial granular sludge process outperformed aerobic granular sludge process in municipal wastewater treatment with less carbon dioxide emissions. Environ. Sci. Pollut. Res. 28, 13616–13623. https://doi.org/10.1007/s11356-020-11565-7

Hao, X., Liu, R., Huang, X., 2015. Evaluation of the potential for operating carbon neutral WWTPs in China. Water Res. 87, 424–431. https://doi.org/10.1016/j.watres.2015.05.050

He, Q., Chen, L., Zhang, S., Chen, R., Wang, H., Zhang, W., Song, J., 2018a. Natural sunlight induced rapid formation of water-born algal-bacterial granules in an aerobic bacterial granular photo-sequencing batch reactor. J. Hazard. Mater. 359, 222–230. https://doi.org/10.1016/j.jhazmat.2018.07.051

He, Q., Chen, L., Zhang, S., Wang, L., Liang, J., Xia, W., Wang, H., Zhou, J., 2018b. Simultaneous nitrification, denitrification and phosphorus removal in aerobic granular sequencing batch reactors with high aeration intensity: Impact of aeration time. Bioresour. Technol. 263, 214–222. https://doi.org/10.1016/j.biortech.2018.05.007

He, Q., Zhang, S., Zou, Z., Zheng, L. an, Wang, H., 2016. Unraveling characteristics of simultaneous nitrification, denitrification and phosphorus removal (SNDPR) in an aerobic granular sequencing batch reactor. Bioresour. Technol. 220, 651–655. https://doi.org/10.1016/j.biortech.2016.08.105

He, Y., Zhu, Y., Chen, J., Huang, M., Wang, P., Wang, G., Zou, W., Zhou, G., 2019. Assessment of energy consumption of municipal wastewater treatment plants in China. J. Clean. Prod. 228, 399–404. https://doi.org/10.1016/j.jclepro.2019.04.320

Ho, S.-H., Chen, C.-Y., Lee, D.-J., Chang, J.-S., 2011. Perspectives on microalgal CO_2-emission mitigation systems - A review. Biotechnol. Adv. 29, 189–198. https://doi.org/10.1016/j.biotechadv.2010.11.001

How, S.W., Lim, S.Y., Lim, P.B., Aris, A.M., Ngoh, G.C., Curtis, T.P., Chua, A.S.M., 2018. Low-dissolved-oxygen nitrification in tropical sewage: An investigation on potential, performance and functional microbial community. Water Sci. Technol. 77, 2274–2283.

https://doi.org/10.2166/wst.2018.143

Huang, W., Li, B., Zhang, C., Zhang, Z., Lei, Z., Lu, B., Zhou, B., 2015. Effect of algae growth on aerobic granulation and nutrients removal from synthetic wastewater by using sequencing batch reactors. Bioresour. Technol. 179, 187–192. https://doi.org/10.1016/j.biortech.2014.12.024

Jahn, L., Svardal, K., Krampe, J., 2019. Nitrous oxide emissions from aerobic granular sludge. Water Sci. Technol. 80, 1304–1314. https://doi.org/10.2166/wst.2019.378

Ji, B., Liu, C., 2022. CO_2 improves the microalgal-bacterial granular sludge towards carbon-negative wastewater treatment. Water Res. 208, 117865. https://doi.org/10.1016/j.watres.2021.117865

Ji, B., Zhang, M., Gu, J., Ma, Y., Liu, Y., 2020a. A self-sustaining synergetic microalgal-bacterial granular sludge process towards energy-efficient and environmentally sustainable municipal wastewater treatment. Water Res. 179, 115884. https://doi.org/10.1016/j.watres.2020.115884

Ji, B., Zhang, M., Wang, L., Wang, S., Liu, Y., 2020b. Removal mechanisms of phosphorus in non-aerated microalgal-bacterial granular sludge process. Bioresour. Technol. 312, 123531. https://doi.org/10.1016/j.biortech.2020.123531

Jiang, L., Li, Y., Pei, H., 2021. Algal–bacterial consortia for bioproduct generation and wastewater treatment. Renew. Sustain. Energy Rev. 149, 111395. https://doi.org/10.1016/j.rser.2021.111395

Jones, E.R., Van Vliet, M.T.H., Qadir, M., Bierkens, M.F.P., 2021. Country-level and gridded estimates of wastewater production, collection, treatment and reuse. Earth Syst. Sci. Data 13, 237–254. https://doi.org/10.5194/essd-13-237-2021

Kampschreur, M.J., Temmink, H., Kleerebezem, R., Jetten, M.S.M., van Loosdrecht, M.C.M., 2009. Nitrous oxide emission during wastewater treatment. Water Res. 43, 4093–4103. https://doi.org/10.1016/j.watres.2009.03.001

Karya, N.G.A.I., van der Steen, N.P., Lens, P.N.L., 2013. Photo-oxygenation to support nitrification in an algal-bacterial consortium treating artificial wastewater. Bioresour. Technol. 134, 244–250. https://doi.org/10.1016/j.biortech.2013.02.005

Knappe, J., Somlai, C., Gill, L.W., 2022. Assessing the spatial and temporal variability of greenhouse gas emissions from different configurations of on-site wastewater treatment system using discrete and continuous gas flux measurement. Biogeosciences 19, 1067–1085. https://doi.org/10.5194/bg-19-1067-2022

Kumar, R., Venugopalan, V.P., 2015. Development of self-sustaining phototrophic granular biomass for bioremediation applications. Curr. Sci. 108, 1653–1661. https://www.researchgate.net/publication/278327434

Larsen, T.A., 2015. CO_2-neutral wastewater treatment plants or robust, climate-friendly wastewater management? A systems perspective. Water Res. 87, 513–521. https://doi.org/10.1016/j.watres.2015.06.006

Lee, D.-J., Chen, Y.-Y., Show, K.-Y., Whiteley, C.G., Tay, J.-H., 2010. Advances in aerobic granule formation and granule stability in the course of storage and reactor operation. Biotechnol. Adv. 28, 919–934. https://doi.org/10.1016/j.biotechadv.2010.08.007

Lee, J.-K., Choi, C.-K., Lee, K.-H., Yim, S.-B, 2008. Mass balance of nitrogen, and estimates of COD, nitrogen and phosphorus used in microbial synthesis as a function of sludge retention time in a sequencing batch reactor system. Bioresour. Technol. 99, 7788–7796. https://doi.org/10.1016/j.biortech.2008.01.057

Lemaire, R., Webb, R.I., Yuan, Z., 2008. Micro-scale observations of the structure of aerobic microbial granules used for the treatment of nutrient-rich industrial wastewater. ISME J. 2, 528–541. https://doi.org/10.1038/ismej.2008.12

Lin, Y.-M., Liu, Y., Tay, J.-H., 2003. Development and characteristics of phosphorus-accumulating microbial granules in sequencing batch reactors. Appl. Microbiol. Biotechnol. 62, 430–435. https://doi.org/10.1007/s00253-003-1359-7

Liu, L., Fan, H., Liu, Y., Liu, C., Huang, X., 2017. Development of algae-bacteria granular consortia in photo-sequencing batch reactor. Bioresour. Technol. 232, 64–71. https://doi.org/10.1016/j.biortech.2017.02.025

Liu, Y., Wang, Z.W., Qin, L., Liu, Y.-Q., Tay, J.-H., 2005. Selection pressure-driven aerobic granulation in a sequencing batch reactor. Appl. Microbiol. Biotechnol. 67, 26–32. https://doi.org/10.1007/s00253-004-1820-2

Liu, Z., Deng, Z., He, G., Wang, H., Zhang, X., Lin, J., Qi Y., Liang, X., 2022. Challenges and opportunities for carbon neutrality in China. Nat. Rev. Earth Environ. 3, 141-155. https://doi.org/10.1038/s43017-021-00244-x

Liu, Z., Ning, F., Hou, Y., Zhang, D., Yang, R., Wang, J., Zhang, A., Chen, Y., Liu, Y., 2022. Deciphering the effect of algae sources on the formation of algal-bacterial granular sludge: Endogenous versus exogenous algae. J. Clean. Prod. 363, 132468. https://doi.org/10.1016/j.jclepro.2022.132468

Lopez, C., Pons, M.N., Morgenroth, E., 2006. Endogenous processes during long-term

starvation in activated sludge performing enhanced biological phosphorus removal. Water Res. 40, 1519–1530. https://doi.org/10.1016/j.watres.2006.01.040

Luo, J., Hao, T., Wei, L., Mackey, H.R., Lin, Z., Chen, G.-H., 2014. Impact of influent COD/N ratio on disintegration of aerobic granular sludge. Water Res. 62, 127–135. https://doi.org/10.1016/j.watres.2014.05.037

Mañas, A., Biscans, B., Spérandio, M., 2011. Biologically induced phosphorus precipitation in aerobic granular sludge process. Water Res. 45, 3776–3786. https://doi.org/10.1016/j.watres.2011.04.031

Mayhew, M., Stephenson, T., 1997. Low biomass yield activated sludge: A review. Environ. Technol. 18, 883–892. https://doi.org/10.1080/09593331808616607

Meng, F., Xi, L., Liu, D., Huang, W., Lei, Z., Zhang, Z., Huang, W., 2019. Effects of light intensity on oxygen distribution, lipid production and biological community of algal-bacterial granules in photo-sequencing batch reactors. Bioresour. Technol. 272, 473–481. https://doi.org/10.1016/j.biortech.2018.10.059

Milferstedt, K., Kuo-Dahab, W.C., Butler, C.S., Hamelin, J., Abouhend, A.S., Stauch-White, K., McNair, A., Watt, C., Carbajal-González, B.I., Dolan, S., Park, C., 2017. The importance of filamentous cyanobacteria in the development of oxygenic photogranules. Sci. Rep. 7, 1–15. https://doi.org/10.1038/s41598-017-16614-9

Mohan, D., Singh, K.P., Sinha, S., Gosh, D., 2004. Removal of pyridine from aqueous solution using low cost activated carbons derived from agricultural waste materials. Carbon N. Y. 42, 2409–2421. https://doi.org/10.1016/j.carbon.2004.04.026

Moore, D.P., Li, N.P., Wendt, L.P., Castañeda, S.R., Falinski, M.M., Zhu, J.-J., Song, C., Ren, Z.J., Zondlo, M.A., 2023. Underestimation of sector-wide methane emissions from United States wastewater treatment. Environ. Sci. Technol. 57, 4082–4090. https://doi.org/10.1021/acs.est.2c05373

Morgenroth, E., Sherden, T., van Loosdrecht, M.C.M., Heijnen, J.J., Wilderer, P.A., 1997. Aerobic granular sludge in a sequencing batch reactor. Water Res. 31, 3191–3194. https://doi.org/10.1016/S0043-1354(97)00216-9

Mosquera-Corral, A., de Kreuk, M.K., Heijnen, J.J., van Loosdrecht, M.C.M., 2005. Effects of oxygen concentration on N-removal in an aerobic granular sludge reactor. Water Res. 39, 2676–2686. https://doi.org/10.1016/j.watres.2005.04.065

Muñoz, R., Guieysse, B., 2006. Algal-bacterial processes for the treatment of hazardous contaminants: A review. Water Res. 40, 2799–2815.

https://doi.org/10.1016/j.watres.2006.06.011

Muylaert, K., Bastiaens, L., Vandamme, D., Gouveia, L., 2017. Chapter 5 - Harvesting of microalgae: Overview of process options and their strengths and drawbacks, in: Gonzalez-Fernandez, C. and Muñoz, R. (Eds.), Microalgae-Based Biofuels and Bioproducts. Woodhead Publications, pp. 113-132. https://doi.org/10.1016/B978-0-08-101023-5.00005-4

Nancharaiah, Y. V., Reddy, G. K. K., 2018. Aerobic granular sludge technology: Mechanisms of granulation and biotechnological applications. Bioresour. Technol. 247, 1128–1143. https://doi.org/10.1016/j.biortech.2017.09.131

Nancharaiah, Y. V., Venkata Mohan, S., Lens, P.N.L., 2016. Recent advances in nutrient removal and recovery in biological and bioelectrochemical systems. Bioresour. Technol. 215, 173–185. https://doi.org/10.1016/j.biortech.2016.03.129

Nereda, 2023. https://neredal.royalhaskoningdhv.com/.Accessed on Jan. 2, 2023.

Nielsen, P. H., McMahon, K. D., 2014. Chapter 4 - Microbiology and microbial ecology of the activated sludge process, in: Jenkins, D and Wanner, J. (Eds.), Activated Sludge - 100 Years and Counting, IWA Publications, pp. 53-75. https://doi.org/10.2166/9781780404943

Oehmen, A., Lemos, P.C., Carvalho, G., Yuan, Z., Keller, J., Blackall, L.L., Reis, M.A.M., 2007. Advances in enhanced biological phosphorus removal: From micro to macro scale. Water Res. 41, 2271–2300. https://doi.org/10.1016/j.watres.2007.02.030

Oehmen, A., Vives, M.T., Lu, H., Yuan, Z., Keller, J., 2005. The effect of pH on the competition between polyphosphate-accumulating organisms and glycogen-accumulating organisms. Water Res. 39, 3727–3737. https://doi.org/10.1016/j.watres.2005.06.031

Ozawa, A., Tsani, T., Kudoh, Y., 2022. Japan's pathways to achieve carbon neutrality by 2050 – Scenario analysis using an energy modeling methodology. Renew. Sustain. Energy Rev. 169, 112943. https://doi.org/10.1016/j.rser.2022.112943

Pancha, I., Chokshi, K., George, B., Ghosh, T., Paliwal, C., Maurya, R., Mishra, S., 2014. Nitrogen stress triggered biochemical and morphological changes in the microalgae *Scenedesmus* sp. CCNM 1077. Bioresour. Technol. 156, 146–154. https://doi.org/10.1016/j.biortech.2014.01.025

Panepinto, D., Fiore, S., Zappone, M., Genon, G., Meucci, L., 2016. Evaluation of the energy efficiency of a large wastewater treatment plant in Italy. Appl. Energy 161, 404–411. https://doi.org/10.1016/j.apenergy.2015.10.027

Pei, M., Zhang, B., He, Y., Su, J., Gin, K., Lev, O., Shen, G., Hu, S., 2019. State of the art of tertiary treatment technologies for controlling antibiotic resistance in wastewater treatment plants. Environ. Int. 131, 105026. https://doi.org/10.1016/j.envint.2019.105026

Pick, U., Rental, M., Chitlaru, E., Weiss, M., 1990. Polyphosphate-hydrolysis - a protective mechanism against alkaline stress? FEBS Lett. 274, 15–18. https://doi.org/10.1016/0014-5793(90)81318-I

Rajta, A., Bhatia, R., Setia, H., Pathania, P., 2020. Role of heterotrophic aerobic denitrifying bacteria in nitrate removal from wastewater. J. Appl. Microbiol. 128, 1261–1278. https://doi.org/10.1111/jam.14476

Ramanan, R., Kim, B.-H., Cho, D.-H., Oh, H.-M., Kim, H.-S., 2016. Algae-bacteria interactions: Evolution, ecology and emerging applications. Biotechnol. Adv. 34, 14–29. https://doi.org/10.1016/j.biotechadv.2015.12.003

RapidTable, n.d. "How to convert lux to watts." https://www.rapidtables.com/calc/light/how-lux-to-watt.html.

Ruban, V., López-Sánchez, J.F., Pardo, P., Rauret, G., Muntau, H., Quevauviller, P., 1999. Selection and evaluation of sequential extraction procedures for the determination of phosphorus forms in lake sediment. J. Environ. Monit. 1, 51–56. https://doi.org/10.1039/a807778i

Samiotis, G., Stamatakis, K., Amanatidou, E., 2021. Assessment of *Synechococcus elongatus* PCC 7942 as an option for sustainable wastewater treatment. Water Sci. Technol. 84, 1438–1451. https://doi.org/10.2166/wst.2021.319

Schönborn, C., Bauer, H.-D.D., Röske, I., 2001. Stability of enhanced biological phosphorus removal and composition of polyphosphate granules. Water Res. 35, 3190–3196. https://doi.org/10.1016/S0043-1354(01)00025-2

Scragg, A.H., Illman, A.M., Carden, A., Shales, S.W., 2002. Growth of microalgae with increased calorific values in a tubular bioreactor. Biomass Bioenerg. 23, 67–73. https://doi.org/10.1016/S0961-9534(02)00028-4

Silva, C., Rosa, M.J., 2021. A practical methodology for forecasting the impact of changes in influent loads and discharge consents on average energy consumption and sludge production by activated sludge wastewater treatment. Sustainability 13, 12293. https://doi.org/10.3390/su132112293

Slade, A.H., Anderson, S.M., Evans, B.G., 2003. Nitrogen fixation in the activated sludge treatment of thermomechanical pulping wastewater: effect of dissolved oxygen. Water Sci.

Technol. 48, 1–8. https://doi.org/10.2166/wst.2003.0446

Smolders, G.J.F., van der Meij, J., van Loosdrecht, M.C.M., Heijnen, J.J., 1994. Stoichiometric model of the aerobic metabolism of the biological phosphorus removal process. Biotechnol. Bioeng. 44, 837–848. https://doi.org/10.1002/bit.260440709

Smolders, G.J.F., van Loosdrecht, M.C.M., Heijnen, J.J., 1995. A metabolic model for the biological phosphorus removal process. Water Sci. Technol. 31, 79–93. https://doi.org/10.2166/WST.1995.0078

Sousa, C., Compadre, A., Vermuë, M.H., Wijffels, R.H., 2013. Effect of oxygen at low and high light intensities on the growth of *Neochloris oleoabundans*. Algal Res. 2, 122–126. https://doi.org/10.1016/j.algal.2013.01.007

Stensel, H. D., Makinia, J., 2014. Chapter 3 - Activated sludge process development, in: Jenkins, D. and Wanner, J. (Eds.), Activated Sludge - 100 Years and Counting, IWA Publications, pp. 33-47. https://doi.org/10.2166/9781780404943.

Sun, Q., Yang, L., 2003. The adsorption of basic dyes from aqueous solution on modified peat-resin particle. Water Res. 37, 1535–1544. https://doi.org/10.1016/S0043-1354(02)00520-1

Świątczak, P., Cydzik-Kwiatkowska, A., 2018. Performance and microbial characteristics of biomass in a full-scale aerobic granular sludge wastewater treatment plant. Environ. Sci. Pollut. Res. 25, 1655–1669. https://doi.org/10.1007/s11356-017-0615-9

Tian, Y., Liu, S., Guo, Z., Wu, N., Liang, J., Zhao, R., Hao, L., Zeng, M., 2022. Insight into greenhouse gases emissions and energy consumption of different full-scale wastewater treatment plants via ECAM tool. Int. J. Environ. Res. Public Health 19, 13387. https://doi.org/10.3390/ijerph192013387

Tiron, O., Bumbac, C., Manea, E., Stefanescu, M., Lazar, M.N., 2017. Overcoming microalgae harvesting barrier by activated algae granules. Sci. Rep. 7, 1–13. https://doi.org/10.1038/s41598-017-05027-3

Tiron, O., Bumbac, C., Patroescu, I. V., Badescu, V.R., Postolache, C., 2015. Granular activated algae for wastewater treatment. Water Sci. Technol. 71, 832–839. https://doi.org/10.2166/wst.2015.010

Tran, H.N., You, S.-J., Hosseini-Bandegharaei, A., Chao, H.-P., 2017. Mistakes and inconsistencies regarding adsorption of contaminants from aqueous solutions: A critical review. Water Res. 120, 88–116. https://doi.org/10.1016/j.watres.2017.04.014

Trebuch, L.M., Oyserman, B.O., Janssen, M., Wijffels, R.H., Vet, L.E.M., Fernandes, T.V.,

2020. Impact of hydraulic retention time on community assembly and function of photogranules for wastewater treatment. Water Res. 173, 115506. https://doi.org/10.1016/j.watres.2020.115506

Vairappan, C.S., 2003. Potent antibacterial activity of halogenated metabolites from Malaysian red algae, *Laurencia majuscula (Rhodomelaceae, Ceramiales)*. Biomol. Eng. 20, 255–259. https://doi.org/10.1016/S1389-0344(03)00067-4

Vasconcelos Fernandes, T., Shrestha, R., Sui, Y., Papini, G., Zeeman, G., Vet, L.E.M., Wijffels, R.H., Lamers, P., 2015. Closing domestic nutrient cycles using microalgae. Environ. Sci. Technol. 49, 12450–12456. https://doi.org/10.1021/acs.est.5b02858

Vergara-Araya, M., Hilgenfeldt, V., Peng, D., Steinmetz, H., Wiese, J., 2021. Modelling to lower energy consumption in a large wwtp in china while optimising nitrogen removal. Energies 14, 5826. https://doi.org/10.3390/en14185826

Wang, J., Lei, Z., Tian, C., Liu, S., Wang, Q., Shimizu, K., Zhang, Z., Adachi, Y., Lee, D.-J., 2021. Ionic response of algal-bacterial granular sludge system during biological phosphorus removal from wastewater. Chemosphere 264, 128534. https://doi.org/10.1016/j.chemosphere.2020.128534

Wang, J., Lei, Z., Wei, Y., Wang, Q., Tian, C., Shimizu, K., Zhang, Z., Adachi, Y., Lee, D.-J., 2020. Behavior of algal-bacterial granular sludge in a novel closed photo-sequencing batch reactor under no external O_2 supply. Bioresour. Technol. 318, 124190. https://doi.org/10.1016/j.biortech.2020.124190

Wang, J., Li, Z., Wang, Q., Chen, X., Lei, Z., Shimizu, K., Zhang, Z., Adachi, Y., Lee, D.-J., 2023a. Revealing calcium ion behavior during anaerobic phosphorus release process in aerobic granular sludge system. Bioresour. Technol. 369, 128474. https://doi.org/10.1016/j.biortech.2022.128474

Wang, J., Li, Z., Wang, Q., Lei, Z., Qian, X., Zhang, Z., Liu, X., Lee, D.-J., 2023b. Use of photo-driven algal-bacterial aerobic granular sludge system to close carbon cycle in biological nutrients removal and sludge anaerobic digestion units in wastewater treatment plants. Chem. Eng. J. 475, 145999. https://doi.org/10.1016/j.cej.2023.145999

Wang, J., Li, Z., Wang, Q., Lei, Z., Yuan, T., Shimizu, K., Zhang, Z., Adachi, Y., Lee, D.-J., Chen, R., 2022a. Achieving stably enhanced biological phosphorus removal from aerobic granular sludge system via phosphorus rich liquid extraction during anaerobic period. Bioresour. Technol. 346, 126439. https://doi.org/10.1016/j.biortech.2021.126439

Wang, J., Wei, Y., Li, Z., Chen, X., Lei, Z., Yuan, T., Shimizu, K., Zhang, Z., Kim, S.-H., Lee,

D.-J., 2022b. Effect of stepwise or one-time illumination strategy on the development of algal-bacterial aerobic granular sludge in sequencing batch reactor. Bioresour. Technol. Reports 17, 100931. https://doi.org/10.1016/j.biteb.2021.100931

Wang, Q., Shen, Q., Wang, J., Zhang, Y., Zhang, Z., Lei, Z., Shimizu, K., Lee, D.-J., 2020. Fast cultivation and harvesting of oil-producing microalgae Ankistrodesmus falcatus var. Acicularis fed with anaerobic digestion liquor via biogranulation in addition to nutrients removal. Sci. Total Environ. 741, 140183. https://doi.org/10.1016/j.scitotenv.2020.140183

Wendell, O. K., Pitt, P.A., Bott C. B., Chandran, K., 2014. Chapter 5 - Nitrogen. Edited by Jenkins, D and Wanner, J., Activated Sludge - 100 Years and Counting, IWA Publishing, pp. 77-91. https://doi.org/10.2166/9781780404943.

Whelan, M.J., Linstead, C., Worrall, F., Ormerod, S.J., Durance, I., Johnson, A.C., Johnson, D., Owen, M., Wiik, E., Howden, N.J.K., Burt, T.P., Boxall, A., Brown, C.D., Oliver, D.M., Tickner, D., 2022. Is water quality in British rivers "better than at any time since the end of the Industrial Revolution"? Sci. Total Environ. 843, 157014. https://doi.org/10.1016/j.scitotenv.2022.157014

Xi, J., Gong, H., Zhang, Y., Dai, X., Chen, L., 2021. The evaluation of GHG emissions from Shanghai municipal wastewater treatment plants based on IPCC and operational data integrated methods (ODIM). Sci. Total Environ. 797, 148967. https://doi.org/10.1016/j.scitotenv.2021.148967

Xu, P., Li, J., Qian, J., Wang, B., Liu, J., Xu, R., Chen, P., Zhou, W., 2023. Recent advances in CO_2 fixation by microalgae and its potential contribution to carbon neutrality. Chemosphere 319, 137987. https://doi.org/10.1016/j.chemosphere.2023.137987

Yan, X., Li, L., Liu, J., 2014. Characteristics of greenhouse gas emission in three full-scale wastewater treatment processes. J. Environ. Sci. (China) 26, 256–263. https://doi.org/10.1016/S1001-0742(13)60429-5

Yang, X., Zhao, Z., Yu, Y., Shimizu, K., Zhang, Z., Lei, Z., Lee, D.-J., 2020. Enhanced biosorption of Cr(VI) from synthetic wastewater using algal-bacterial aerobic granular sludge: Batch experiments, kinetics and mechanisms. Sep. Purif. Technol. 251, 117323. https://doi.org/10.1016/j.seppur.2020.117323

Yong, J.J.J.Y., Chew, K.W., Khoo, K.S., Show, P.L., Chang, J.-S., 2021. Prospects and development of algal-bacterial biotechnology in environmental management and protection. Biotechnol. Adv. 47, 107684.

https://doi.org/10.1016/j.biotechadv.2020.107684

Zakaria, M.S., Hassan, S., Nor, M.F.M., 2015. Calorific value of the sewage sludge in the thermal dryer. ARPN J. Eng. Appl. Sci. 10, 10245–10248. http://large.stanford.edu/courses/2017/ph240/huang1/docs/zakaria.pdf

Zhang, B., Guo, Y., Lens, P.N.L., Zhang, Z., Shi, W., Cui, F., Tay, J.-H., 2019. Effect of light intensity on the characteristics of algal-bacterial granular sludge and the role of N-acyl-homoserine lactone in the granulation. Sci. Total Environ. 659, 372–383. https://doi.org/10.1016/j.scitotenv.2018.12.250

Zhang, B., Lens, P.N.L., Shi, W., Zhang, R., Zhang, Z., Guo, Y., Bao, X., Cui, F., 2018. Enhancement of aerobic granulation and nutrient removal by an algal–bacterial consortium in a lab-scale photobioreactor. Chem. Eng. J. 334, 2373–2382. https://doi.org/10.1016/j.cej.2017.11.151

Zhang, H.-L., Sheng, G.-P., Fang, W., Wang, Y.-P., Fang, C.-Y., Shao, L.-M., Yu, H.-Q., 2015. Calcium effect on the metabolic pathway of phosphorus accumulating organisms in enhanced biological phosphorus removal systems. Water Res. 84, 171–180. https://doi.org/10.1016/j.watres.2015.07.042

Zhang, H., Gong, W., Bai, L., Chen, R., Zeng, W., Yan, Z., Li, G., Liang, H., 2020. Aeration-induced CO_2 stripping, instead of high dissolved oxygen, have a negative impact on algae–bacteria symbiosis (ABS) system stability and wastewater treatment efficiency. Chem. Eng. J. 382, 122957. https://doi.org/10.1016/j.cej.2019.122957

Zhang, Z., Li, H., Zhu, J., Weiping, L., Xin, X., 2011. Improvement strategy on enhanced biological phosphorus removal for municipal wastewater treatment plants: Full-scale operating parameters, sludge activities, and microbial features. Bioresour. Technol. 102, 4646–4653. https://doi.org/10.1016/j.biortech.2011.01.017

Zhao, Z., Liu, S., Yang, X., Lei, Z., Shimizu, K., Zhang, Z., Lee, D.-J., Adachi, Y., 2019. Stability and performance of algal-bacterial granular sludge in shaking photo-sequencing batch reactors with special focus on phosphorus accumulation. Bioresour. Technol. 280, 497–501. https://doi.org/10.1016/j.biortech.2019.02.071

Zhao, Z., Yang, X., Cai, W., Lei, Z., Shimizu, K., Zhang, Z., Utsumi, M., Lee, D.-J., 2018. Response of algal-bacterial granular system to low carbon wastewater: Focus on granular stability, nutrients removal and accumulation. Bioresour. Technol. 268, 221–229. https://doi.org/10.1016/j.biortech.2018.07.114

Acknowledgements

First of all, I would like to express the greatest appreciation from the bottom of my heart towards my supervisors, Profs. Zhongfang LEI, Zhenya ZHANG, Kazuya SHIMIZU and Yasuhisa ADACHI for providing me the opportunity to conduct the research, and for their careful guidance and kind help. Special appreciation to my chief supervisor, Prof. Zhongfang LEI, for her patient and kind help throughout my study. The thesis would not be completed without their supervision and guidance.

Special thanks should go to my thesis committee members, Profs. Zhongfang LEI, Helmut YABAR, Tian YUAN, Motoo UTSUMI, and Yasuhisa ADACHI, for their patient reading, listening, valuable suggestions and comments. All the instructors provided great help for me to improve my thesis and future research.

I want to express the special appreciation towards the program of "Support for Pioneering Research Initiated by the Next Generation (SPRING)" from Japan Science and Technology Agency (JST), Japan for the precious scholarship, which provided me the opportunity to study at the University of Tsukuba with energy and enough time.

I would like to thank my lab mates and friends for the assistance and help in my research and life. Thanks to Dr. Jixiang WANG, Dr. Qian WANG, Dr. Xingyu CHEN, Mr. Xiaochuan DONG, Mr. Yankai ZHAO, Miss Wenjun LIU, Miss Ge GAO, Mr. Yunqiang FAN, Miss Ke JIN, Miss Ziyin Ai and other friends for their countless assistance during my three-year doctoral study.

The deepest gratitude goes to my husband (Jixiang WANG), my younger sister (Zejing LI) and my son (Jinzhao WANG) for their endless love. My husband gives me endless supporting and cares that always make me feel strong in my life. Special thanks to my parents for their love, care, and unselfish support throughout my life.

Last but not least, I would like to express my most sincere gratitude to my supervisor, Prof. Zhongfang LEI. Thanks for her selfless care, kind help, professional guidance, and friendly suggestion during these five years. I will definitely remember her teachings and would be a serious, responsible, and kind person like her.

Publications

[1] **Li, Z.**, Wang, J., Liu, W., Zhao, Y., Lei, Z., Yuan, T., Shimizu, K., Zhang, Z., Lee, D.-J., 2023. Photosynthetic oxygen-supported algal-bacterial aerobic granular sludge can facilitate carbon, nitrogen and phosphorus removal from wastewater: Focus on light intensity selection. Bioresour. Technol., 388, 129752.

[2] **Li, Z.**, Wang, J., Liu, J., Chen, X., Lei, Z., Yuan, T., Shimizu, K., Zhang, Z., Lee, D.-J., Lin, Y., Adachi, Y., van Loosdrecht, M. C., 2023. Highly efficient carbon assimilation and nitrogen/phosphorus removal facilitated by photosynthetic O_2 from algal-bacterial aerobic granular sludge under controlled DO/pH operation. Water Res., 238, 120025.

[3] **Li, Z.**, Wang, J., Chen, X., Lei, Z., Yuan, T., Shimizu, K., Zhang, Z., Lee, D.-J. ,2022. Insight into aerobic phosphorus removal from wastewater in algal-bacterial aerobic granular sludge system. Bioresour. Technol., 352, 127104.

[4] Wang, J., **Li, Z.**, Wang, Q., Lei, Z., Qian, X., Zhang, Z., Liu, X., Lee, D.-J., 2023. Use of photo-driven algal-bacterial aerobic granular sludge system to close carbon cycle in biological wastewater nutrients removal and sludge anaerobic digestion units in wastewater treatment plants. Chem. Eng. J., 475,145999.

[5] Wang, J., **Li, Z.**, Wang, Q., Chen, X., Lei, Z., Shimizu, K., Zhang Z., Adachi Y., Lee, D.-J., 2023. Revealing calcium ion behavior during anaerobic phosphorus release process in aerobic granular sludge system. Bioresour. Technol., 369, 128474.

[6] Chen, X., Mai, J., Dong, X., Wang, Q., **Li, Z.**, Yuan, T., Lei, Z., Zhang, Z., Shimizu, K., Lee, D. -J., 2023. Enhanced alginate-like exopolymers recovery from algal-bacterial aerobic granular sludge: Optimal cultivation condition and contribution of bacteria and microalgae during the transport/storage period. Bioresour. Technol., 382, 129155.

[7] Chen, X., Wang, J., Wang, Q., **Li, Z.**, Yuan, T., Lei, Z., Zhang, Z., Shimizu, K., Lee, D. -J., 2022. A comparative study on simultaneous recovery of phosphorus and alginate-like exopolymers from bacterial and algal-bacterial aerobic granular sludges: Effects of organic loading rate. Bioresour. Technol., 357, 127343.

[8] Wang, J., Wei, Y., **Li, Z.**, Chen, X., Lei, Z., Yuan, T., Zhang Z., Adachi Y., Lee, D.-J., Chen, R., 2022. Effect of stepwise or one-time illumination strategy on the development of algal-bacterial aerobic granular sludge in sequencing batch reactor. Bioresour. Technol. Rep., 17, 100931.

[9] Wang, J., **Li, Z.**, Wang, Q., Lei, Z., Yuan, T., Shimizu, K., Zhang, Z., Adachi Y., Lee, D.-

J., Chen, R., 2022. Achieving stably enhanced biological phosphorus removal from aerobic granular sludge system via phosphorus rich liquid extraction during anaerobic period. Bioresour. Technol., 346, 126439.